FABRICATION, CHARACTERIZATION AND DEGRADATION OF PHB AND PHBV MICROSPHERES FOR LIVER CELL GROWTH

CHAW SU THWIN

NATIONAL UNIVERSITY OF SINGAPORE

2004

FABRICATION, CHARACTERIZATION AND DEGRADATION OF PHB AND PHBV MICROSPHERES FOR LIVER CELL GROWTH

CHAW SU THWIN

(B.Eng.(Chemical) Yangon Technological University)

A THESIS SUBMITTED

FOR THE DEGREE OF MASTER OF ENGINEERING

DEPARTMENT OF CHEMICAL AND BIOMOLECULAR ENGINEERING

NATIONAL UNIVERSITY OF SINGAPORE

2004

Acknowledgements

The author would like to express her deepest thanks and appreciation to her supervisor Associate Professor Dr. Tong Yen Wah for his valuable advice and excellent guidance imparted into this research project, preparation of this manuscript and above all, his understanding and help in different ways, all the time.

The author would like to express her gratitude to the National University of Singapore for providing the research scholarship and the opportunity to pursue the master degree program in its Department of Chemical and Biomolecular Engineering.

The author would like to thank the staff members of the Department of Chemical and Biomolecular Engineering, especially Ms. Lee Chai Keng, Mr. Boey Kok Hong, Ms. Samantha Farm, Madam Khoh Leng Khim and Ms. Tay Choon Yeng for providing technical support which made the research project possible to be accomplished.

The author would gratefully acknowledge her colleagues, Mr. Hidenori Nishioka, Ms. Ko Choon Ying, Mr. Jeremy Daniel Lease and Madam Liu Shaoqiong for their suggestions and discussions on this research.

The special appreciation is expressed to the author's lovely parents Mr. Maung Maung Thwin and Madam Khin Sein, and also brother Mr. Ye Thiha Thwin for their prayers,

devotion and encouragement given while she was studying in the National University of Singapore.

Finally, the author would express her deepest thanks to her husband Mr. Kyaw Tun for his unconditional love, kind understanding and encouragement throughout these years.

Table of Contents

Acknowledgements **i**

Table of Contents **iii**

Summary **viii**

List of Tables **xi**

List of Figures **xiii**

List of Symbols **xvii**

Chapter 1. Introduction **1**

1.1. General Introduction **1**

1.2. Research Scope **4**

1.3. Research Objectives **5**

Chapter 2. Literature Review and Background **6**

2.1. Liver Tissue Engineering **6**

2.2. Biodegradable Polymers for Tissue Engineering **14**

2.2.1. Synthetic Biodegradable Polymers 14

2.2.2. Natural Biodegradable Polymers 14

2.2.3. PHA, PHB and PHBV 16

2.2.3.1. PHA 16

2.2.3.2. PHB and PHBV 17

2.2.4. Miscible and Immiscible Polymers with PHB and PHBV 21

2.2.5. Other Uses of PHB and PHBV 22

2.3. Applications of PHB and PHBV in Tissue Engineering 23

Chapter 3. Materials and Methods 26

3.1. Materials 26

3.2. Preparation of Scaffolds 26

3.2.1. Fabrication of Microspheres 26

3.2.2. Preparation of Thin Films 28

3.3. Polymer Characterizations 28

3.3.1. Particle Size Analysis 28

3.3.2. SEM Observations 29

3.3.3. Contact Angle Measurement 29

3.3.4. Gel Permeation Chromatography (GPC) Analysis 30

3.3.5. Differential Scanning Calorimetry (DSC) Measurement 30

3.3.6. Proton-Nuclear Magnetic Resonance (^{1}H-NMR) Analysis 31

3.3.7. X-ray Photoelectron Spectroscope (XPS) Analysis 31

3.3.8. Fourier Transform Infrared (FTIR) Examination 31

3.4. Degradation of Microspheres 32

3.4.1. Mass Loss Analysis 32

3.5. Liver Cell Culture on Polymer Scaffolds 33

3.5.1. Preparation of the Controls 33

3.5.2. Preparation of Cell Culture Medium 33

3.5.3. Human Liver Cell Line (Hep3B) 34

3.5.4. Cell Culture 34

3.5.5. Cell Seeding on Polymer Scaffolds 35

3.5.6. Fixation of the Cells for SEM 36

3.5.7. Live/Dead Assay for Laser Confocal Micrograph 36

3.6. Cell Viability Test 37

3.6.1. Haemocytometer Cell Counting 37

3.6.2. [3-(4,5-dimethylthiazol-2-yl)-2-yl]-diphenyltetrazolium bromide] MTT Assay 37

3.6.2.1. Statistical Analysis 38

3.7. Direct Contact Cytotoxicity Test (ISO 10993-5) 39

3.7.1. Mouse Fibroblast Cell Line (L-929) Culture 39

3.7.2. Preparation of Materials 40

3.7.3. Preparation of Neutral Red (NR) Solution 40

3.7.4. Preparation of Formal-calcium Solution 40

3.7.5. Placement of the Specimens onto the Cell Surface 41

3.7.6. Neutral Red (NR) Assay 41

3.7.6.1.Statistical Analysis 42

3.8. Liver Cell Functionality Tests 42

3.8.1. EROD Assay for Cytochrome P-450 activity 42

3.8.1.1. Statistical Analysis 43

3.8.2. Albumin Secretion Synthesis by ELISA 43

3.8.2.1. Statistical Analysis 44

Chapter 4. Results and Discussion 45

4.1. PHB and PHBV Scaffolds 45

4.1.1. 2D Thin Films 45

4.1.2. 3D Microspheres 47

4.2. Size Distribution of Microspheres 49

4.3. The Size, Shape and Surface Studies of Microspheres **51**

4.3.1. Effect of Copolymer Composition 51

4.3.2. Effect of Polymer Solution Concentration 52

4.3.3. Effect of Emulsifier Concentration 54

4.3.4. Effect of Oil/First Aqueous Volume Ratio 56

4.3.5. Effect of Solvent 58

4.3.6. Effect of Homogenizing Speed 60

4.3.7. Effect of Homogenizing Time 61

4.3.8. Effect of Stirrer Height 62

4.3.9. Effect of Evaporation Temperature 64

4.3.10. Other Affecting Parameters for the Size of Microspheres 66

4.4. Degradation of Microspheres **66**

4.4.1. SEM Results 67

4.4.2. Mass Loss Analysis 71

4.5. Polymer Characterizations **73**

4.5.1. Contact Angle measurement 73

4.5.2. Gel Permeation Chromatography (GPC) Analysis 75

4.5.3. Differential Scanning Calorimetry (DSC) Measurement 77

4.5.4. Proton-Nuclear Magnetic Resonance (^{1}H-NMR) Analysis 81

4.5.5. X-ray Photoelectron Spectroscope (XPS) Analysis 84

4.5.6. Fourier Transform Infrared (FTIR**)** Examination 86

4.6. Direct Contact Cytotoxicity Test **88**

4.7. Liver Cells Seeding on Polymer Scaffolds **90**

4.7.1. Liver Cells Growth on 2D Polymer Thin Films 91

4.7.2. Liver Cells Growth on 3D Polymer Microspheres 92

4.8. Cell Viability Test 96

4.8.1. Cell Proliferation Determination by MTT assay 97

4.9. Measurement of Liver Cell Functionalities 99

4.9.1. Cytochrome P-450 Activity 100

4.9.2. Synthesis of Albumin Secretion 102

Chapter 5. Conclusion and Recommendation 104

5.1. Conclusion 104

5.2. Recommendation 109

Bibliography 110

Summary

Tissue engineering is considered to be a biomedical emerging area for the development of a new generation of implants for damaged tissues. Constructing engineered liver tissue is one of the major targets for tissue engineering with the goal of reducing the implantation cost and solving the shortage of liver donors. One new approach of tissue engineering is the use of microsphere scaffolds to guide cells growth.

Recently, poly(3-hydroxybutyrate) (PHB) and poly(3-hydroxybutyrate-*co*-3-hydroxy-valerate) (PHVB), both microbial polyesters, have received increasing attention in tissue engineering application due to their biodegradability, biocompatibility and non-toxicity. This study focuses on the fabrication of three-dimensional microspheres of PHB and PHVB copolymers with 5%, 8% and 12% PHV content respectively by the oil-in-water emulsion solvent evaporation as the artificial scaffolds. Two-dimensional thin films were also produced in comparison with the microspheres for growth, proliferation and functionalities of the liver cells.

Surface properties of the polymers such as porosity, surface smoothness or roughness, and physical properties such as wettability, crystallinity, T_m, T_g and polymer

degradation rate were found to vary with PHV content. Some influencing parameters being studied related to size, shape and surface of the microspheres are copolymer composition, polymer and emulsifier concentration, solvent and so forth.

To study the degradation of the microspheres, *in vitro* degradation was evaluated up to a one year period. The mass loss or molecular weight loss of the polymers was observed to increase with increasing HV content such as 16.5%, 22%, 26% and 34% for PHB, PHBV(5%), PHBV(8%) and PHBV(12%) microspheres, respectively. SEM results revealed that bulk erosion was faster than surface erosion. The contact angle measurement indicated that PHB is the most hydrophilic (75.3ºC) while PHBV(12%) is the most hydrophobic (81.9ºC). DSC data illustrated that increasing HV content resulted in decreasing crystallinity, T_m and T_g of the polymers. Together with the ^{1}H-NMR results, these showed that amorphous regions degraded faster than crystalline region during degradation. FTIR and XPS analysis performed to determine chemical structure and chemical compositions of the microspheres showed similar trends.

The cytotoxicity of the polymers was evaluated by ISO 10993-5 standard direct contact cytotoxicity test using a mouse fibroblast cell line, L-929. The cytotoxicities of PHB, PHBV(5%), PHBV(8%) and PHBV(12%) films were found to be 18.4%, 12.7%, 10.6% and 12.7% respectively, which were low compared to 100% for the positive control.

Human hepatoma cell line, Hep3B, was cultured *in-vitro* both on the microspheres and thin films. The cells grew as a monolayer on the thin films while multilayer cells were observed to bridge the microspheres and developed into cell-polymer aggregates after

one week culture. MTT results showed that the cell proliferation on the microspheres were more than 2-5 times higher than that on thin films at 6 days of culture.

Two hepatic specific functions, albumin secretion and cytochrome P-450 activity, were evaluated by EROD and ELISA assays. EROD results showed that the P-450 activity of Hep3B cells on the PHB, PHBV(5%) and PHBV(8%) microspheres were 2 times higher than that on thin films at day 6 of culture. At the same period, ELISA results revealed that Hep3B attached on the PHB, PHBV(5%) and PHBV(8%) microspheres secreted albumin 1 to 2 times higher than that on thin films.

List of Tables

Table 4.1. Comparison of the mean diameter of PHB, PHBV(5%), PHBV(8%) and PHBV(12%) microspheres. 50

Table 4.2. Comparison of the effect of polymer concentration on the typical PHBV(8%) microspheres. 53

Table 4.3. Comparison of the effect of emulsifier concentration on the typical PHBV(8%) microspheres. 56

Table 4.4. Comparison of the effect of oil/first aqueous volume ratio on the typical PHBV(8%) microspheres. 58

Table 4.5. Comparison of the effect of solvent on the typical PHBV(8%) microspheres. 59

Table 4.6. Comparison of the effect of homogenizing speed on the typical PHBV(8%) microspheres. 61

Table 4.7. Comparison of the effect of homogenizing time on the typical PHBV(8%) microspheres. 62

Table 4.8. Comparison of the effect of stirrer height on the typical PHBV(8%) microspheres. 64

Table 4.9. Comparison of the effect of evaporation temperature on the typical PHBV(8%) microspheres. 65

Table 4.10. Mass loss of the PHB, PHBV(5%), PHBV(8%) and PHBV(12%) microspheres one year after degradation. 73

Table 4.11. Contact angle measurements of the PHB, PHBV(5%), PHBV(8%) and PHBV(12%) thin films. 74

Table 4.12. GPC results of PHB, PHBV(5%), PHBV(8%) and PHBV(12%) microspheres before and after degradation. 75

Table 4.13. DSC results of PHB, PHBV(5%), PHBV(8%) and PHBV(12%) microspheres before and after degradation. 78

Table 4.14. ^{1}H-NMR integrated area assignments for the representative 83

PHBV(8%) microspheres.

Table 4.15. The signal intensity ratio of protons b4 and v4 for PHBV(5%), PHBV(8%) and PHBV(12%) microspheres after degradation. 84

Table 4.16. Atomic percentage of carbon and oxygen elements on the PHB and PHBV microspheres before degradation. 86

List of Figures

Fig. 2.1. Repeating molecular structure of PHBV: (a) PHB and (b) PHV. 18

Fig. 3.1. The fabrication processes of the PHB and PHBV microspheres by the oil-in water (o/w) emulsion solvent evaporation technique. 27

Fig. 3.2. Direct contact cytotoxicity test procedure using mouse fibroblast cell line (L-929). 42

Fig. 4.1. SEM scans of thin films with different PHV content: (A) PHB, (B) PHBV(5%), (C) PHBV(8%) and (D)PHBV(12%). Images on the left column are at 3000 x magnification while images on the right column are at 7500 x magnification. Size of the bar is 1 μm. 46

Fig. 4.2. SEM scans of microspheres with different PHV contents: (A) PHB, (B) PHBV(5%), (C) PHBV(8%) and (D) PHBV(12%). Images on the left column are at 50 x magnification while images on the right column are at 600 x magnification. Size of the bar of the left column is 500 μm while size of the bar of the right column is 20 μm. 48

Fig. 4.3. Particle size distribution of (A) PHB, (B) PHBV(5%), (C) PHBV(8%) and (D) PHBV(12%) microspheres as measured by a Coulter particle size analyzer. 49

Fig. 4.4. SEM scans of PHBV(8%) with different polymer solution concentrations: (A) 2% and (B) 8%. Size of the bar is 500 μm. 52

Fig. 4.5. Particle size distribution of the PHBV(8%) microspheres with 2% polymer solution concentration. 53

Fig. 4.6. SEM scans of the PHBV(8%) microspheres using different emulsifier concentrations: (A) 0.01 (w/v %) and (B) 0.15 (w/v %). Size of the bar is 500 μm. 55

Fig. 4.7. Particle size distribution of the PHBV(8%) microspheres with various emulsifier concentration: (A) 0.01 (w/v %) and (B) 0.15 (w/v %). 55

Fig. 4.8. SEM scans of the PHBV(8%) microspheres using oil/first aqueous volume ratio of 5 : 1. Size of the bar is 500 μm. 57

Fig. 4.9. Particle size distribution of the PHBV(8%) microspheres with oil : first aqueous volume ratio (5:1). 57

Fig. 4.10. SEM scans of the representative PHBV(8%) microspheres using different solvent: (A) DCE and (B) DCM. Size of the bar is 20 μm. 58

Fig. 4.11. Particle size distribution of the PHBV(8%) microspheres with various solvents: (A) DCE and (B) DCM. 59

Fig. 4.12. Particle size distribution of the typical PHBV(8%) microspheres with various homogenizing speed: (A) 19,000 rpm and (B) 13,000 rpm. 60

Fig. 4.13. Particle size distribution of the PHBV(8%) microspheres with various homogenizing time: (A) 10 s and (B) 20 s. 61

Fig. 4.14. SEM scans of PHBV(8%) microspheres using different stirrer height: (a) equal to 1 inch and (b) higher than 1 inch. Size of the bar of (A) is 500 μm and that of (B) is 200 μm. 63

Fig. 4.15. Particle size distribution of the PHBV(8%) microspheres with various stirrer height: (A) > 1 inch and (B) ≈ 1 inch. 64

Fig. 4.16. Particle size distribution of the PHBV(8%) microspheres with various evaporation temperature: (A) 30ºC and (B) 55ºC. 65

Fig. 4.17. SEM scans of the microspheres after 1 year in vitro degradation: (A) PHB, (B) PHBV(5%), (C) PHBV(8%) and (D) PHBV(12%). The magnification is 600 x and the size of the bar is 10 μm. 68

Fig. 4.18. SEM scans of the microspheres: (A) PHB, (B) PHBV(5%), (C) PHBV(8%) and (D) PHBV(12%). A1, B1, C1 and D1 represent before degradation; the size of the bar is 5 μm. A2, B2, C2 and D2 represent one year after degradation; the size of the bar is 1 μm. 69

Fig. 4.19. SEM scans of cross-sectional internal morphology of the microspheres: (A) PHB, (B) PHBV(5%), (C) PHBV(8%) and (D) PHBV(12%). A1, B1, C1 and D1 represent before degradation. A2, B2, C2 and D2 represent one year after degradation. Size of the bar of A1, A2 and C1 is 50 μm and that of the rest is 20 μm. 70

Fig. 4.20. Mass loss analysis of the PHB, PHBV(5%), PHBV(8%) and PHBV(12%) microspheres as a function of time. 72

Fig. 4.21. Changes in weight average molecular weight of the PHB, PHBV(5%), PHBV(8%) and PHBV(12%) microspheres as a function of degradation time. 76

Fig. 4.22. Melting endotherms of the representative PHB and PHBV(5%) microspheres before (solid line) and one year after degradation (dashed line). 79

Fig. 4.23. Crystallization exotherms of the representative PHBV(5%) microspheres before (solid line) and one year after degradation (dashed line). 80

Fig. 4.24. The relation between degradation rate (mass loss %) and crystallinity % of the PHB, PHBV(5%), PHBV(8%) and PHBV(12%) microspheres. 81

Fig. 4.25. Chemical formula of PHBV copolymer: (A) PHB and (B) PHV. The letters (b1 to b4 and v1 to v5) correspond to the specific chemical shift regions identified by ^{1}H-NMR spectroscopy in Fig. 4.27. 81

Fig. 4.26. The 400 MHz ^{1}H-NMR spectra of the representative PHBV(8%) microspheres (A) before and (B) after degradation. 83

Fig. 4.27. C1s regions of XPS spectra of the representative (A) PHB and (B) PHBV(5%) microspheres. 85

Fig. 4.28. FTIR spectra for the PHB, PHBV(5%), PHBV(8%) and PHBV(12%) microspheres before (thick line) and one year after degradation (dashed line). 87

Fig. 4.29. Optical micrographs of mouse fibroblast cell line, L-929, cultured on TCP on (A) day 1 and (B) day 3. 88

Fig. 4.30. Optical micrographs of L-929 mouse fibroblasts seeded on polymer films, after 48 h incubation: (A) PHB, (B) PHBV(5%), (C) PHBV(8%) and (D) PHBV(12%). 89

Fig. 4.31. Cytotoxicity results for positive control (white bar), negative control (black bar) and polymer thin films (dotted bars). Values represent means ± SD, n = 5. Statistical analysis was performed by Student *t*-test. $*p < 0.01$. 90

Fig. 4.32. Optical micrographs of Hep3B attached on TCP: (A) 30 min and (B) 4 days, after seeding. 91

Fig. 4.33. Scanning electron micrographs of Hep3B cells adhere on the typical PHBV(5%) thin films, 3 days after culture. Size of the scale bar is 10 μm. 91

Fig. 4.34. Laser confocal micrograph of Hep3B grow on the representative PHBV(8%) thin film. 92

Fig. 4.35. Optical micrographs of Hep3B growth characteristics on the representative PHBV(12%) microspheres. (A) day 2, (B) day 4, (C) day 6, (D) day 8, (E) day 10, (F) day 12, (G) day 14 and (H) day 16. 93

Fig. 4.36. SEM micrographs of Hep3B seeded on the microspheres after 2 weeks: (A) PHB, (B) PHBV(5%) and (C) PHBV(8%). Size of the scale bar of A1, B1 and C1 is 100 μm and that of A2, B2 and C2 is 10 μm 94

Fig. 4.37. SEM scans of cell-cell and cell-substrate interactions on the (A & B) PHBV(8%), and (C & D) PHBV(5%) microspheres after two weeks. Size of the scale bar is 10 μm. 95

Fig. 4.38. 2D confocal microscopy images of Hep3B cells seeding on the typical PHB microspheres on 5 days of culture. 96

Fig. 4.39. MTT results of Hep3B viability on 2 days culture onto positive control (white bar), negative control (black bar), thin films (dotted bars) and microspheres (hatched bars). Values represent means ± SD, n = 2. Statistical analysis was performed by Student *t*-test. *$p < 0.05$. 97

Fig. 4.40. MTT results of Hep3B viability on 6 days culture onto positive control (white bar), negative control (black bar), thin films (dotted bars) and microspheres (hatched bars). Values represent means ± SD, n = 2. Statistical analysis was performed by Student *t*-test. *$p < 0.05$. 97

Fig. 4.41. Cytochrome P-450 activity of Hep3B cells attached onto controls, thin films and microspheres on 2 days (dotted bars), 4 days (black bars) and 6 days (hatched bars). Values represent means ± SD, n = 3. Statistical analysis was performed by Student *t*-test. *$p < 0.05$. 101

Fig. 4.42. Albumin secretion of Hep3B cells attached onto controls, thin films and microspheres on 2 days (dotted bars), 4 days (black bars) and 6 days (hatched bars). Values represent means ± SD, n = 3. Statistical analysis was performed by Student *t*-test. *$p < 0.05$. 102

List of Symbols

2D	Two-dimensional
3D	Three-dimensional
BSA	Bovine serum albumin
Cr	Crystallization
DCM	Dichloromethane
DCE	Dichloroethane
DMEM	Dulbecco's modified Eagle's medium
DMSO	Dimethyl sulphoxide
DSC	Differential scanning calorimetry
ECM	Extracellular matrix
ELISA	Enzyme-linked immunosorbent assay
EROD	Ethoxyresorufin-*O*-dealkylase
FBS	Fetal bovine serum
FTIR	Fourier-transform infrared spectroscopy
GPC	Gel permeation chromatography
HDPE	High density polyethylene
Hep3B	Human hepatoma cell line
^{1}H-NMR	Proton-Nuclear magnetic resonance
KBr	Potassium bromide
LSCM	Laser scanning confocal microscope
NR	Neutral red

MTT	3-(4,5-dimethylthiazol-2-yl)-2,5-diphenyltetrazolium bromide
L-929	Mouse fibroblast cell line
LSCM	Laser scanning confocal microscope
P-450	Cytochrome P-450
PBS	Phosphate buffer solution
PHB	Poly(3-hydroxybutyrate)
PHBV	Poly(3-hydroxybutyrate-*co*-3-hydroxyvalerate)
PHBV(5%)	Poly(3-hydroxybutyrate-*co*-3-hydroxyvalerate) (5% HV content)
PHBV(8%)	Poly(3-hydroxybutyrate-*co*-3-hydroxyvalerate) (8% HV content)
PHBV(12%)	Poly(3-hydroxybutyrate-*co*-3-hydroxyvalerate) (12% HV content)
ppm	Parts per million
PVA	Polyvinyl alcohol
rpm	Revolutions per minute
SEM	Scanning electron microscope
TCP	Tissue culture plate
THF	Tetrahydrofuran
T_g	Glass transition temperature
T_m	Melting temperature
TCP	Tissue culture plate
TMB	3,3',5',5-tetramethylbenzidine
UV	Ultraviolet
w/v%	Weight per volume percent
XPS	X-ray photoelectron spectroscopy
ZDBC	polyurethane film containing 0.25% zinc dibutyldithiocarbamate

Greek Letters

δ	delta
λ	wavelength (nm)

Subscripts

g	glass transition
m	melting

Chapter 1

Introduction

1.1 General Introduction

The goal of tissue engineering is to develop biomaterials to facilitate, repair, regenerate or replace damaged or diseased tissues [Matthew, 2002]. The range of tissue engineering applications are extensive with studies on the liver, lung, skin, corneal, blood vessels, cartilage, tendon, muscles, nerves, heart valve leaflets, kidney, and pancreatic islets among others.

This research focuses on liver tissue engineering. The liver performs various metabolic functions which include the secretion of bile for digestion, metabolizing proteins, carbohydrates and fats, storage of glycogen and vitamins, synthesizing blood-clotting factors, removing wastes and toxic matter from the blood, regulating blood volume, and destroying old red blood cells. Among these, the most important function of the liver is the secretion of blood serum proteins, such as albumin, that are supplied to the blood. Apart from this, a liver is able to restore its original form and perform normal functions through spontaneous regeneration if the liver is damaged. This specific quality of the liver promotes further investigation for liver tissue engineering.

The most common liver failures today are due to chronic hepatitis, cirrhosis and alcoholic liver disease. Due to the increasing number of liver patients and liver donor

shortage, waiting time of patients for liver transplantation is increasing year by year. In the US alone in 2002, about 17000 patients were on the registration lists for liver transplant while more than half of the patients die annually waiting for a donated liver. Estimated liver transplantation cost is approximately US$75000 or more depending on case-by-case treatment or surgery. With this great demand, liver tissue engineering is increasingly seen as a solution to the problem of liver donor shortage and would reduce the cost of liver transplantation.

The parenchymal liver cells, hepatocytes, are anchorage dependent cells and they generally need a scaffold or support to attach, grow and proliferate to accomplish further cell functionalities. Accordingly, some major requirements of the polymeric scaffolds used for tissue engineering include biodegradability, biocompatibility, non-toxicity and high porosity. In addition, they must possess a suitable surface texture for cell attachment. Novel tissue engineering technique uses three dimensional scaffolds as structural templates for cell adhesion and subsequent tissue formation, since 3D scaffolds have more available surface area for cell attachment and adequate porosity for nutrients and oxygen transport. Therefore, 3D porous microspheres are attractive for liver tissue engineering. This research presents work on the fabrication of biodegradable porous polymer microspheres as temporary scaffolds for liver cell growth, in order to create desired engineered liver tissue for the regeneration of diseased livers. Polymers selected in this study are microbial PHB and three PHBV copolymers with HV contents of 5%, 8% and 12%, which are herein described as PHB, PHBV(5%), PHBV(8%) and PHBV(12%). PHB and PHBVs are the most widely used of the poly(β-hydroxyalkanoate) (PHA) family of thermoplastic aliphatic polyester.

A variety of methods to fabricate microspheres for specific applications have been previously developed. In this work, the microspheres were fabricated by an oil-in-water (o/w) emulsion solvent evaporation technique. Two-dimensional thin films were also made using the same polymers to compare the results of cell attachment, growth and functionalities with that of 3D microspheres.

The size, shape and surface morphology of the microspheres were examined for their effect by changing copolymer composition, polymer solution concentration, emulsifier concentration, oil/first aqueous volume ratio, solvent, homogenizing speed, homogenizing time, stirrer height, evaporation temperature, stirring speed, stirring time, lyophilization time and molecular weight of the polymer to guide liver cell growth.

This work also focuses on the hydrolytic degradation that has been evaluated by time-dependent changes in gravimetric mass loss (erosion) and molecular weight loss of the microspheres using GPC. To further study this degradation, PHB and PHBV microspheres and thin films were characterized before and after degradation by a few different methods. The internal and external surface morphological examinations of the microspheres were performed using SEM. The degradation of the microspheres depended on the crystallinity, T_m and T_g which was analyzed by DSC, and ^{1}H-NMR was used to prove the degradation results obtained by GPC and DSC. FTIR and XPS analysis were performed to determine chemical structure and chemical compositions of the microspheres. Additionally, the wettability of the polymers was determined by static water contact angle measurement because the cell attachment was believed to be related with the hydrophilicity of the polymers.

To ensure that PHB and PHBV are biocompatible for medical purposes, a direct contact cytotoxicity test was conducted by following the ISO 10993-5 method. L-929 mouse fibroblasts were cultured on PHB and PHBV thin films, while HDPE was used as a negative control and ZDBC was used as a positive control in this test.

To create artificial liver tissue *in vitro*, human hepatoma cell lines, Hep3B, were cultured on both 3D microspheres and 2D polymer thin films. The cell adhesion and growth were examined by an optical microscope, SEM and LSCM, while the cell viability and proliferation were assessed by trypan blue exclusion and MTT assay.

Although the liver perform various functions, only the most important hepatic functions such as cytochrome P-450 activity and albumin secretion were evaluated for both the microspheres and thin films. P-450 activity for detoxification of the liver cells was measured by an ethoxyresorufin-*O*-deethylase (EROD) assay. Serum albumin, the important blood protein in our body, secretion by the liver cells was also evaluated by an enzyme-linked immunosorbent (ELISA) assay.

1.2. Research Scope

This research focuses on the fabrication of novel PHB and PHBV microspheres as three-dimensional artificial scaffolds for liver cell growth, proliferation and functions to compare with the traditional two-dimensional thin films. It is hypothesized that PHB and PHBV can be used as a biocompatible and biodegradable scaffold for enhancing liver cell growth and that microspheres are unique 3D scaffolds that enables formation of tissues.

1.3. Research Objectives

The objectives of this research were to:

1. Fabricate novel PHB and PHBV copolymer (5%, 8% and 12% HV content) microspheres to be used as biodegradable scaffolds for liver tissue engineering
2. Study the size, shape and surface of the microspheres form various synthesis parameters
3. Conduct *in vitro* biodegradation of microspheres
4. Characterize and analyze of the microspheres before and after degradation
5. Examine the cytotoxicity of the polymers
6. Evaluate liver cell growth, proliferation and functions both on the microspheres and thin films.

Chapter 2

Literature Review and Background

2.1. Liver Tissue Engineering

Tissue engineering became a popular sub-area within the biomedical field since the 1970s, with many different definitions for the subject being derived. In 1988, the National Science Foundation coined the term "tissue engineering" as "the application of the principles and methods of engineering and the life sciences toward the fundamental understanding of structure-function relationships in normal and pathological mammalian tissues and the development of biological substitutes to restore, maintain, or improve functions" [Recum, 1999]. The objective of tissue engineering is to create not only engineered tissue but also biological substitutes. Therefore, the factors required for tissue engineering include cells and artificial scaffolds for cell growth [Lewandrowski, 2002].

Tissue engineering can be broadly classified into two main areas: organ transplantation and tissue regeneration. The current difficulties of organ transplantation are the lack of available organs at the required time and lack of close donor-recipient interaction. Moreover, the organs to be transplanted must survive outside the body for a period of time just before transplantation. In addition, organ donors can only meet less than half of the total organ demands [Rubinsky, 2002].

Tissue engineering is growing rapidly as an empirical approach to overcome the lack of available organs and donor shortages. In tissue engineering, the tissue foundation is assembled *in vitro* and subsequently implanted, which thus requires both seeding of the cells and artificial scaffolds. The task of a tissue engineer is to construct the desired scaffold for the intended tissue formation. Currently, the range of applied tissue engineering is very extensive, including but not limited to the liver, lung, skin, corneal, blood vessels, cartilage, tendon, muscles, nerves, heart valve leaflets, kidney, and pancreatic islets. In this list, liver is the only organ that can regenerate itself in the body. For this reason, we are concentrating on liver tissue engineering and this work is focused on creating artificial scaffolds for liver cell growth *in vitro*.

The dark, reddish brown, wedge-shaped liver is the largest gland in the human body, weighing about 3 pounds. A liver performs sophisticated functions with linked organs such as the stomach, intestine, gall bladder and pancreas. Normal liver functions include secretion of bile for digestion; metabolizing proteins, carbohydrates and fats; storage of glycogen and vitamins; synthesizing blood-clotting factors; detoxification of both endogenous products and xenobiotics; regulation of blood volume and destroying old red blood cells; and secretion of blood serum proteins, including albumin, that are supplied to the blood. A liver is made up of many types of cells such as sinusoidal endothelial cells, Kupffer cells, stellate cells, biliary epithelial cells and hepatocytes. Sixty percent of the liver is made up of hepatic cells or hepatocytes which are about 20-30 μm (± 5 μm) in size. Most of the liver-specific metabolic functions are performed by hepatocytes [Selden and Hodgson, 2002], and therefore, the term “hepatocyte” will be used herein to refer to the “liver cell”.

The most common liver failures are chronic hepatitis (hepatitis A, B and C), cirrhosis, liver cancer and diseases caused by alcohol. The replacement of liver is only transplanted when the patient has end-stage liver disease. Today, liver patients face the problem of organ donor shortages. While the demands of donated liver are increasing, the available organs for transplantation are decreasing. The shortage of donors arises in part due to the traditional beliefs of various peoples in some parts of the world. In the US alone, at the end of 2002, about 17000 patients were waiting for liver transplantation. More than half of the patients die annually while waiting for donated liver. Estimated liver transplantation cost is approximately US$75000 depending on the stage of treatment or surgery. In order to reduce the cost of organ transplantation and liver donor shortage, engineered liver tissues are generated *in vitro*. As previously mentioned, the liver has the capacity to regenerate itself, even after transection. By applying this natural ability, liver tissue engineering has an increased chance of success.

Various methods for liver transplantation include organ transplantation, hepatocellullar transplantation and the use of extracorporeal devices. The liver organ transplantation originated with cadaveric (dead body) transplantation. The first human liver cadaveric transplantation was performed in 1963 [Starzl, 1963]. Although most of the donated livers are obtained from cadaveric donors, available cadaveric livers are still less than the demand. The next advancement in liver organ transplantation was the split liver transplantation. In split liver transplantation, a cadaveric liver is divided into a small right lobe and a larger left lobe, and then transplanted in a child and in an adult respectively [Ghobrial, 2000]. Split liver transplantation is however more complicated than whole liver transplantation. To solve these complicated problems, living donor

transplantation was first investigated in children in 1988. It was only later that adult-to-adult living donor transplantations were extensively performed [Raja, 1989], [Hashikura, 1994]. Xenotransplanation, or the transplantation of animal organs, has also been performed to treat patients with end-stage organ failure. Pig organs have been shown to have significant physiological similarities with human organs. Unfortunately, the drawbacks of xenotransplanation include the damage of blood vessel, blockage and graft failure [Starzl, 1993]. Xenogeneic cells can also induce immune reactions within the host against cells and proteins synthesized by the xenogeneic hepatocytes.

One of the commonly used strategies in liver tissue engineering is the implantation of isolated cells. However, isolated hepatocytes have limited potential to divide for further uses in addition to the loss of their normal functions. To overcome this problem, the *in vivo* culture conditions and growth factor combinations can be modified to enhance proliferating adult hepatocytes. Growth factors support tissue regeneration and induce angiogenesis that promote supply of oxygen and nutrients to ensure cell survival. Some investigations have been attempted to modify the culture media to improve the hepatocyte morphology and liver specific functions by adding low concentrations of hormones, vitamins or amino acids [Allen and Bhatia, 2002]. Some research has explored use of providing extracellular matrix (ECM) for hepatocyte growth, proliferation and differentiation. The ECM has also been shown to affect the shape and morphology of cells [Mooney, 1992]. Hepatocytes are known to lose their liver specific functions while they are in culture. For long term survival and maintenance of liver specific functions, a lot of investigations have been performed. These include co-culture of hepatocytes with other cells of the liver such as non-

parenchymal stellate cells [Riccalton-Banks, 2003], and pancreatic islets [Kneser, 1999].

Primary cells (autogeneic, allogeneic or xenogeneic) and stem cells were originally used as isolated cell transplantation to overcome the shortage of donor livers, but their availability is limited. Subsequently, primary cells were subcultured into cell lines. The proliferation rate of the cell lines is much higher than that of primary cells, which therefore enables maintaining of the cells *in vitro* for longer periods of time. *In vitro* cell culture needs suitable scaffolds for cell attachment, growth, proliferation and differentiation. Tissue engineering *in vitro* requires at least three steps: the mass production of the cells in conventional culture dishes, the induction of differentiation of the cells, and the maintenance of differentiation. The latter two steps need novel tissue carriers such as two or three dimensional scaffolds for anchorage dependent cells. Monolayer cell culture on two-dimensional thin film may lose their phenotypic characteristics such as morphology or surface markers after repeated passages. Therefore, three-dimensional scaffolds are used to promote cell development, including appropriate cell-cell or cell-matrix interactions, normal cell functions and stability of the cells. In addition, diverse 3D scaffolds can be used to improve surface area per volume ratio compared with 2D scaffolds, which is a useful quality to promote high cell yield. *In vitro* cell culture has thus developed using 3D cell culture in which cells are given the required physiological conditions to provide adequate levels of nutrients to cells assembled in tissue formation [Doyle and Griffiths, 2001].

Three dimensional extracorporeal liver supports have been designed using different technologies such as membranes [Krasteva, 2002], spheroids [Riccalton-Banks, 2003],

suspension reactor microcarriers, bioreactors [Li, 1993, Sussman, 1994 and Flendrig, 1997], hollow fiber cartridges, perfusion beds, matrices such as sponges [Chung, 2002], foams [Ranucci, 2000], multicompartment interwoven fibers [Gerlach, 1994] and gel entrapment [Dunn, 1991]. As a major current technology, spheroids are encapsulated suspended multicellular aggregates in which cells adhere to each other rather than to a substrate. The drawback, however, of spheroid aggregates is the difficulty in stabilizing the cells [Sun, 1987 and Joly, 1997] and diffusion limitations [Piskin, 1997]. In the late 1980s, hollow fiber extracorporeal devices were first used for clinical applications with primary hepatocytes, but they have shown limited success [Matsumura, 1987].

Three-dimensional microspheres have been widely used for biomedical applications, especially drug delivery and protein release profiles. Jain fabricated PLGA microspheres by oil-in-water (o/w) single emulsion, water-in-oil-in-water (w/o/w) double emulsion, phase separation or coacervation and spray drying [Jain, 2000] for drug release. The o/w single emulsion solvent evaporation technique is widely used to fabricate the microspheres for controlled drug release because it is simple, economical and easy to process. The disadvantage of using the o/w single emulsion is poor encapsulation efficiencies of water-soluble drugs. To overcome this problem, a water-in-oil-in-water (w/o/w) double emulsion solvent evaporation technique was developed. Although the w/o/w process has additional steps, this method can be used for water-soluble drugs like peptides, proteins and vaccines as well as water-insoluble drugs like steroids. Phase separation or coacervation process is also used for both water-soluble and water-insoluble drugs but this process is more complex than w/o/w process. In addition, phase separation process tends to produce agglomerated particles and it is

difficult to remove the remaining solvent from the microspheres. To solve these problems, spray drying method is used to produce the microspheres for drug release. The spray drying method is more rapid, easier to scale-up, more convenient and less dependent on the solubility parameter of the polymer and the drug than the former methods. For example, Géze et al. studied the release characteristics of a radiosensitizer from PLGA/LMW-PLA microspheres fabricated by a phase separation technique. They reported that the drug release from the microspheres occurred over six weeks which was the standard time course of conventional radiation therapy [Géze, 1999]. Another example, Etrl et al. evaluated the anticancer agent camptothecin release rate correlated with the size of the PLGA microspheres and encapsulation efficiency. They concluded that PLGA microspheres could be used for cancer treatment by chemoembolization and implantation during surgical excision of the tumor [Ertl, 1999]. Kassab et al. fabricated L-PLA and PLGA microspheres to monitor the release rate of amphotericin B, an antifungal drug. They concluded that the drug release from PLGA microspheres were more than that of PLA [Kassab, 2002]. For clinical application, some researchers have attempted to use magnetic microspheres in separation of red blood cells from the whole blood for photopheresis treatment of white blood cells [Chatterjee, 2001].

Biodegradable polymers have played an important role in biomedical applications including tissue engineering. The polymer scaffold must be biodegradable to ensure the gradual replacement of the scaffold with new tissue as well as to distribute growth factors or nutrients to the target tissue. To support tissue formation for anchorage-dependant cells, polymer scaffold should provide a highly biocompatible surface to stimulate cell adhesion, migration, proliferation and differentiated function. Cell

adhesion to the polymer substrate is influenced by chemical structure and surface topography [Recum, 1999]. The surface morphology of a polymer scaffold is important because it directly interacts with the cell or the host. The surface of a polymer scaffold can be modified in various ways, such as by changing the chemical group functionality, surface charge and wettability. Some investigators have attempted to modify the surface to maximize cellular attachment by coating with a bioactive compound or peptide [Simon, 1999].

A significant amount of work has been done on identifying a suitable scaffold design for various applications which provide not only adequate sites for cellular attachment but also permit adequate diffusion of nutrients and gases. Biodegradable polymers have been synthesized into various shapes by using different fabrication methods for specific applications. Solid forms of polymeric biomaterials include hollow fiber, tube, film, membrane, disc, powder, bead, fiber, rod, and microsphere.

One of the widely used implantable materials for controlled release and tissue engineering is the microcapsule which has a core containing the active ingredient enveloped by a wall. Their size, core compositions, wall thickness and pore size can be controlled by the type of polymers and the processing environment. The suitable size of a microcapsule for encapsulation of cells is around 50-300 μm [Lim, 1984]. Youan et al. studied BSA protein release profiles of PLG and PCL oily core microcapsules with different degradation times [Youan, 2001].

To fabricate artificial scaffolds for cell growth, different researchers used different kinds of materials such as ceramics, metals, composites and polymers including both

biodegradable and non-degradable polymers. The following section will focus on polymers used for fabricating scaffolds in tissue engineering.

2.2. Biodegradable Polymers for Tissue Engineering

Biodegradable polymers have so far been classified into two main types: synthetic and natural polymers. Both possess their specific advantages and disadvantages.

2.2.1. Synthetic Biodegradable Polymers

Synthetic polymers have been used in tissue engineering because of their advantages such as ease of use, strength, durability, resistance to chemical and biological corrosion, and low production cost. They can be made into the required shape, surface area, wettability and porosity by controlling mechanical and physical properties. They can also be made easily into complex shapes and structures. However, they may produce undesirable biological responses such as poor cell attachment and growth. In addition, their degradation products may be toxic to the host. For instance, Poly(α-hydroxy acids), specifically poly(lactic acid) (PLA), poly(glycolic acid) (PGA) and their copolymer (PLGA) were the most widely used synthetic aliphatic polyesters in medical applications since the 1970s. They were used clinically due to their high purity, convenient processing and good mechanical properties. In addition, their biodegradability can be controlled by changing their molecular weight and copolymer compositions.

2.2.2. Natural Biodegradable Polymers

To overcome the lack of intrinsic biological activity of synthetic polymers, natural biodegradable polymers were used. They possess specific biological property such as

good biocompatibility. Another advantage is that the degradation products are non-toxic which are then transformed into carbon dioxide and water over a period of time. They are normally enzymatically degradable, possessing various degradation rates. On the other hand, limited control over molecular weight, the potential for unfavorable immunological responses and poor mechanical properties are the disadvantages of natural based polymers. Some examples of natural polymers used for tissue engineering scaffolds are collagen, polysaccharides, alginate, chitosan, glycosaminoglycan and hyaluronic acid.

Among them, collagen scaffolds have been produced in the forms of sponges, woven and non-woven meshes, gels and porous composites. They have been successfully utilized as skin, cartilage and nerve regeneration. Another type of natural polymer is polysaccharides, which are polymers of five-carbon (pentose) or six-carbon (hexose) sugar molecules. They have been widely used in tissue engineering because most of them are biodegradable, hydrophilic and non-toxic. They possess high molecular weights and extended chain configurations that enhances highly viscous gel formation. An example is chitosan, a partially or fully deacetylated derivative of chitin. The primary source of chitosan is shells from crab, shrimp, and lobster. It is the most promising polysaccharide because of its excellent ability to be processed into porous structure. It is hydrolyzed enzymatically *in vivo*. Chitosans have been investigated as woven and non-woven fiber-based structural materials. Glycosaminoglycan is also a polysaccharide that occurs within the extracellular matrix (ECM) of most animals. A third type of natural polymer, hyaluronic acid has high molecular weight and gel-forming ability and has been used in wound healing. Catapano et al. reported that the primary hepatocytes cultured in non-woven fabrics of the hyaluronic acid esters

retained liver-specific functions such as urea synthesis and ammonia elimination for longer-term than on collagen films [Catapano, 2001].

The last example is microbial polyester, natural aliphatic polyester such as PHB and PHBV which have been attractive for a wide range of environmental industries, such as agriculture, marine and packaging. More recently, they have been attractive for medical applications because of their biodegradability, biocompatibility and non-cytotoxicity. These natural polymers have better biocompatibility compared with synthetic polymers but they are more difficult to prepare in a controlled manner [Brown, 2002].

2.2.3. PHA, PHB and PHBV

2.2.3.1. PHA

Poly(hydroxyalkanoic acids) (PHA) are thermoplastic, aliphatic, biodegradable polyesters produced as a storage compound for carbon and energy by many bacterial species when an excess carbon source is present. Different block copolymer of PHA can be formed by changing different carbon sources. PHAs are found in the cytoplasm of cells in the form of inclusion bodies or granules. Of the bacterially synthesized polyesters, PHA has been most widely used in medical applications.

In general, polyesters can be classified into two types, poly(α-esters) such as PLA, PGA, PLGA and poly(β-esters) such as PHB, PHBV, and PHBHHx. The repeat units that make up poly(β-esters) are all in the [R]-configuration which results in isotactic polyesters [Ashby, 1997]. The bacteria can be synthesized and their growth conditions control the chemical composition and molecular weight of PHA (2×10^5 to 3×10^6

Da) [Lee, 1996]. More than a hundred different PHAs consisting of different monomers, such as straight, branched, saturated, unsaturated and aromatic, have been found. PHA is produced industrially by hypochlorite extraction, centrifugation, cross-flow filtration and flocculation [Zinn, 2001].

PHA received particular interest in the medical field since it was reported as a polymer having good biodegradability and biocompatibility. Because of this interest, PHA was widely studied and found to be in the cell envelope of eukaryotes [Reusch, 2000]. Therefore, PHA represents a class of polymers that has immense potential for medical applications that include sutures, surgical meshes, swabs, trileaflet heart valves [Sodian, 2000], cardiovascular fabrics, pericardial patches, vascular grafts, spinal cages, bone graft substitutes, meniscus regeneration, internal fixation devices (e.g. screws) and urological stents.

2.2.3.2. PHB and PHBV

PHB and PHBV are the most well known and useful polymers of the poly(β-esters) family. A number of studies have shown that PHB and PHBV appear to be a suitable material to serve as a substrate in tissue engineering [Sodian, 2000 and Köse, 2003 and Nebe, 2001]. A study by Nebe et al. showed that the material had no cytotoxic effect, with the cells attaching to the material and proliferating. PHB is a stereoregular, linear, head-to-tail polymer of β-hydroxybutyric acid. The empirical formula of PHB is $(C_4H_6O_2)_n$. The molecular structures of PHB and PHV are shown in figure 2.1.

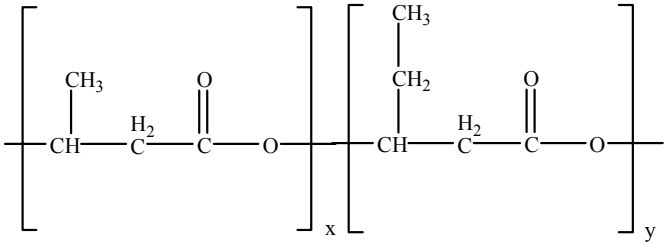

(a) (b)

Fig. 2.1. Repeating molecular structure of PHBV: (a) PHB and (b) PHV.

PHB was described in the microbiological literature since 1901 [Sharp, 1985]. Maurice Lemoigne from the Institut Pasteur was the first scientist who observed granule-like inclusions in the cytoplasm fluid of bacteria in 1925. PHB was produced and stored inside the bacterial cell walls in granules. *Alcaligenes eutrophus*, which was the first bacteria used for the industrial production of PHB, could accumulate large quantities of PHB as discrete intercellular granules by careful control of the fermentation process, i.e., up to 80% of the weight of the dried cell can be in the form of PHB granules. PHB was recovered from the cell by various procedures such as solvent extraction. The resulting PHB materials are highly crystalline thermoplastic with several characteristics, such as melting point, degree of crystallinity and glass-rubber transition temperature are comparable to those of isotactic polypropylene (PP). However, PHB is stiffer, more brittle and more crystalline than PP.

Many papers have showed that PHB is a polymer with excellent biocompatibility, having a lack of toxicity [Saito, 1991], and compatibility in contact with tissue [Doyle, 1991] and blood [Malm, 1994]. For these reasons, PHB has been widely used in biomedical applications including controlled drug release. However, the most serious disadvantage of PHB is its increasing brittleness with time, and its processing temperature range is limited compared to polyethylene and isotactic polypropylene. Moreover, the production cost of PHB (approximately £8000 per ton) is more than ten

times higher than that of PVC, PP (approximately £500 per ton) and HDPE (approximately £600 per ton) [Amass, 1998]. This high brittleness and high production cost of PHB thus limits its applications. Currently there are two possible ways to improve thermal processability and mechanical properties of PHB, i.e., copolymerization of PHB with other monomers and blending of PHB with other polymeric materials.

In 1952, Kepes and Péaud Lenoël observed that Lenoigne's isolated polyester was high molecular weight linear polyester [Kepes, 1952]. Williamson and Wilkinson were the first to report the molecular weight and physical properties of PHB [Williamson and Wilkinson, 1958]. In the 1950s, Baptist and Werber produced pound quantities of PHB and obtained a patent of the production and isolation processes [Hocking and Marchessault, 1994]. In 1968, ICI in the UK produced PHB by single cell protein technology for animal feed. In the 1970s, ICI produced PHB commercially from the bacterium *Alcaligenes eutrophus* based on a two-stage batch reactor. Another kind of micro-organism used to produce PHB was *Pseudomonas oleovorans*. Peter King published ICI's work on PHB in 1981 [King, 1982].

In 1985, ICI first commercialized and patented the production procedure of poly(3-hydroxybutyrate-*co*-3-hydroxyvalerate) (PHBV) with the trade name *'Biopol'* by *Alcaligenes eutrophus*. Biopol is now produced commercially by Monsanto. The empirical formula of PHBV is $(C_5H_8O_2)_m$. PHBV was produced by fermentation with a high yield, comparable to those of PHB. The physical properties of PHBV can be controlled by varying the composition of the copolymers. The range of HV mole fractions can be varied from 0 to 100%. The properties of PHB can be greatly

improved by increasing the concentration of PHV. For example, T_g, T_m and crystallinity decrease with increasing PHV composition.

Polymer scaffolds for tissue engineering should have suitable mechanical properties which determine the usefulness of the scaffolds. Increasing PHV content affects the mechanical properties of PHBV copolymers such as (i) reducing Young's modulus and tensile strength, (ii) increasing toughness and notched Izod impact strength, and (iii) improving flexibility of the copolymers. PHB has a variety of mechanical properties comparable to synthetically produced degradable polyesters such as polylactides. Several groups have attempted to improve the mechanical properties of PHB polymer by two-step drawing and annealing [Aoyagi, 2003], or by the addition of plasticizers [Savenkova, 2000]. In addition, fillers were used to reduce the price and plasticizers were used to improve flexibility of the polymer [Amass, 1998].

Various parameters that can affect the degradation of the polymers include size, shape, surface to volume ratio, porosity, diffusion of water into polymer bulk, copolymer composition, molecular weight, molecular weight distribution, hydrophilicity and hydrophobicity, crystallinity and amorphous state, T_g, process of chain cleavage, chemical structure or composition, degradation rate of polymer backbone, pH, solvent used, speed of solvent removal, and stirring rate [Anderson and Shive, 1997, Göpferich, 1997, Kiss and Vargha-Butlaer, 1999, Peppas and Langer, 1994 and Vert, 1984]. Degradability of PHB and PHBV polymers has been found to vary widely with their comonomer compositions. The degradation rate of PHB and PHBV polymer can also be changed with modification of end group, pH of buffer solution, degree of crystallinity, molecular weight, surface area, HV content in the copolymer and

blending of two or more polymers. The degradation processes can be broadly classified into two types: chemical (acid or base catalyzed hydrolytic degradation and oxidation degradation) and biological (degradation by microorganisms or enzymes catalyzed degradation or both). In this research, hydrolytic degradation of the PHB and PHBV microspheres were studied for one year period. During hydrolytic degradation, water diffused into the microspheres through the porous cavities and initiated random hydrolytic chain scission of the ester bond in the polymer backbone, resulting in the formation monomeric hydroxyacid.

2.2.4. Miscible and Immiscible Polymers with PHB and PHBV

In order to reduce production cost and brittleness, PHB or PHBV was blended with two or more polymers. Blending with other degradable polymer causes higher flexibility and elongation at break [Dufresne and Vincendon, 2000]. Miscibility, immiscibility and properties of the blends depend on the glass transition and the composition of PHB or PHBV, which can be measured by thermal or mechanical testing. Many papers have been published about different polymers that could or could not be blended with PHB or PHBV. Non-biodegradable natural cellulose esters such as cellulose acetate butyrate (CAB) and cellulose acetate propionate (CAP) could be blended with up to 50% of PHB or PHBV, as Scandola et al. found in 1992 [Scandola, 1992]. Synthetic non-biodegradable polymers which have been found to be blended with PHB and PHBV include poly(vinyl acetate) (PVAc) [Greco and Martuscelli, 1989], poly(vinyl chloride) (PVC) [Dave, 1990], poly(vinyl phenol) [Iriondo, 2000], poly(epichloro-hydrin) (PECH) [Paglia, 1993], poly(methyleneoxide) (PMO) [Avella, 1997], low-density polyethylene (LDPE) [O'lkhov, 2000] and poly(vinyl alcohol) (PVA) [Azuma, 1992]. Miscible synthetic biodegradable polymers include

poly(ethylene oxide) (PEO) [Avella and Martuscelli, 1998], poly(L-lactide) (PLLA) [Blumm and Owen, 1995] and poly(D,L-lactide) (PLA) [Zhang, 1996]. Poly(methyl methacrylate) (PMMA) was immiscible with PHB at room temperature, however, it is miscible in the melt state [Lotti, 1993]. Cao et al. blended P(3HB) and chemically synthesized poly(3-hydroxypropionic acid) (P(3HP)) by solvent casting [Cao, 1998]. Conversely, poly(ε-caprolactone) (PCL) [Shuai, 2001], poly(γ-benzyl-L-glutamate) (PBLG) [Deng, 2001], ethylene-propylene rubber (EPR), poly(ethylene-co-vinyl acetate) (EVA), poly(l,4-butylene adipate) (PBA) [Kim, 1999] and poly(cyclohexyl methacrylate) (PCHMA) [Lotti, 1993] are immiscible with PHB.

2.2.5. Other Uses of PHB and PHBV

Besides medical applications, PHB and PHBV have been used in the packaging industry, automobile industry and agricultural industry. The first commercial product made of PHBV was introduced in the market as injection blow molded hair shampoo bottles in Germany by Wella AG, Darmstadt in 1990 [Amass, 1998]. PHB packaging film is five times less permeable to CO_2 than that of poly(ethylene terephthalate) (PET) and is as strong as PP film, but not as tough as PET film. By addition of glass fiber filling [King, 1982], PHB can be strengthened to be similar to nylon. Other potential assets of PHB and PHBV were motor oil containers, paper coating materials, sanitary napkins and diapers. PHBV has been used in agricultural applications as controlled release of pesticides and fertilizers. Holmes reported that PHBV was suitably used for the release of insecticide into soil [Holmes, 1985]. Scherzer reported that PHBV has excellent gas barrier properties. In particular, PHBV membrane has extremely low oxygen permeability [Scherzer, 1997].

2.3. Applications of PHB and PHBV in Tissue Engineering

Besides being biodegradable, both PHB and PHBV and their degradable products have shown to be biocompatible and non-toxic. For these reasons, they have been evaluated for various medical applications. Uses in such applications include controlled release, wound dressing, surgical implants, biomaterials for tissue engineering and other medical purposes.

Many papers have reported the use of PHA micro- and nanospheres as drug carriers for anticancer therapy. Kassab et al. fabricated rifampicin loaded PHB microspheres for chemoembolization. They reported that the drug release rate could be controlled by the drug loading and the size of the microspheres [Kassab, 1997]. Sendil et al. made a similar study. They compared the tetracycline antibiotic release in PHBV microspheres with 7, 14 and 22% PHV contents and encapsulation efficiencies. However, they did not focus on degradation of the microspheres because the drug release was completed before degradation occurred [Sendil, 1999]. Doyle et al. scrutinized that PHB scaffolds did not provoke chronic inflammatory response after implantation in rabbits up to 12 months [Doyle, 1991]. Malm et al. observed that PHB patches assembled as atrial septal walls in calves and the patches degraded 12 months after implantation under optical microscope [Malm, 1992]. Malm et al. have also reported the implantation of PHB non-woven patches into the right ventricular outflow tract and pulmonary artery of weanling sheep in 1994, and they reported that there were no aneurysms for up to 2 years [Malm, 1994].

The results reported by Kostopoulos and Karring in 1994 showed that the mandible bone of rats filled on PHB membrane after 6 months, but only 40% of bone filled on

control without PHB regeneration in rats [Kostopoulos and Karring, 1994]. Another study of bone healing was also carried out in 1994 by Gotfredsen et al. It was reported that an inflammatory reaction and less marginal bone healing were found by using PHBV membrane reinforced with polyglactin 910 [Gotfredsen, 1994]. Köse et al. modified PHBV(8%) foams with sucrose by oxygen plasma treatment to improve the hydrophilicity of the surface for the seeding of stromal fibroblasts [Köse, 2003].

Gogolewski et al. (1993) monitored the comparison of cell responses such as acute inflammation and tissue necrosis for PLGA, PHB and PHBV in mice up to six months. They concluded from their analysis that there were no signs of abscess formation on all of the polyesters and the extent of tissue response was the same for all. However, PLGA was found to degrade faster than PHBV *in vivo* [Gogolewski, 1993].

According to Rivard et al., protein production of isolated fibroblasts on PHBV sponges was twice as high as that on collagen sponges [Rivard, 1995]. Hu et al. compared the biocompatibility of PHBV(5%) membrane grafted with hyaluronic acid (HA) and chitosan (CS) using L-929 fibroblasts. They reported that PHBV-HA had high cell proliferation and low cell attachment, meanwhile, PHBV-CS showed low cell proliferation and high cell attachment [Hu, 2003]. Duvernoy et al. evaluated PHB as pericardial substitutes [Duvernoy, 1995]. Saad et al. studied the cell response of mouse macrophages, primary rat peritoneal macrophages and mouse fibroblasts (3T3) cultured on short chain PHB block copolymer [Saad, 1996].

PHBV strips deployed on stents implanted in porcine coronary arteries induced inflammatory responses after one month implantation, while PLGA strips evoked less

responses. *In vivo* observations were not found to be expected from *in vitro* preliminary tests. The possible reasons could be due to polymer biodegradation products and implantation conditions, as Giesssen et al. pointed out [Giessen, 1996].

In conclusion, the PHB and PHBV are biodegradable, biocompatible and non-cytotoxic, and therefore they can be considered as potential candidates for tissue engineering. In addition, they have been proven to support cell growth and proliferation. However, PHB and PHBV microspherical scaffolds has yet to be studied for liver cell growth. In this research, the PHB and PHBV microspheres were fabricated by o/w single emulsion solvent evaporation technique as artificial three-dimensional scaffolds for human hepatoma cell line, Hep3B, growth. The fabrication of porous three-dimensional microspheres is not only to optimize cell viability and growth, but also to tailor these scaffolds for specific tissue engineering applications. Hep3B was used in this work because it could be considered as a potential source of the cell for tissue engineering as it exhibit higher growth rate and it is easily obtainable. In addition, the *in-vitro* experiments are usually easy, fast and less expensive than those of *in-vivo*. For these reasons, Hep3B cells were cultured onto the PHB and PHBV scaffolds *in vitro* which were designed as temporary scaffolds to guide the growth and promote the proliferation of the cells. The concept of using biodegradable polymer microspheres as scaffolds for liver cell growth is believed to provide an innovative approach in liver tissue engineering.

Chapter 3

Materials and Methods

3.1. Materials

Poly(3-hydroxybutyrate) (PHB) homopolymer and poly(3-hydroxybutyrate-*co*-3-hydroxyvalerate) copolymers with three different PHV contents (5, 8 and 12%) such as PHBV(5%), PHBV(8%) and PHBV(12%) were purchased from Aldrich Chemical Co., USA.

3.2. Preparation of Scaffolds

3.2.1. Fabrication of Microspheres

The PHB and PHBV microspheres were prepared as 3D scaffolds by using an oil-in-water (o/w) emulsion solvent evaporation technique as described by Yang et al. [Yang, 2000]. Briefly, an initial weight (P_i) of 0.6 g of polymer powder was first dissolved in 12 mL of chloroform (GR grade, EM Science, USA) under vigorous stirring in a water bath maintained at 60ºC. Then, 1mL of the first aqueous volume, phosphate-buffered saline (PBS) (pH 7.4, Sigma) with 0.05 w/v% poly(vinyl alcohol) (PVA) (80 mol% hydrolyzed, average M_w 6000, Polysciences) was added to 10 mL of the polymer-organic solvent solution. Emulsification was subsequently carried out using a homogenizer (T25B, Ika Labortechnik, Germany) at 16000 rpm for 15 s. The homogenized mixture was immediately poured into a bulk solution of 300 mL PBS with 0.05 w/v% PVA, the second aqueous volume. The solution was then placed under

continuous mechanical stirring (RW20, Ika Labortechnik, Germany) at 300 rpm for 3 h to evaporate the organic solvent. The temperature was maintained at 38ºC with a magnetic hotplate stirrer (Cimarec Thermolync) throughout the evaporation phase. The fabrication process of the microspheres is shown in Fig. 3.1.

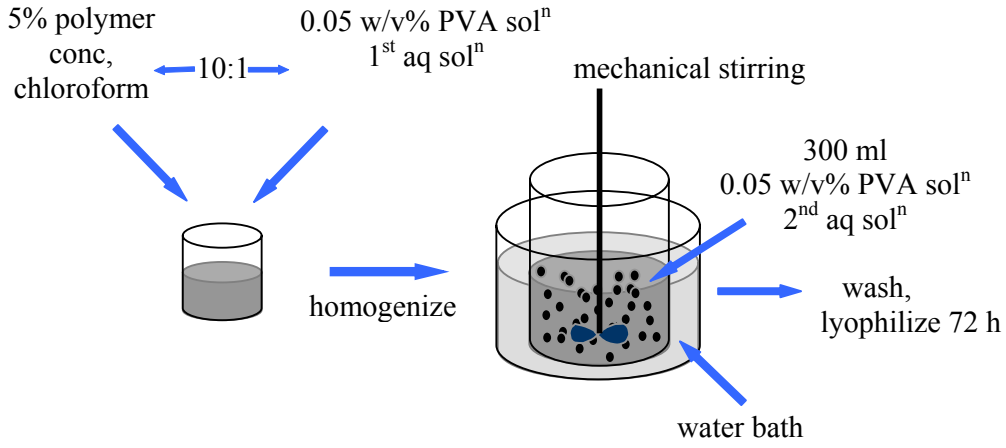

Fig. 3.1. The fabrication processes of the PHB and PHBV microspheres by an oil-in-water (o/w) emulsion solvent evaporation technique.

The resulting microspheres were washed with deionized water at least 5 times, collected into a glass vial and weighed by using an analytical balance (Mettler Toledo, AB 204-S, Switzerland). They were then frozen in liquid nitrogen (–196ºC) for 1 min and placed in a lyophilizer (Martin Christ Laboratory Freeze Dryer Alpha 1-4) for 7 days to remove any remaining solvent and to get a constant weight of dried microspheres, *P*.

The yield percent of the produced microspheres was approximately 70-80% which can be calculated by the following equation:

$$\%Yield = \frac{P}{P_i} \times 100 \qquad (3.1)$$

where,

P = dry polymer weight (mg)

P_i = initial weight of polymer powder (mg)

3.2.2. Preparation of Thin Films

Polymer thin films were prepared as 2D scaffolds in comparison with 3D microspheres for liver cell growth and proliferation, to evaluate liver specific functions, as well as to examine hydrophilicity and cytotoxicity of the films. Briefly, 0.6 g of polymer powder was first dissolved in 12 mL of chloroform under vigourous stirring in a water bath at 60ºC for 5 min. The polymer solution was poured into a 50 mm glass Petri dish and dried under a fume hood overnight to obtain polymer thin films with 200 μm thickness. The resulting polymer films were lyophilized in the freeze drier for 7 days to remove any remaining solvent.

3.3. Polymer Characterizations

Polymer characterizations involve precise measurements of the polymers to analyze their physical and chemical properties. The PHB and PHBV microspheres and thin films were characterized by Coulter particle size analyzer, SEM, water contact angle, GPC, DSC, ^{1}H-NMR, XPS and FTIR.

3.3.1. Particle Size Analysis

The cells attachment on the microspheres was believed to depend on the size of the microsphere scaffolds, and hence, the microspheres were produced with the aim of detaining uniform size and the sizes measured by a particle size analyzer. Briefly, 15 mL of the microspheres were re-dispersed in deionised water and the size distributions

of the microspheres were determined using a Coulter particle size analyzer (Coulter LS 230, USA). Tween® 80 (Polyoxyethylene-sorbitan monooleate) (Aldrich) was used as a surfactant in the process and the mixture was sonified using an ultrasonic sonicator (Ultrasonic LC20H).

3.3.2. SEM Observations

The external surface textures and internal morphologies of the microspheres before and after *in vitro* degradation were observed using a scanning electron microscope (SEM) (JEOL, JSM-5600VL). To observe internal cross-sectioned SEM images, samples were sectioned with a cryostat (Leica CM3050) using a tissue freezing medium and razor blade (set at 100 μm cut). The microspheres and cross-sectioned samples were mounted onto brass stubs using double-sided adhesive tape and vacuum-coated twice with a thin layer of platinum using the Auto Fine coater (JEOL, JFC-1300) for 40 s prior to examination.

3.3.3. Contact Angle Measurement

Hydrophilicity and hydrophobicity of the polymer films were measured by a static water contact angle (First Ten Angstrom, FTA 100 series, Virginia, USA) and drop shape analysis software version 1.96. To measure wettability, the polymer thin films were made as mentioned in section 3.2.2. A water droplet was placed on the surface of the polymer thin film and its dispersion depended on the hydrophobicity of the polymer. For each film, at least five measurements on different surface locations were averaged.

3.3.4. Gel Permeation Chromatography (GPC) Analysis

The molecular weight of a polymer plays an important role in determining the characteristics of polymer degradation. Hence, the number- and weight-average molecular weights (M_n and M_w) and polydispersity (M_w/M_n) of the polymer microspheres before and after *in vitro* degradation were determined using gel permeation chromatography (GPC) or size exclusion chromatography (SEC) (Agilent Technology 1100 series, part number 79911GP-MXC, Germany, Isocratic pump, Chemstation software) with a Refractive index detector (RI-G1362A), and an Aligent Technologies PLgel Mixed-C column (79911GP-MXC) (300 × 7.5 mm, 5 μm) (M_w range 200 to 3 millions). Briefly, 3 mg of the microspheres was dissolved in 1 mL of HPLC grade chloroform (Fluka) and the polymer solution was filtered with 0.47 μm PTFE syringe filter (25 mm diameter, Alpha Analytical). Then 30 μL of the polymer solution were injected for analysis. The mobile phase was HPLC grade chloroform at a flow rate of 1 mL/min at 30ºC. The calibration was carried out using polystyrene standards with narrow molecular weight distribution.

3.3.5. Differential Scanning Calorimetry (DSC) Measurement

Thermal analysis of polymer microspheres was examined using a Mettler oscillating differential scanning calorimeter (DSC 822e, STARe software, USA). Briefly, 2-3 mg of microspheres was put in a sealed aluminum pan. An empty pan with lid was used as a reference. The pans were hermetically sealed to prevent water evaporation during scanning. After calibration with indium, specimens were scanned from –100ºC to 200ºC at a heating rate of 10ºC/min, using nitrogen as a purge gas at 10 ml/min. After being held at 200ºC for 1 min, the specimens were cooled down to –100ºC at a cooling

rate of 10ºC/min. Melting temperature, T_m, was taken as the onset of the melting peak. A non-isothermal crystallization temperature, T_c, was obtained from the cooling process.

3.3.6. Proton-Nuclear Magnetic Resonance (^{1}H-NMR) Analysis

^{1}H-NMR spectra of the PHB and PHBV microspheres were carried out not only to determine their chemical structures but also to confirm the degradation mechanism of the microspheres by GPC and DSC. Briefly, 5 mg of microsphere was dissolved in 2 mL of deuterated chloroform ($CDCl_3$) (99.9 atom %D, Aldrich). Polymer solution was then filtered with 0.47 μm PTFE syringe filter (25 mm diameter, Alpha Analytical) before being transferred into an NMR tube. The ^{1}H-NMR experiments were performed on a Bruker Avance 400 spectrometer (400 MHz) and chloroform-d was used as a solvent. Chemical shifts were expressed in parts per million (δ) using residual protons in the indicated solvent as the internal standard.

3.3.7. X-ray Photoelectron Spectroscopy (XPS) Analysis

X-ray photoelectron spectroscopy (XPS) was used to investigate the surface chemical compositions of the polymer microspheres. XPS spectra were analyzed using a Kratos AXIS HSi XPS spectrometer (Kratos Analytical, UK) with a monochromatic Aluminium K-α x-ray source. The spectra were processed and quantified using the Kratos software provided with the instrument.

3.3.8. Fourier Transform Infrared (FTIR) Examination

Fourier transform infrared (FTIR) spectroscopy was employed to determine the chemical structure (functional groups) of the polymer microspheres. Briefly, 200 mg

of KBr powder (FTIR grade) and 2 mg of polymer microspheres were mixed and ground in a mortar and pestle. They were then compressed into pellets under a pressure of 10,000 kg/in^{-2} for 10 min prior for IR examination. A blank KBr pellet was used as a standard. FTIR spectra were collected on a Fourier Transform infrared spectrometer (Excalibur Series, BioRad Laboratories, FTS 135, USA). The IR frequency range of interest is 4000 cm^{-1} to 400 cm^{-1}.

3.4. Degradation of Microspheres

To determine the degradation mechanism of the PHB and PHBV microspheres, i*n vitro* hydrolytic degradation was carried out over a one year period. Briefly, 20 mg of dried microspheres were dispersed in 10 mL PBS buffer solution (pH 7.4) at 37ºC in a 12 mL glass vial. The buffer solution was changed with fresh PBS buffer solution twice a week to maintain pH of the medium at 7.4. The microspheres were periodically taken out when they were allowed to degrade to various time points. At each time point, the supernatant from each sample was removed and polymer microspheres were washed with deionized water at least 5 times to remove water soluble low molecular weight degraded species. Then they were frozen in liquid nitrogen for 1 min and lyophilized for 7 days to remove remaining solvent and to obtain a constant weight. After lyophilization, the samples were stored at 4ºC for further analysis.

3.4.1. Mass Loss Analysis

In vitro degradation of the microspheres was evaluated by measuring mass loss and molecular weight loss at each time point. Mass loss of microspheres was measured by an analytical microbalance (Mettler Toledo, AB 204-S, Switzerland).

3.5. Liver Cell Culture on Polymer Scaffolds

3.5.1. Preparation of the Controls

For liver cell culture, positive control, negative control, polymer thin films and microspheres were prepared prior to culture. To prepare a positive control, a glass coverslip (22 × 22 × 0.16 mm, Superior Marienfeld, Germany) was rinsed with detergent and deionized water, and then air-dried. The coverslip was put into a 30 mm glass Petri dish and exposed to UV 1 h prior to plating. Subsequently, the coverslip was coated with 1 mL of 1 mg/mL poly(L-lysine) aqueous solution (PLL; Sigma, MW = 37000 g/mol) for 3 days at room temperature on an automatic shaker at 100 rpm. Then, 20 μL of a 1 mg/mL aqueous solution of laminin (Invitrogen) was added and incubated for 12 h at 37ºC. Polyurethane film containing 0.1% zinc diethyldithio-carbamate (ZDBC) was used as a negative control for Hep3B culture. Both controls were then sterilized by irradiation under UV overnight and washed three times each with 70% ethanol, sterilized deionized water, and sterilized PBS solution and immersed in culture medium for 10 min just before use. The polymer thin films prepared as in section 3.2.2 were cut into circular shape with a 19 mm diameter using a cork borer. The controls, thin films and microspheres were sterilized by UV irradiation overnight and washed three times each with 70% ethanol, sterilized deionized water, and sterilized PBS solution and immersed in culture medium for 10 min just before use.

3.5.2. Preparation of Cell Culture Medium

Fetal Bovine Serum (FBS) (Gibco) was inactivated in a water bath at 56ºC for 30 min. Then, the cell culture medium was prepared with Dulbecco's modified Eagle's

medium (DMEM) supplemented with 10% of the FBS, 2 mM L-glutamine (Sigma), 55 mg sodium pyruvate (Sigma) and 1% antibiotic antimycotic solution (100 units/mL penicillin G, 100 μg/mL streptomycin sulfate, and 0.25 μg/mL amphotericin B) (Gibco). The cell culture medium was changed every 3 days to reduce the effects of the polymer degradation products and to ensure sufficient nutrient supply.

3.5.3. Human Hepatoma Cell Line (Hep3B)

Human hepatoma cell line (Hep3B, ATCC) was obtained from Cell Resource Center for Biomedical Research, Institute of Development, Aging and Cancer, Tohoku University. Hep3B cell lines were used because their proliferation rate is high and they biologically represent human primary hepatocytes.

3.5.4. Cell Culture

For the cell culture of Hep3B cells, frozen cells stored in liquid nitrogen were thawed in a water bath at 37ºC for 30 s and mixed gently with growth medium. They were then centrifuged at 1500 g for 5 min to remove cryopreservatives and cultured in a T25 cell culture flask for 24-48 h.

Cell proliferation was observed with an inverted microscope and the cells were subcultured after reaching approximately 90% confluence. Briefly, 2 mL of sterilized PBS solution was added into a T25 polystyrene cell culture flask, shaken gently and discarded. Then, 2 mL of trypsin/EDTA (ethylenediaminetetra-acetic acid) solution (0.25% trypsin/0.02% EDTA, Gibco) was added to the flask, gently shaken to detach the cells, and the solution was aspirated. The cells were incubated in an incubator at 37ºC for 2-3 min. When the cells were detached from the flask, 4 mL of fresh medium

was put into the flask. The suspension of the cells was removed through gentle pipetting. The suspension medium was transferred into a 15 mL centrifuge tube and centrifuged at 1500 rpm for 5 min at room temperature. After centrifugation, almost all of the supernatant was aspirated. Then, 5 mL of fresh medium was added into the conical tube and triturated to create a uniform cell suspension. Then, the cell suspension was put into a new T25 flask. The culture medium was renewed every 3 days.

When there were excess cells, they were frozen and kept for future experiments. The excess cells were sedimented by centrifugation to form a pellet and the medium was decanted. Then, the cells were stored in the freezing medium, serum supplemented growth medium containing a cryopreservative, and 10% dimethylsulphoxide (DMSO) which protects the cells from disruption during the freezing and thawing process. After gentle mixing, the cell suspension was placed in a 1 mL cryotube and labeled with the name of the cell line, the number of cells per vial, and the freezing date. The concentration of the freezing cells was about 1×10^7 cells/mL. Then the cryotube was frozen in a polystyrene box with the freezing rate of lºC/min for 4 h and –80ºC (Ultra low temperature freezer, Nuaire, NU-6580) for overnight before placing in liquid nitrogen for long-term storage.

3.5.5. Cell Seeding on Polymer Scaffolds

For the microspheres, a cell density of 1×10^5 cells/mL of Hep3B immersed in 2 mL of culture medium was put into a 15 mL conical tube with the sterile microspheres and shaken gently for 10 min, allowing the cells to adhere onto the microspheres. Then the microspheres were transferred into a 30 mm diameter polystyrene Petri dish and

incubated in a 5% CO_2 incubator at 37ºC. For thin films and controls, the sterile films were put into 30 mm diameter polystyrene Petri dish, and then 1×10^5 cells/mL of Hep3B immersed in 2 mL of culture medium was put into the Petri dish and incubated in a 5% CO_2 incubator at 37ºC. Cell adhesion, growth and proliferation on the scaffolds were studied under an optical microscope, SEM and LSCM at various time points.

3.5.6. Fixation of the Cells for SEM

To fix the cells under SEM, attached cells on the polymer scaffolds were rinsed twice with PBS solution and fixed with 4% glutaraldehyde for 48 h. Then, the sample was washed twice with PBS solution and dehydration was accomplished using a graded series of ethanol (50%, 60%, 70%, 80%, 90%, and 100%, twice). The polymer scaffolds were air dried overnight, mounted onto an aluminum stub and sputter-coated with platinum for 40 s before viewing under SEM.

3.5.7. Live/Dead Assay for Laser Scanning Confocal Micrograph

To examine Hep3B cells under laser scanning confocal microscope (LSCM), live/dead assay was evaluated. The basis for this test is differential permeability of live and dead cells to green florescent and red fluorescent stains. Live-dead solution was prepared by adding 20 μL of green florescent SYTO® 10 nucleic acid stain (Molecular Probes) and 10 μL of red fluorescent DEAD Red™ (ethidium homodimer-2, Molecular Probes) in 10 mL of sterile PBS solution and shaken for 15 min using a vortex mixer.

The Hep3B cells were cultured on a 4-chambered cover glass (Lab-tek) with the seeding density of 2×10^3 cells/mL. The old culture medium was replaced with fresh

medium and 100 μL of live/dead solution was added into the medium, and kept in the dark for 1 h at room temperature. A confocal micrograph was obtained by using a laser scanning confocal microscope (Leica, DM-IRE 2). The florescent green-colored cells were live cells while the florescent red-colored cells were dead cells. The stock solution was kept in the dark in the fridge for further use.

3.6. Cell Viability Tests

3.6.1. Haemocytometer Cell Counting

The viable cells were counted by haemocytometer during cell culture (Hausser Scientific, USA). Briefly, 100 μL of the cell suspension was pipetted out and put into a 1 mL cryotube and mixed with 100 μL 0.4% trypan blue solution (Sigma) which stained dead cells blue while leaving live ones unstained (colorless). Then, 20 μL of the mixed solution was placed on a haemocytometer and only the live cells were counted under an optical microscope. The total number of the cells present in the medium was calculated as the average cell counts/1 $mm^2 \times 2 \times 10^4 \times$ mL of cell suspension medium. The amount of fresh medium was calculated to dilute the cell suspension to get the required cell density.

The cell viability was calculated by the following equation:

$$\text{Cell viability \%} = \frac{\text{total number of cells - number of blue cells}}{\text{total number of cells}} \times 100 \qquad (3.2)$$

3.6.2. [3-(4,5-dimethylthiazol-2-yl)-2-yl]-diphenyltetrazolium bromide] MTT Assay

Cell proliferation was assessed using methylthiazol tetrazolium (MTT) assay. The MTT assay is based on the cleavage of a water-soluble yellow tetrazolium salt in metabolically active mitochondria to water-insoluble purple formazan crystals by the action of dehydrogenase enzymes. The amount of the formazan formation can be measured spectrophotometrically, where the absorbency measurement is directly proportional to the number of living cells. To prepare MTT solution, 5 mg of MTT (thiazolyl blue) powder (Numi Lab Supplies) was dissolved in 1 mL sterile PBS (pH 7.4) solution and shaken for 15 min by a vortex meter. The polymer scaffolds including controls, thin films and microspheres were sterilized in the same procedure described in section 3.5.1. Hep3B cells were cultured on the scaffolds with the seeding density of 5×10^4 cells/well/mL in a 12-well tissue culture plate. After reading 90% confluence, the original medium was aspirated, rinsed twice with 1 mL of sterilized PBS solution, and replaced with 1 mL of serum-free DMEM medium. Then, 100 μL of MTT/PBS solutions were added into the medium and incubated at 37ºC for 4 h. After MTT formazan formation, the culture medium and MTT were removed and rinsed twice with PBS solution. To dissolve insoluble formazan crystals, 1 mL of dimethyl sulfoxide (DMSO) was added to each well and mildly shaken for 15 min. Then, 1 mL of the above formazan solution was taken from each well and added to a new 12-well plate. Two parallel samples were prepared. The absorbencies of the samples were measured spectrophotometrically in a Microplate Reader (GENios, XFluor4 software) set at wavelengths 560 nm (test) and 620 nm (reference). DMSO was used as a blank.

3.6.2.1. Statistical Analysis

Data are presented as means ± SD of the mean. Statistical comparisons were performed using Students *t*-test. Statistical significance was set at $*p < 0.05$.

3.7. Direct Contact Cytotoxicity Test (ISO 10993-5)

There are three different types of cytotoxicity tests, consisting of the direct contact test, indirect contact test and extract test. Since all the polymer samples and controls were in solid state circular thin films (7mm dia) with flat surfaces, the direct contact cytotoxicity test was used in this study. This test evaluates both the qualitative and quantitative assessment of the cytotoxicity.

The cytotoxicity test was principally based on neutral red dye which penetrates the cell membranes and stains the lysosomes of the viable cells red. Therefore, the higher the viable cells, the more neutral red dye is taken in. However, if the cell membrane is damaged by any toxic substance caused by the scaffold, the cell cannot retain the neutral red dye. Hence, a bigger inhibition zone signifies the sample is more cytotoxic, while a smaller inhibition zone indicates the sample is less cytotoxic.

3.7.1. Mouse Fibroblast Cell Line (L-929) Culture

For cytotoxicity test, mouse fibroblast cell lines, L-929 cells (ATCC, CCL1, USA), were cultured in Dulbecco's modified Eagles medium (DMEM: Sigma) supplemented with 10% Fetal Bovine Serum (FBS) (Gibco), 1% non-essential amino acid solution (Sigma), 1% 10 mM Sodium Pyruvate (Sigma), 1% 2 mM L-Glutamine, and 1.5 g/L sodium bicarbonate solution, at a suspension density of 2.5×10^5 cells in 3 mL of media in a 50 mm plastic Petri dish. The Petri dish was shaken by gentle horizontal

rotation to distribute the cells evenly, and then left undisturbed at 37ºC and 5% CO_2 for two days to allow cells attachment.

3.7.2. Preparation of Materials

The polymer films were prepared by cutting with a cork borer to get circular shape films with fixed dimensions of 7 mm in diameter and 0.2 mm in height. In this test, the negative control means a control which does not produce a cytotoxic response while the positive control provides a reproducible cytotoxic response. The negative control was made from high density polyethylene (HDPE) with 2 mm thickness, and the positive control was made from polyurethane film containing 0.25% zinc dibutyldithiocarbamate (ZDBC) (Hatano Research Institute, Japan) with 0.5 mm thickness. The polymer films were washed with 70% ethanol and sterilized deionized water, followed by washing with PBS solution 5 times each. They were UV-sterilized overnight before use.

3.7.3. Preparation of Neutral Red (NR) Solution

The neutral red solution was prepared using neutral red dye. At each run the dye was diluted to a final concentration of 50 μg/mL in complete medium, 18-24 h before use to allow for precipitation of undissolved dye. Immediately before use, the dye-media was centrifuged at 1500 × g for 5min and the supernatant was used for the NR assay. NR solution was shielded by aluminum foil to protect from light and kept in the dark for further use.

3.7.4. Preparation of Formal-calcium Solution

Formal-calcium solution was prepared by dissolving 10 mL of 4% formaldehyde (Sigma) and 10 mL of 10% anhydrous calcium chloride into 80 mL of water.

3.7.5. Placement of the Specimens onto the Cell Surface

After the cells reached 80% confluency, the existing media was removed from the cells. The individual specimens were placed on the cell layer in the center of each Petri dish by using a sterilized forceps. Then, 1 mL of the fresh medium was carefully added to the top of the cell surface to cover exactly the monolayer of the cells. The cells were incubated at 37ºC and 5% CO_2 for 2 days.

3.7.6. Neutral Red (NR) Assay

The supernatants were removed. On the bottom of the culture dishes, the outline of the inhibition zones of the specimen were marked with a permanent marker and the specimens were removed. The monolayer cells were washed with PBS solution to remove any debris or dead cells. Then, 4 mL of medium containing 50 μg/mL NR solutions were added to each Petri dish to cover the cells. The cells were incubated for an additional 3 h at 37ºC in the dark. The dyes were removed and each well was washed rapidly with 4 mL of formal-calcium solution. This step was used to remove excess unincorporated NR and also to enhance attachment of cells to the substratum. Because fixation damages the lysosomes, the exposure time was limited to about 2-3 min. This step was carried out in the flow hood for protection from fumes. After removing the formal calcium solution, the Petri dishes were left to dry in the open air before quantitative analysis of any significant zone of inhibition around the biocomposites. Fig. 3.2 is a schematic diagram to describe the step by step procedures of the direct contact cytotoxicity test performed.

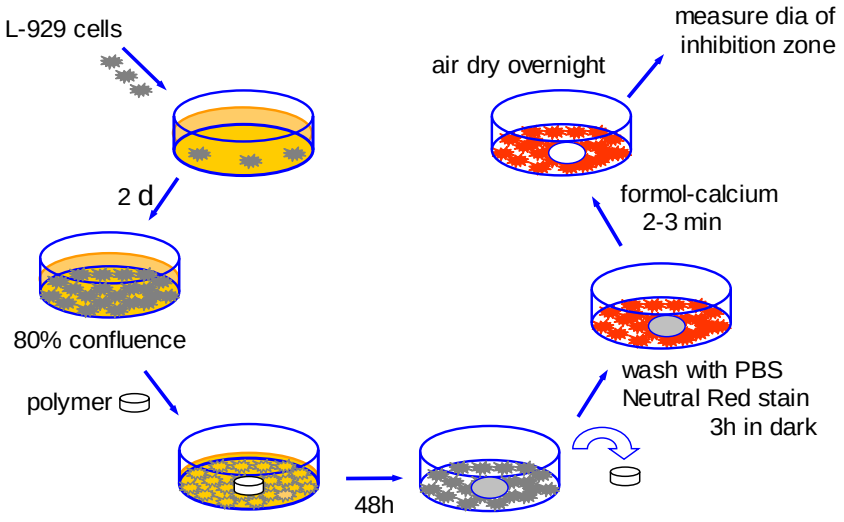

Fig. 3.2. Direct contact cytotoxicity test procedure using mouse fibroblast cell line (L-929).

3.7.6.1. Statistical Analysis

The results were taken as an average of five replicates. Data are presented as means ± SD. Statistical comparisons were performed using Students *t*-test. *p*-values < 0.01 were considered statistically significant.

3.8. Liver Cell Functionality Tests

3.8.1. EROD Assay for Cytochrome P-450 activity

Cytochrome P-450 (CYP-450) enzymes play an important role for detoxification in the liver. To measure P-450 activity of Hep3B, an ethoxyresorufin-*O*-deethylase (EROD) assay was used, adapted from a method described by Burke and Mayer [Burke and Mayer, 1975]. For this test, the polymer scaffolds including controls, thin films and microspheres were sterilized as previously mentioned in section 3.5.1. Hep3B cells were cultured on the scaffolds with the seeding density of 5×10^4 cells/well/mL in a 12-well tissue culture plate. After reaching 90% confluency, the original medium was

aspirated, and stored for albumin assay. The wells were washed twice with 1 mL sterilized PBS solution and incubated for 30 min in the dark at 37ºC in PBS containing 0.5 mL 5 µM 7-ethoxyresorufin and 0.5 mL 10 µM dicumarol (3,3'-methylene-bis(4-hydroxy-coumarin)) (Sigma). The fluorescence of the supernatant was measured using a microplate reader (GENios) at 535 nm excitation and 595 nm emission.

3.8.1.1. Statistical Analysis

The results were taken as an average of three replicates. Data are presented as means ± SD. Statistical comparisons were performed using Students *t*-test. Statistical significance was set at $*p < 0.05$.

3.8.2. Albumin Secretion Synthesis by ELISA

The albumin secretion of liver cells in the culture media was determined on 2, 4 and 6 days using enzyme-linked immunosorbent assay (ELISA) (Human albumin ELISA quantitation kit, Bethyl Laboratories, Inc., E80-129). There are three types of ELISA; direct ELISA, indirect ELISA and antibody-sandwich ELISA for detection of soluble antigens; the latter was chosen for use in this study. At various time points, the supernatant was aspirated from the wells and centrifuged at 15000 rpm for 5 min, filtered with 0.45 µm PTFE filter and stored at –20ºC until use. Calibrator or standard solution (human reference serum, RS10-110) was diluted in sample diluent from 10000 ng/mL to 6.25 ng/mL. Next, 96-well cell culture plates (Nunc) were coated with coating antibody (1 in 100 dilutions of coating antibody (goat anti-human albumin-affinity purified) and coating buffer (0.05 M sodium carbonate, pH 9.6), incubated for 1 h at room temperature in the dark, and washed three times with washing solution (0.05% Tween/saline, pH 8.0). Then, they were blocked by adding 200 µL blocking

(postcoat) solution (1% bovine serum albumin (BSA) in PBS) to each well, incubated for 30 min and washed three times with washing solution. Then, 100 µL of controls, samples and standard solutions were added into each well, incubated for 1 h and washed five times with Tween/saline. Plates were then incubated with a 1 in 70000 dilution of HRP detection antibody (goat anti-human albumin-HRP conjugate, A80-129P) and sample/conjugate diluent (0.05% Tween/saline, pH 8.0) for 1 h and washed five times with washing solution. Finally, 200 µL of [3,3',5',5-tetramethylbenzidine] (TMB) (Sigma) was added into each well and incubated for 1 h. A blue solution was formed. Reaction was terminated by adding 100 µL of stopping solution (0.5 M H_2SO_4) for 30 min. The solution was observed to change to yellow color and the mean optical density (OD) of the solution in each well was determined using ELISA reader at 450 nm.

3.8.2.1. Statistical Analysis

The results were taken as an average of three replicates. Data are presented as means ± SD. Statistical comparisons were performed using Students *t*-test. Statistical significance was set at $*p < 0.05$.

Chapter 4

Results and Discussion

Tissue engineering scaffolds are designed to provide a support structure for the engineered tissue. The scaffolds are essential for anchorage dependent cells to support their growth and proliferation while the cells are adhered to their surface. Furthermore, the scaffolds should allow for the proper distribution of nutrients and waste, enabling the cells to function normally. In addition to assisting natural tissue replacement, it should be biocompatible with the host cells and be biodegradable by releasing non-toxic by-products.

In this research, PHB and PHBV were examined for use as biodegradable polymers with high potential for biomedical applications. Porous PHB and PHBV scaffolds were fabricated not only to optimize liver cell viability and growth, but also to provide normal cell functionalities. Therefore, PHB and PHBV polymers were made into 2D thin films and 3D microspheres as artificial scaffolds for human liver cell growth for liver tissue engineering.

4.1. PHB and PHBV Scaffolds

4.1.1. 2D Thin Films

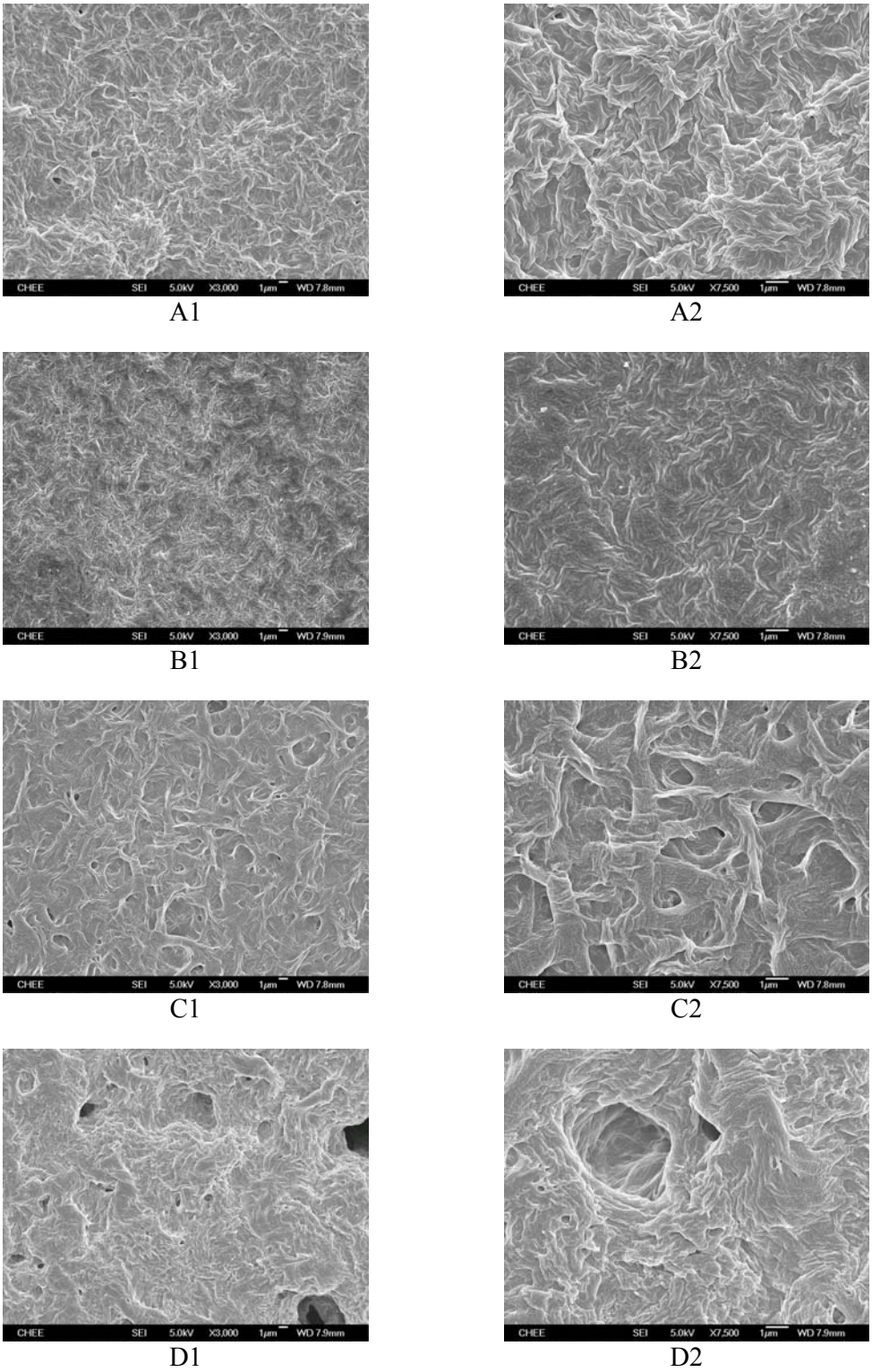

Fig. 4.1. SEM scans of thin films with different PHV content: (A) PHB, (B) PHBV(5%), (C) PHBV(8%) and (D)PHBV(12%). Images on the left column are at 3000 x magnification while images on the right column are at 7500 x magnification. Size of the bar is 1 μm.

It is well known that polymer thin films are useful for both *in vitro* studies and *in vivo* implantations. In this research, PHB, PHBV(5%), PHBV(8%) and PHBV(12%) were fabricated as 2D thin films with 200 μm thickness in order to compare cell viability, proliferation and liver specific functions with 3D microspheres. Figure 4.1 shows the SEM images of PHB and PHBV thin films at two different magnifications.

The morphologies of PHB and PHBV thin films were comparatively different with different PHV composition. The polymer surface was observed to be progressively rougher when HV content was increased in the copolymers. Hence, the surfaces of PHBV(8%) and PHBV(12%) films were rougher than that of PHB and PHBV(5%) films. The smoothness or roughness of the scaffold is one of the determining factors for cells growth. Generally, the cells prefer a smooth surface than rough surface to seed on. Hence, the growth of the liver cells on PHBV(12%) films was the lowest compared to other films as will be shown later in section 4.8.1.

4.1.2. 3D Microspheres

To study 3D scaffolds for liver cell growth, PHB, PHBV(5%), PHBV(8%) and PHBV(12%) were fabricated as microspheres by an oil-in-water (o/w) emulsion solvent evaporation technique. The microspheres were targeted to be made in the size range between 100-200 μm (± 30 μm) which was observed to be the most suitable size for liver cell (size, 20-30 μm ± 5 μm) growth.

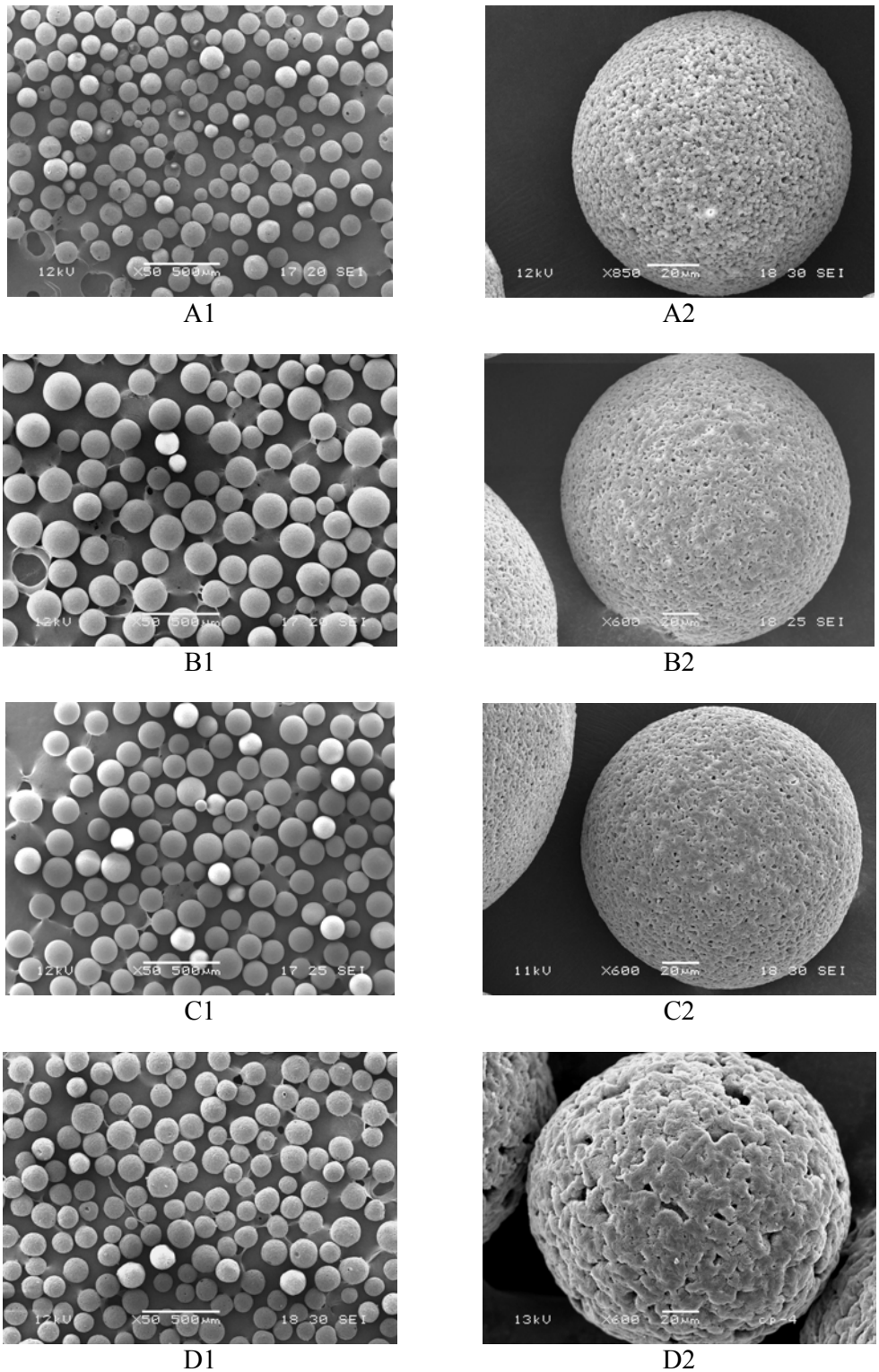

Fig. 4.2. SEM scans of microspheres with different PHV contents: (A) PHB, (B) PHBV(5%), (C) PHBV(8%) and (D) PHBV(12%). Images on the left column are at 50 x magnification while images on the right column are at 600 x magnification. Size of the bar of the left column is 500 μm while size of the bar of the right column is 20 μm.

External morphology of the microspheres was examined by using scanning electron micrographs and the images were shown in Figure 4.2. It can be seen that all of the microspheres were well defined and spherical in shape having multi-vesicles on the external surface due to the removal of internal water droplets after lyophilization. Similar with thin films, the surfaces of the microspheres with higher PHV content was found to be rougher than that with low PHV composition. Hence, PHBV(12%) microspheres have more porous and rougher surface than the other three types of the microspheres, resulting the lowest cells growth.

4.2. Size Distribution of Microspheres

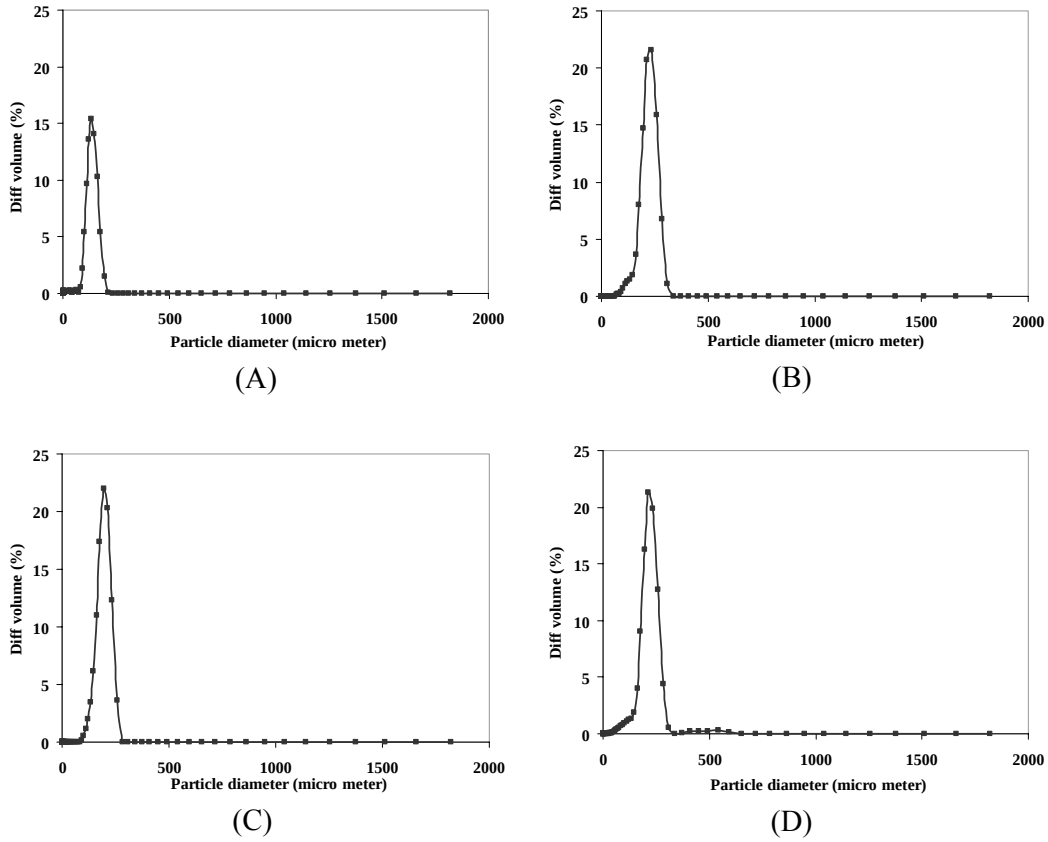

Fig. 4.3. Particle size distribution of (A) PHB, (B) PHBV(5%), (C) PHBV(8%) and (D) PHBV(12%) microspheres as measured by a Coulter particle size analyzer.

The size distributions of the PHB, PHBV(5%), PHBV(8%) and PHBV(12%) microspheres were measured by a Coulter particle size analyzer. The results obtained are shown in Figure 4.3. Herein, the mean diameter of the microspheres as determined by the Coulter counter will be used to refer to the differential volume size distribution.

Table 4.1 represents the mean diameter and standard deviation of PHB and PHBV microspheres measured using a Coulter particle size analyzer. The mean diameter of PHB microspheres, at 229.7 μm, was slightly higher than that of all the other PHBV microspheres. A possible explanation for this could be due to the longer chain length of PHB. For example, the highest molecular weight of PHB, 851100 Da, led to more extensive chain entanglement that in turn caused an increase in viscosity of the organic phase. Thus, bigger PHB microspheres were produced during fabrication. Conversely, PHBV(8%) had the lowest molecular weight, 575980 Da, resulting in the smallest mean diameter of the studied microspheres at 196.4 μm. Meanwhile, the PHBV(5%) (221.4 μm, 754820 Da) and PHBV(12%) (211.2 μm, 680970 Da) microsphere sizes are in between the first two.

Table 4.1. Comparison of the mean diameter of PHB, PHBV(5%), PHBV(8%) and PHBV(12%) microspheres.

Polymer	Mean diameter (μm)	Standard deviation (μm)
PHB	229.7	1.31
PHBV(5%)	221.4	1.25
PHBV(8%)	196.4	1.20
PHBV(12%)	211.2	1.37

4.3. The Size, Shape and Surface Studies of Microspheres

The external morphology of the microspheres is vital for cell-polymer interaction. There are a great number of studies published in the literature referring to modification of polymer scaffolds for tissue engineering. Therefore, in this research, the parameters influencing the size, shape and surface morphology of PHB and PHBV microspheres were studied extensively. These parameters include (1) copolymer composition, (2) polymer solution concentration, (3) emulsifier concentration, (4) oil/first aqueous volume ratio, (5) solvent, (6) homogenizing speed, (7) homogenizing time, (8) stirrer height, (9) evaporation temperature, (10) stirring speed, (11) stirring time, (12) lyophilization time and (13) molecular weight of the polymer. Although the SEM scans and Coulter counter results of PHBV(8%) microspheres was typically chosen a representative in section 4.3.1 to 4.3.9, similar surface morphologies and the size distribution were found to observed for PHB, PHBV(5%) and PHBV(12%) microspheres.

4.3.1. Effect of Copolymer Composition

It is well known that copolymer composition is one of the influencing factors on surface morphology of the microspheres produced by copolymers as shown in Fig. 4.2. The external surfaces of PHBV(5%) and PHBV(8%) were quite similar; although, those of PHB and PHBV(12%) were observed to be different. SEM scans at high magnification showed that PHB microspheres possessed very small rounded polymer particulates attached on the external surface (Fig. 4.2A & Fig. 4.18A). It may be possible that even though the same amount of emulsifier was used for the four different kinds of polymer during fabrication, some of the longer molecular chains of PHB polymer were not completely emulsified by PVA during emulsification since

PHB has the highest molecular weight among these polymers. In the case of PHBV(12%), the external surface of these microspheres was rougher than others because they were more porous (Fig. 4.2D & Fig. 4.18D). A possible explanation for hydrophobic PHBV(12%) possessing rough surface is that water droplets close to the surface coalesced and formed a highly porous external surface after being freeze dried. Both PHBV(5%) (Fig. 4.2B & Fig. 4.18B), and PHBV(8%) (Fig. 4.2C & Fig. 4.18C) have porous external surfaces, but were not as rough as PHB or PHBV(12%).

4.3.2. Effect of Polymer Solution Concentration

Polymer solution concentration affected not only the external surface but also the size of the microspheres. The optimal polymer solution concentration used in this work was found to be 5% which was the optimal concentration used for the rest of the studies to obtain a smooth surface morphology and narrow size distribution of the microspheres.

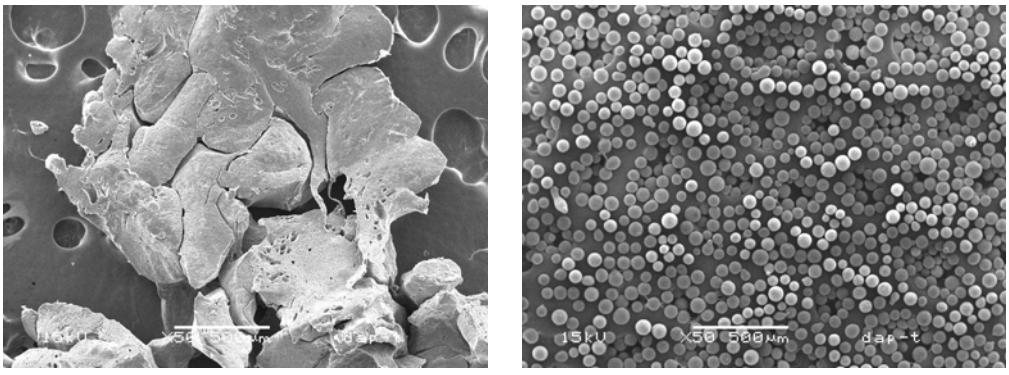

(A) (B)

Fig. 4.4. SEM scans of PHBV(8%) with different polymer solution concentrations: (A) 2% and (B) 8%. Size of the bar is 500 µm.

Fig. 4.4A shows that the polymer formed aggregates after 72 h of freeze-drying when the polymer solution was increased to 8% concentration. It was found that the higher

the polymer solution concentration, the more difficult it is for PVA to isolate the polymer chain, leading to bigger polymer aggregates. Meanwhile, the polymer maintained microspherical shapes (Fig. 4.4B) and gave almost uniform size when the polymer solution was decreased to 2% concentration as measured by Coulter particle size analyzer (Fig. 4.5). However, the mean diameter of the microspheres was dramatically reduced to 76.1 μm which is not suitable for liver cell growth as the size of Hep3B cells were 20-30 μm ± 5 μm. Hence, the polymer solution concentration was chosen to be 5%, resulting in the smooth surface microspheres with the mean diameter of 221.4 μm as seen earlier.

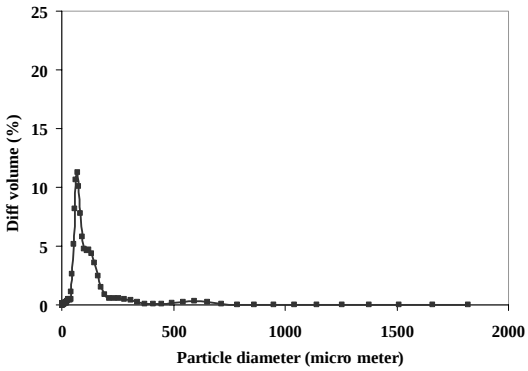

Fig. 4.5. Particle size distribution of the PHBV(8%) microspheres with 2% polymer solution concentration.

Table 4.2. Comparison of the effect of polymer concentration on the typical PHBV(8%) microspheres.

Polymer solution concentration (%)	Mean diameter (μm)	
	Volume mean diameter	Standard deviation
8	-	-
5	221.4	2.15
2	76.1	2.70

As shown in Table 4.2, the mean diameter of the microspheres produced with 2% polymer solution concentration was 76.1 μm and that of 5% polymer solution

concentration was 221.4 μm. Meanwhile, the polymer aggregates formed by using 8% polymer solution concentration could not be measured. It is possible that the same amount of PVA could thoroughly emulsify the polymer with lower concentration, resulting smaller microspheres.

4.3.3. Effect of Emulsifier Concentration

In the o/w solvent evaporation microsphere fabrication, emulsion stability is one of the important considerations because the emulsifier enhances the stability of the particles formed. In this research, PVA was used as the emulsifier or surfactant to reduce the interfacial tensions between the profiles and stabilize them against coalescence. Generally, these surfactant molecules generate a repulsive steric entropic force between particles formed in the emulsion at the microsphere's surface by extending their hydrophilic ends into the aqueous phase. This presents a barrier between the microspheres and keeps them apart from each other.

The SEM image shows a majority of the representative PHBV(8%) microspheres formed an elongated drum-shape structures when 0.01 w/v% emulsifier concentration was used, as shown in Fig. 4.6A. This could be due to a constant fluctuation in the surfactant density during the solvent evaporation phase and this may lower surfactant concentration in certain spots on the microspheres. This reduced steric repulsion enables two microspheres to come approach each other and the repulsive forces could be overcome by the attractive Van der waals forces between them. This would draw the surfaces closer and the two surfactant films could then fuse to create direct contact between the two microspheres. Hence, even in the presence of surfactant, coalescence of microspheres could potentially still take place through the diffusion and subsequent

re-orientation of PHBV solution between the microspheres. Meanwhile, when 0.15 w/v% emulsifier concentration was used, microspherical particles with smaller size and rougher surfaces were formed as seen in Fig. 4.6B. The smaller size may be due to a larger abundance of PVA molecules which isolates the polymer into smaller microspheres, while the rougher surface may be a result of a higher water content at the surface that evaporates leading to the highly porous external surfaces of the microspheres.

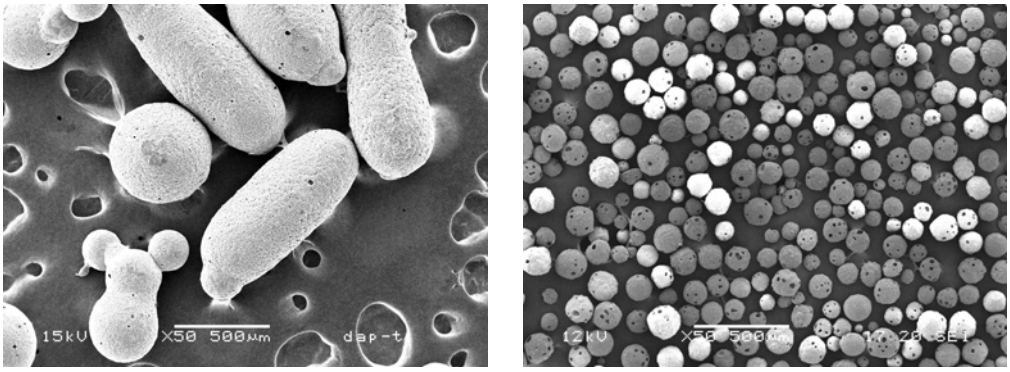

(A) (B)

Fig. 4.6. SEM scans of the PHBV(8%) microspheres using different emulsifier concentrations: (A) 0.01 (w/v %) and (B) 0.15 (w/v %). Size of the bar is 500 µm.

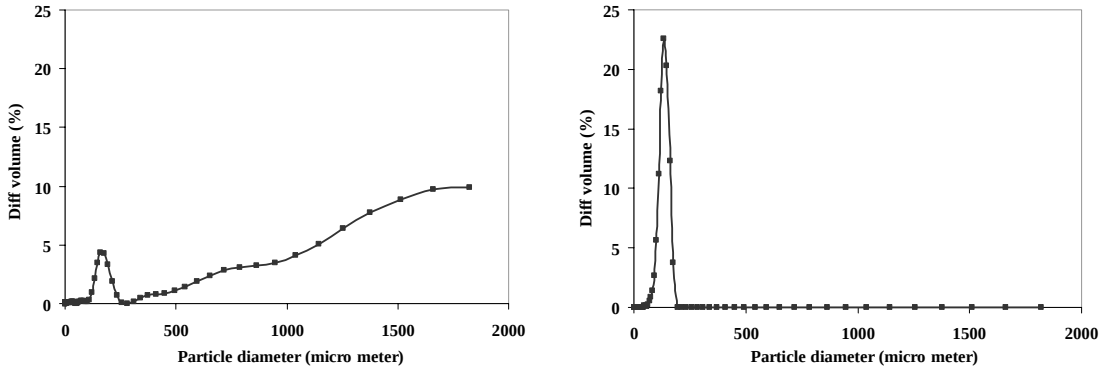

(A) (B)

Fig. 4.7. Particle size distribution of the PHBV(8%) microspheres with various emulsifier concentration: (A) 0.01 (w/v %) and (B) 0.15 (w/v %).

Quantitatively, Table 4.3 shows the changes in the size of typical PHBV(8%) microspheres with different PVA concentrations. Due to the required size distribution of the microspheres, sizes around 220 μm was obtained when a PVA concentration of 0.05 w/v % was used; this was used as the optimum PVA concentration for further experiments. However, a significant decrease in mean microsphere size from 669.8 μm to 135.9 μm was observed when the PVA concentration was increased from 0.01 to 0.15 w/v %. This was contrary to the results obtained by Yang [Yang, 2001] who had indicated that there was a slight decrease in the size of POE-PEG-POE microspheres by increasing PVA concentration. It may be possible that different polymers could be affected in different manners by PVA concentration.

Table 4.3. Comparison of the effect of emulsifier concentration on the typical PHBV(8%) microspheres.

Emulsifier concentration (w/v %)	Mean diameter (μm)	
	Volume mean diameter	Standard deviation
0.01	669.8	3.27
0.05	221.4	2.15
0.15	135.9	1.20

4.3.4. Effect of Oil/First Aqueous Volume Ratio

The effect of oil/first aqueous volume ratio on the fabrication of the microspheres was also studied. The initially used ratio was 5:1, and the resultant particles tended to form a mass of attached microspheres (Fig. 4.8). This is due to insufficient PVA concentration to isolate individual microspheres, giving rise to a high frequency of coalescence. The oil/first aqueous volume ratio was later changed to 10:1, and was found to produce totally unattached microspheres with smooth surface (Fig. 4.2C1).

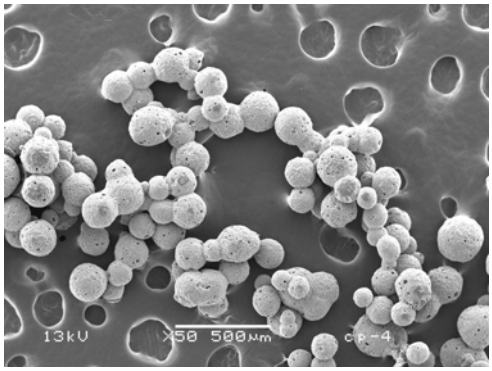

Fig. 4.8. SEM scans of the PHBV(8%) microspheres using oil/first aqueous volume ratio of 5 : 1. Size of the bar is 500 µm.

Figure 4.9 shows a wide volume distribution of the representative PHBV(8%) microspheres plotted against the particle size when the oil/first aqueous volume ratio used was 5:1 even though other process parameters were kept constant. This possibly resulted from the coalescence of smaller microspheres to form larger particles. Therefore, the oil/first aqueous volume ratio was later raised to 10:1 and the particle size was effectively reduced to acquire nearly uniform microspheres with 221.4 µm mean diameter (see Fig. 4.3C).

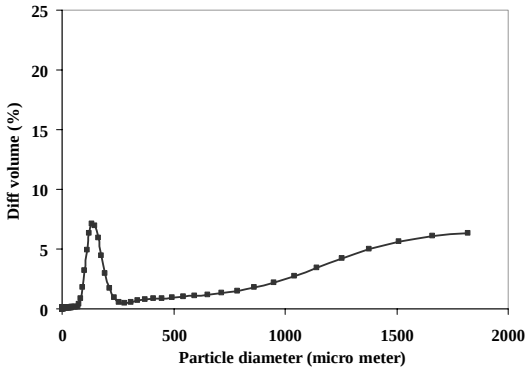

Fig. 4.9. Particle size distribution of the PHBV(8%) microspheres with oil : first aqueous volume ratio (5:1).

Table 4.4 shows the mean particle size of microspheres produced using the two different oil/first aqueous volume ratios. It can be concluded that lower oil/first

aqueous volume ratio (5:1) gave a wider range of size distribution with larger microspheres (367.1 μm). Therefore, the ratio of 10:1 was used in further experiments.

Table 4.4. Comparison of the effect of oil/first aqueous volume ratio on the typical PHBV(8%) microspheres.

Oil : first aqueous volume ratio	Mean diameter (μm)	
	Volume mean diameter	Standard deviation
5:1	367.1	3.60
10:1	221.4	2.15

4.3.5. Effect of Solvent

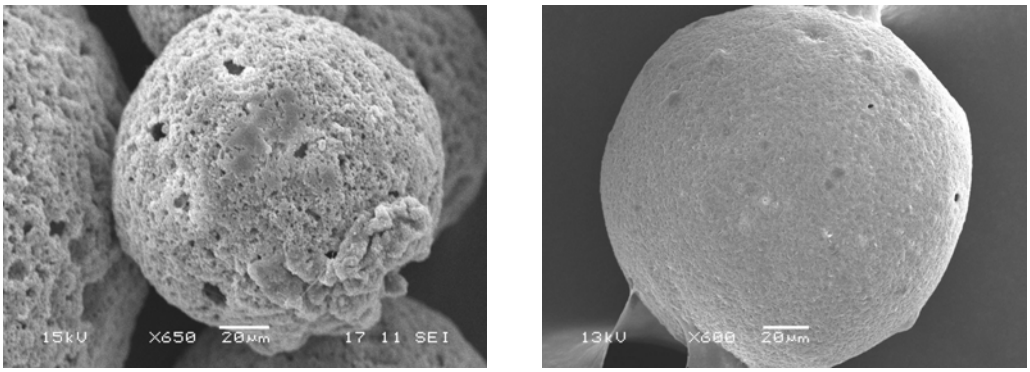

(A) (B)

Fig. 4.10. SEM scans of the representative PHBV(8%) microspheres using different solvent: (A) DCE and (B) DCM. Size of the bar is 20 μm.

The choice of solvent can significantly affect the surface of the microspheres. When dichloroethane (DCE) was used as the solvent during fabrication, the resultant microspheres exhibited a very rough external surface with high porosity, as shown in Fig. 4.10A. The surface of the microspheres was observed to be not as rough when dichloromethane (DCM) was used as a solvent although some polymer lumps were found on the microsphere surface. It may be possible that the PHB and PHBV polymers could not totally dissolve in DCE and DCM. However, the polymers were fully dissolved in chloroform, resulting in the microspheres with smooth surfaces and

rounded-shape as shown in Fig 4.2C. Similar morphology was observed for PHB, PHBV(5%) and PHBV(12%) microspheres.

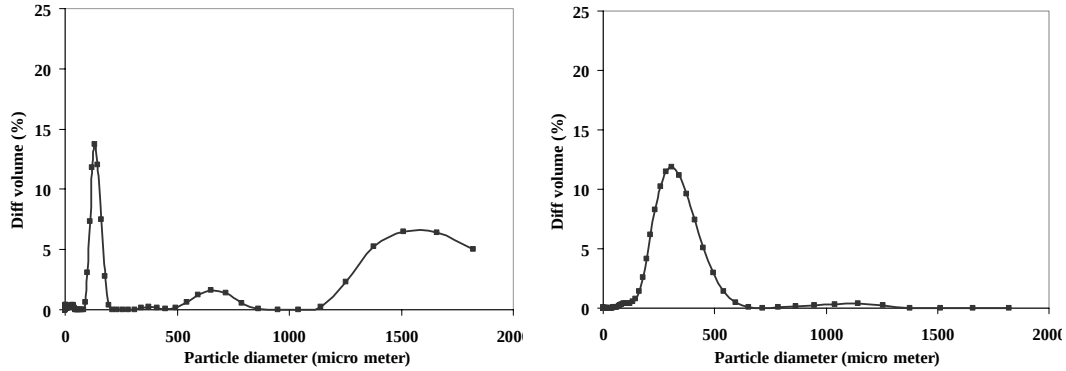

Fig. 4.11. Particle size distribution of the PHBV(8%) microspheres with various solvents: (A) DCE and (B) DCM.

The Coulter counter results showed that the size distribution of the typical PHBV(8%) microspheres with DCE as the solvent was broader than that when DCM was used (Fig. 4.11). However, a narrow size distribution of the microspheres was observed with chloroform and thus used for further experiments (Fig. 4.3C).

Table 4.5. Comparison of the effect of solvent on the typical PHBV(8%) microspheres.

Solvent	Mean diameter (μm)	
	Volume mean diameter	Standard deviation
DCE	223.6	4.58
Chloroform	221.4	2.15
DCM	306.8	1.48

From Table 4.5, the mean diameter of the PHBV(8%) microspheres made with DCE was 223.6 μm and that of DCM was 306.8 μm. The size of the microspheres was obtained around 220 μm when chloroform was used, see Table 4.1. Therefore, DCM

could be considered as better solvent than DCE. However, chloroform was chosen as the most suitable solvent especially for PHB and PHBV for further experiments.

4.3.6. Effect of Homogenizing Speed

The homogenizing speed was varied to observe the effect on the mean size of the microspheres. Figure 4.12A shows a narrow range of differential volume distributions of the typical PHBV(8%) microspheres plotted against the particle diameter with homogenizing speed set at 19000 rpm. A broader range of differential volume distributions was produced when the homogenizing speed was set at 13000 rpm, as shown in figure 4.12B. All other process parameters were kept constant. However, a narrow size distribution of the PHBV(8%) microspheres was observed by Coulter size analyzer when the homogenizing speed was set at 16000 rpm, as shown in Fig. 4.3C.

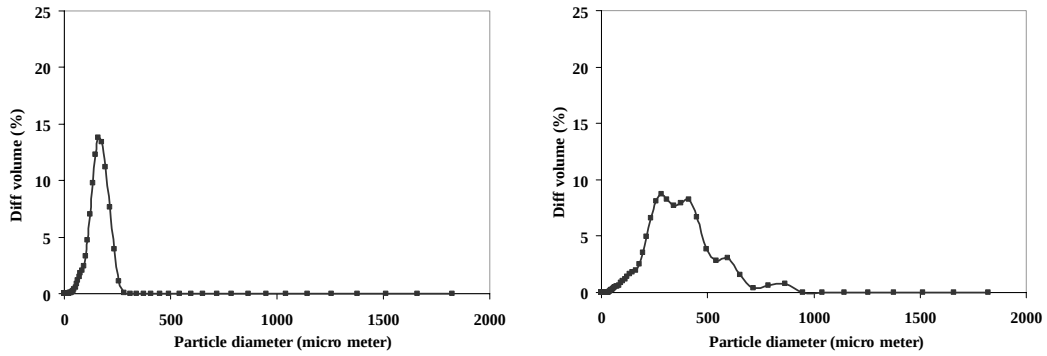

Fig. 4.12. Particle size distribution of the typical PHBV(8%) microspheres with various homogenizing speed: (A) 19,000 rpm and (B) 13,000 rpm.

Table 4.6 shows the mean diameter of the typical PHBV(8%) microspheres with different homogenizing speeds. It was observed that faster homogenizing speed yielded much smaller microspheres while slower speed yielded much bigger microspheres. Therefore, the optimum homogenizing speed was chosen to be 16000

rpm with the resulting mean microspheres size of 221.4 μm for further studies (Table 4.1).

Table 4.6. Comparison of the effect of homogenizing speed on the typical PHBV(8%) microspheres.

Homogenizing speed (rpm)	Mean diameter (μm)	
	Volume mean diameter	Standard deviation
19000	152.1	1.42
16000	221.4	2.15
13000	297.1	1.71

4.3.7. Effect of Homogenizing Time

The homogenizing time was also studied for the effect on the size distribution of the microspheres. Figure 4.13A shows the range of differential volume distributions of the typical PHBV(8%) microspheres plotted against the particle diameter with a homogenizing time of 10 s.

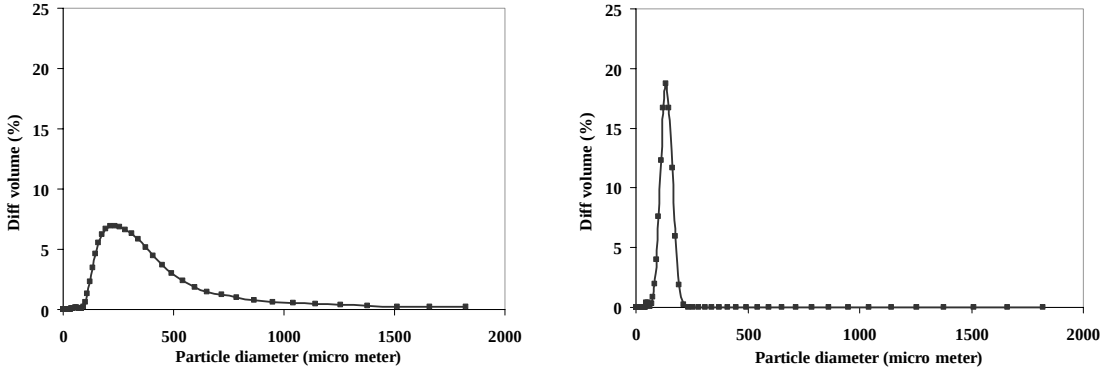

(A) (B)

Fig. 4.13. Particle size distribution of the PHBV(8%) microspheres with various homogenizing time: (A) 10 s and (B) 20 s.

In contrast, the range of size distribution was evidently reduced when the homogenizing time was doubled (20 s), as shown in Fig. 4.13B. Therefore, it can be

seen that the shorter homogenizing time gave a wider size distribution of the microspheres while the longer homogenizing time gave a narrower size distribution. However, the optimum homogenizing time was chosen for 15 s to get the required size of the microspheres of about 220 μm.

Table 4.7 shows the mean diameter of the typical PHBV(8%) microspheres with various homogenizing times. It showed that the microspheres fabricated with 20 s homogenizing time had their size distributed over a broader range (276.3 μm) as compared to the smaller microspheres (134.9 μm) produced with 10 s homogenizing time. The optimum homogenizing time used in this work was chosen to be 15 s, which produced the microspheres with the mean size (221.4 μm), as shown in Table 4.1.

Table 4.7. Comparison of the effect of homogenizing time on the typical PHBV(8%) microspheres.

Homogenizing time (s)	Mean diameter (μm)	
	Volume mean diameter	Standard deviation
20	276.3	1.98
15	221.4	2.15
10	134.9	1.24

4.3.8. Effect of Stirrer Height

The effect of stirrer height on the size of the microspheres was also investigated. Figure 4.14 represents SEM scans of the representative PHBV(8%) microspheres obtained with different stirrer heights. However, it should be taken into account that the stirrer height adjustment depends on the size of the beaker, the volume of the second aqueous solution, the stirring speed and the size of the stirrer.

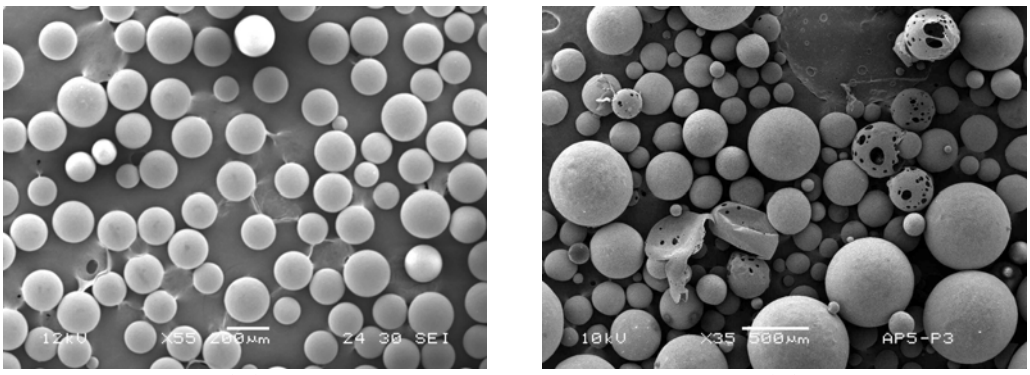

(A) (B)

Fig. 4.14. SEM scans of PHBV(8%) microspheres using different stirrer height: (a) equal to 1 inch and (b) higher than 1 inch. Size of the bar of (A) is 500 µm and that of (B) is 200 µm.

In order to obtain a more uniform size of the microspheres in this work, the stirrer height was adjusted to one inch above the bottom of the 600 mL beaker in 300 mL of the second aqueous solution (Fig. 4.14A). A stirrer height of greater than 1 inch clearly has an effect on the size of the microspheres by producing widely distributed sizes of the microspheres (Fig. 4.14B). However, the stirrer height did not influence the surface morphology as all of the resulting microspheres had a smooth surface. It can be seen from Fig. 4.15A that a very wide size distribution of the microspheres was formed when the stirrer height was set higher than one inch from the bottom of the beaker. A possible explanation is as follows. During the first thirty minutes of fabrication, polymer solution was soft, heavy and not as stable as a microspherical structure. When the stirrer was set above one inch, rotating microspheres with high molecular weight could not be thoroughly stirred and separated during emulsification. This enabled microspheres to coalesce and form bigger microspheres. Only microspheres with smaller particles can be successfully stirred near the upper surface of the second aqueous solution, forming smaller microspheres. A narrow size distribution was obtained when the stirrer height was set to around one inch from the bottom of the beaker (Fig. 4.15B). All other process parameters were kept constant.

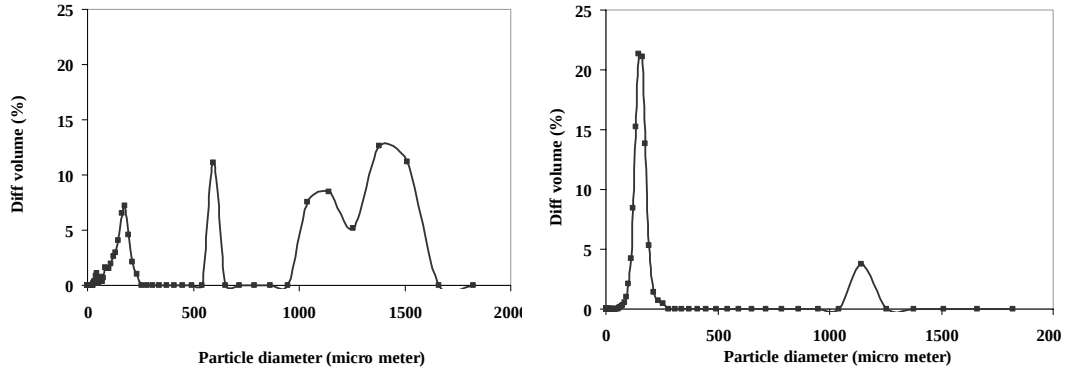

(A) (B)

Fig. 4.15. Particle size distribution of the PHBV(8%) microspheres with various stirrer height: (A) > 1 inch and (B) ≈ 1 inch.

Table 4.8 shows the mean diameter of the typical PHBV(8%) microspheres with different stirrer heights. The size of the microspheres dramatically decreased from 448.7 μm to 167.4 μm when the stirrer height was reduced from greater than 1 inch to one inch above the bottom of the beaker.

Table 4.8. Comparison of the effect of stirrer height on the typical PHBV(8%) microspheres.

Stirrer height (inch)	Mean diameter (μm)	
	Volume mean diameter	Standard deviation
> 1	448.7	3.12
≈ 1	167.4	1.54

4.3.9. Effect of Evaporation Temperature

The evaporation temperature is another parameter that can affect the size distribution of the microspheres because of the effect on the solvent removal rate. A higher evaporation temperature leads to rapid evaporation of the solvent inside the microspheres, which might result in the formation of smaller microspheres. Lower evaporation temperature produces larger microspheres due to a slower solvent removal rate.

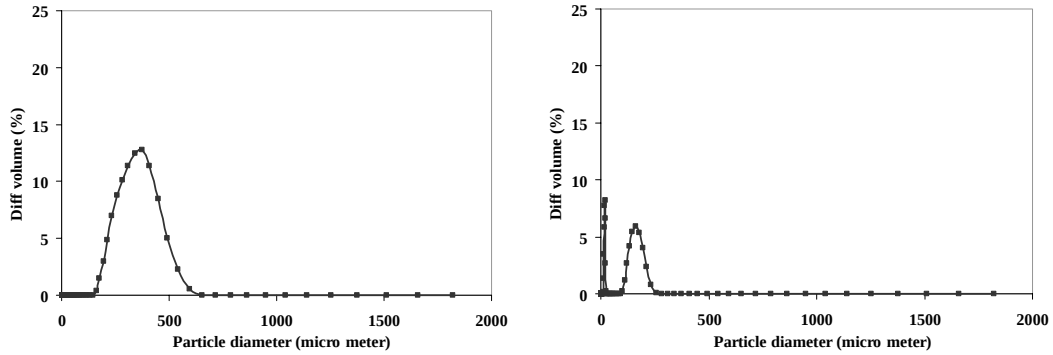

(A) (B)

Fig. 4.16. Particle size distribution of the PHBV(8%) microspheres with various evaporation temperature: (A) 30ºC and (B) 55ºC.

Figure 4.16A shows differential volume distributions of the typical PHBV(8%) microspheres with evaporation temperature maintained at 30ºC, resulting in a mean diameter of 341.2 μm. A narrower size distribution was obtained when the evaporation temperature was kept at 55ºC (Fig. 4.16B), obtaining a mean diameter was 127.4 μm. The mean size of the PHBV(8%) microspheres was 221.4 μm (Table 4.9) when the evaporation temperature was set at 38ºC although all other process parameters were kept constant. Therefore, the evaporation temperature of 38ºC was used for further experiments.

Table 4.9. Comparison of the effect of evaporation temperature on the typical PHBV(8%) microspheres.

Evaporation temperature (ºC)	Mean diameter (μm)	
	Volume mean diameter	Standard deviation
30	341.2	1.31
38	221.4	2.15
55	127.4	3.52

4.3.10. Other Parameters Affecting the Size of Microspheres

Apart from the influencing parameters mentioned above, there are additional factors that can be varied to optimize the applicable size of the microspheres, as described in the previous work of Jain [Jain, 2000]. Additional experiments were carried out to examine these effects and only a brief description of the findings is described here. For instance, stirring speed could be increased so that more mechanical energy could be supplied to break up the emulsion particles, resulting in smaller size. On the other hand, the stirring speed could also be lowered for larger microspheres to be obtained. Other parameters that have been studied were the stirring time and the lyophilization time, since it was known that longer stirring time and lyophilization time generally result in smaller particles. Hence, shorter stirring time and lyophilization time could logically yield bigger particles. Another important parameter is the molecular weight of the polymer. Higher molecular weight of the polymer could lead to bigger microspheres, whereas lower molecular weight could lead to smaller microspheres (Table 4.1 & 4.12), which was fully agreed with the previous report by Gillard et al. [Gillard, 1999].

4.4. Degradation of Microspheres

In tissue engineering, the polymer scaffolds used must be biodegradable after tissue formation, releasing non-toxic byproducts after a certain time. Different polymers have different degradation rates, which are determined by the energy required to break bonds or the location of the bonds. Polymers with hydrolysable groups can be degraded faster when there are catalysts such as water, oxygen, UV, or heat present. The degradation processes can be broadly classified into two types: chemical (acid or base catalyzed hydrolytic degradation and oxidation degradation) and biological

(degradation by microorganisms or enzymes catalyzed degradation or both). In this study, the hydrolytic degradation of PHB and PHBV microspheres with varying PHV contents was carried out by ester hydrolysis in phosphate buffer (PBS) solution at 37ºC up to a one year period.

Degradation and erosion mechanisms of the microspheres were monitored by examining their external and internal morphologies, as well as mass and molecular weight loss. In the initial period of degradation, the ester bonds were cleaved randomly and the molecular weight of the polymer decreased slightly from the polymer bulk but there was almost no mass loss. In the later period of study, the rate of both mass loss and molecular weight loss was faster due to the additional chain cleavage of the ester bonds. To study these effects, an analytical balance was used to measure the gravimetric mass loss, while the molecular weight loss was evaluated by GPC at different time points. The degradation of external surface and internal morphology of the microspheres were examined by SEM.

4.4.1. SEM Results

Figure 4.17 represents SEM scans of the external morphology of PHB and PHBV microspheres after a degradation time of one year. The degraded microspheres became smaller in size with irregular shapes due to both surface and bulk erosion when compared to the shape before degradation (Fig. 4.2).

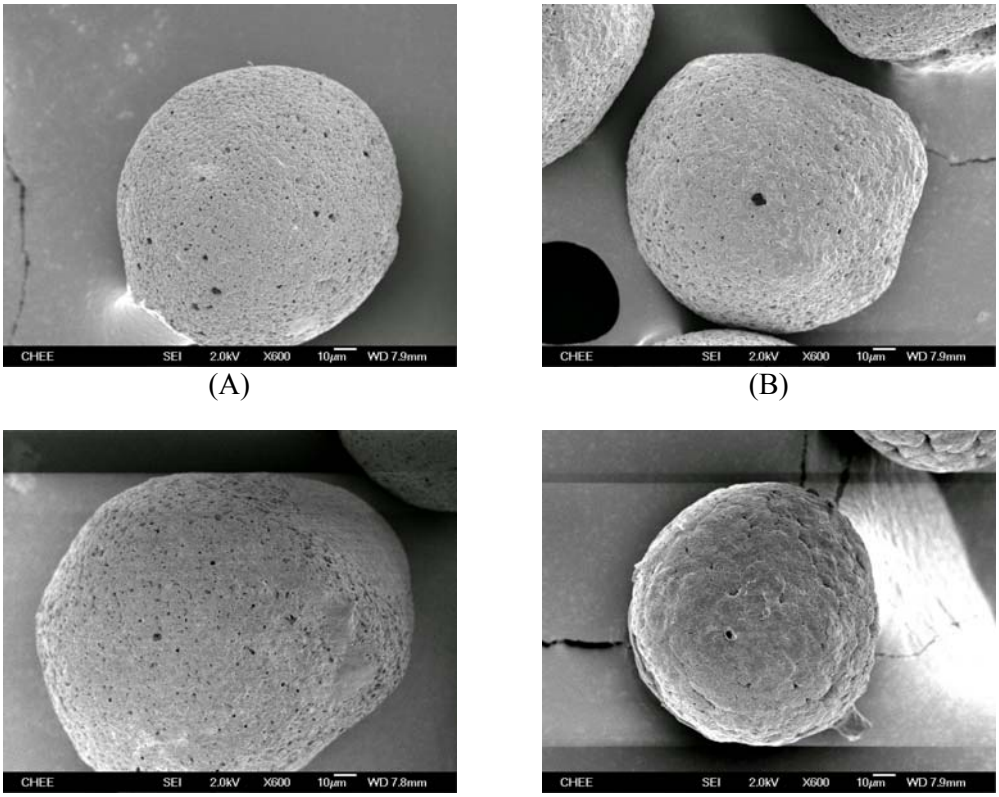

Fig. 4.17. SEM scans of the microspheres after 1 year *in vitro* degradation: (A) PHB, (B) PHBV(5%), (C) PHBV(8%) and (D) PHBV(12%). The magnification is 600 x and the size of the bar is 10 µm.

Fig. 4.18 shows the external surface of the PHB and PHBV microspheres before (left column) and after one year degradation (right column). Due to the different PHV composition, the degradation of microspheres resulted in different surface textures. PHB microspheres had many clusters or clumps on the surface while the PHBV(5%), PHBV(8%) and PHBV(12%) microspheres had knitted wavy surfaces. The images of A2, B2, C2 and D2 showed that surface erosion was homogeneous for all the microspheres and the surfaces were rather smooth after degradation compared to the original rough surfaces before degradation.

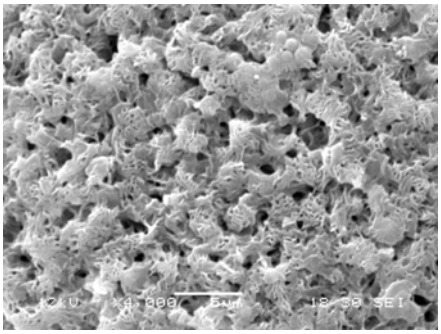
A1

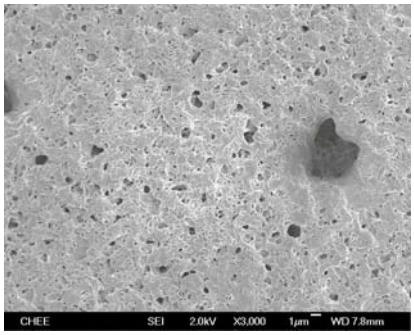

A2

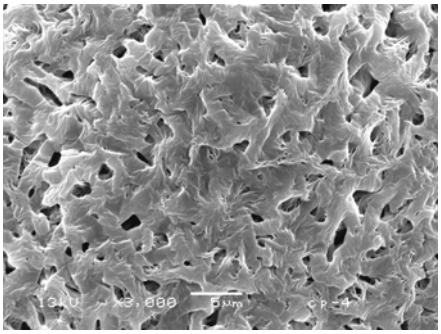
B1

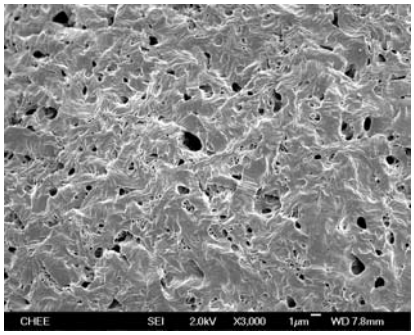

B2

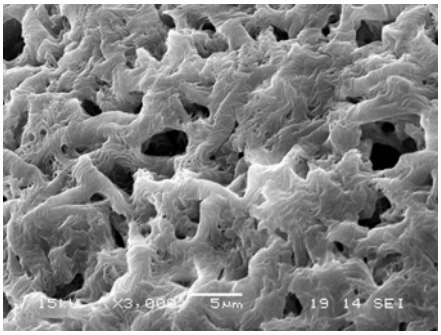
C1

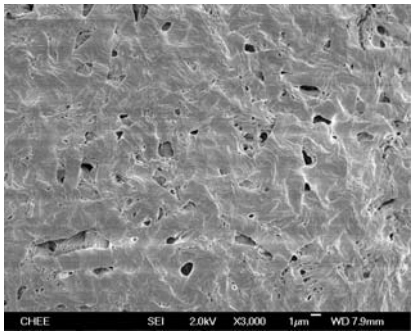

C2

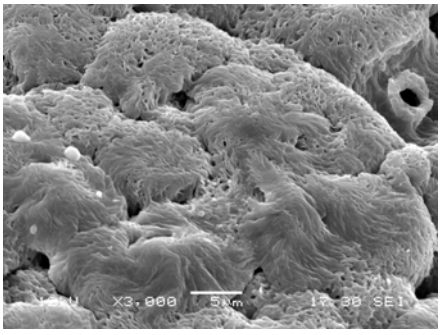
D1

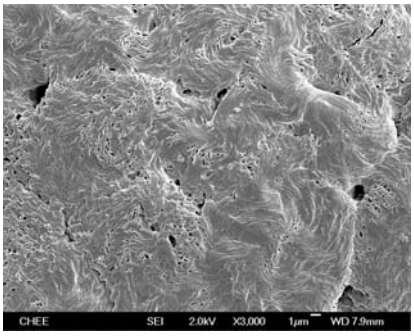

D2

Fig. 4.18. SEM scans of external surface of the microspheres: (A) PHB, (B) PHBV(5%), (C) PHBV(8%) and (D) PHBV(12%). A1, B1, C1 and D1 represent before degradation; the size of the bar is 5 μm. A2, B2, C2 and D2 represent one year after degradation; the size of the bar is 1 μm.

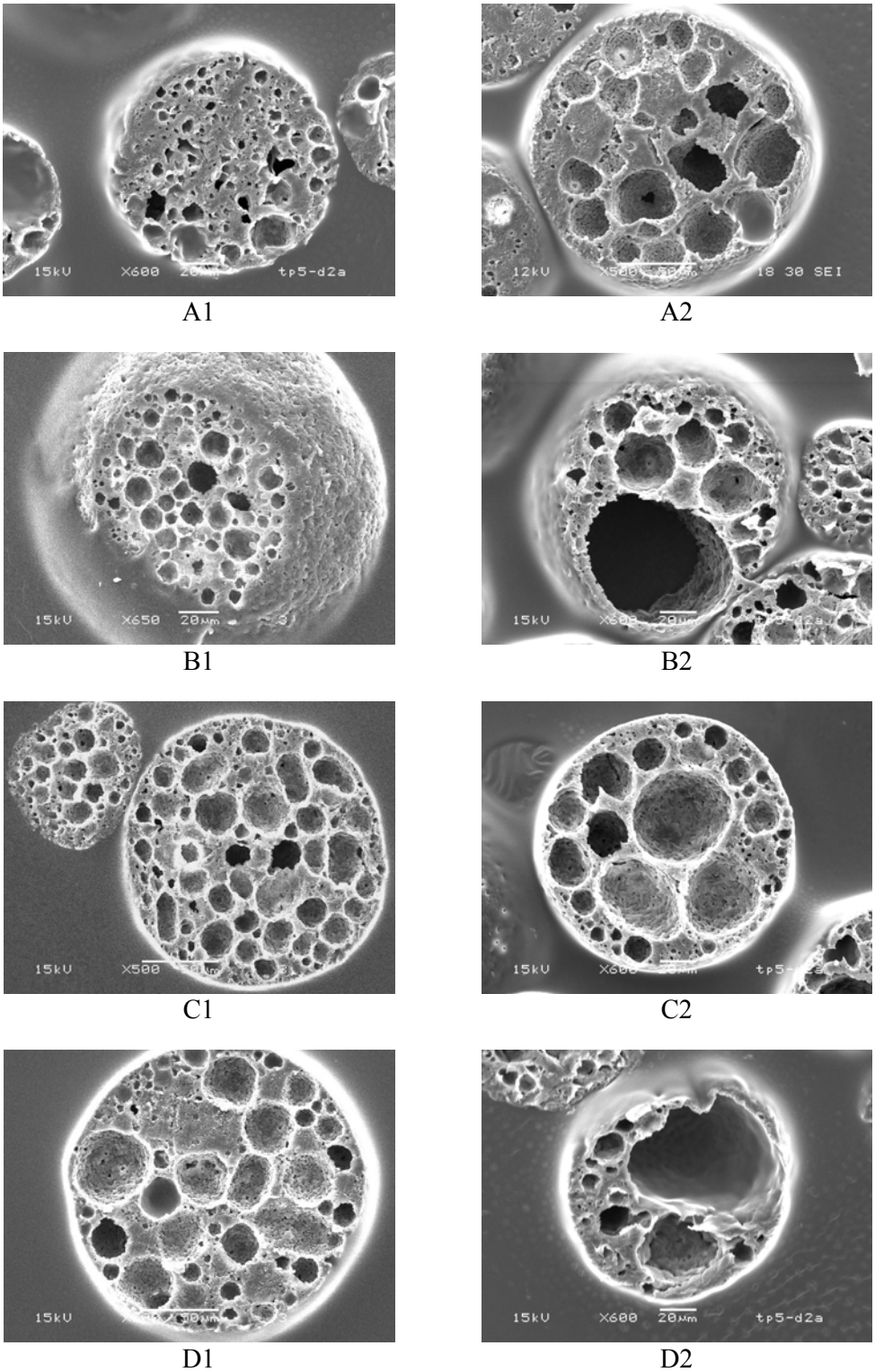

A1 A2

B1 B2

C1 C2

D1 D2

Fig. 4.19. SEM scans of cross-sectional internal morphology of the microspheres: (A) PHB, (B) PHBV(5%), (C) PHBV(8%) and (D) PHBV(12%). A1, B1, C1 and D1 represent before degradation. A2, B2, C2 and D2 represent one year after degradation. Size of the bar of A1, A2 and C1 is 50 µm and that of the rest is 20 µm.

SEM images of the internal morphologies of PHB, PHBV(5%), PHBV(8%) and PHBV(12%) microspheres were illustrated in Fig. 4.19, with A1, B1, C1 and D1 representing cross-sections of the microspheres before degradation. All of the microspheres can be seen to possess internal vesicles. A possible explanation was that PHB and PHBV were relatively hydrophobic and internal water droplets coalesce with each other due to the hydrophobic surrounding, which evaporated and formed small vesicles after being freeze dried. Among them, PHB microspheres possessed less vesicles and a denser core than the other microspheres. This might be due to PHB being more hydrophilic, allowing a fine distribution of smaller water droplets in the polymer matrix, which resulted in a denser internal core after freeze drying. On the other hand, the more hydrophobic PHBV copolymers were observed to have bigger vesicles. After one year degradation, the size of the vesicles increased (see Fig. 4.19 A2, B2, C2 and D2), which was evident in more amorphous copolymers. However, the more crystalline PHB microspheres seemed to have less dense internal cores than PHBV copolymers after degradation. This was because that for a semicrystalline polymer, the amorphous region degraded faster than the crystalline region during hydrolytic degradation as was observed by Yang et al. [Yang, 2001].

4.4.2. Mass loss Analysis

The rate of erosion of PHB and PHBV microspheres were monitored by measuring the mass loss at specific time points up to a period of one year. SEM images confirmed that mass loss occurred both in the bulk (bulk erosion) and at the surface of the microspheres (surface erosion). It can be seen from SEM images shown in figure 4.17-4.19 that bulk erosion was more evident in the core than surface erosion for PHB and PHBV microspheres. These erosion results agreed with Burkersroda et al. who

previously theorized that when water diffusion into the polymer matrix is faster than the degradation of the polymer backbone, bulk erosion will be dominant. Conversely, when the degradation of the polymer backbone is faster than the diffusion of water; the hydrolysis of the bonds on the polymer surface will be dominant on water diffusion and surface erosion will be faster than bulk erosion [Burkersroda, 2002].

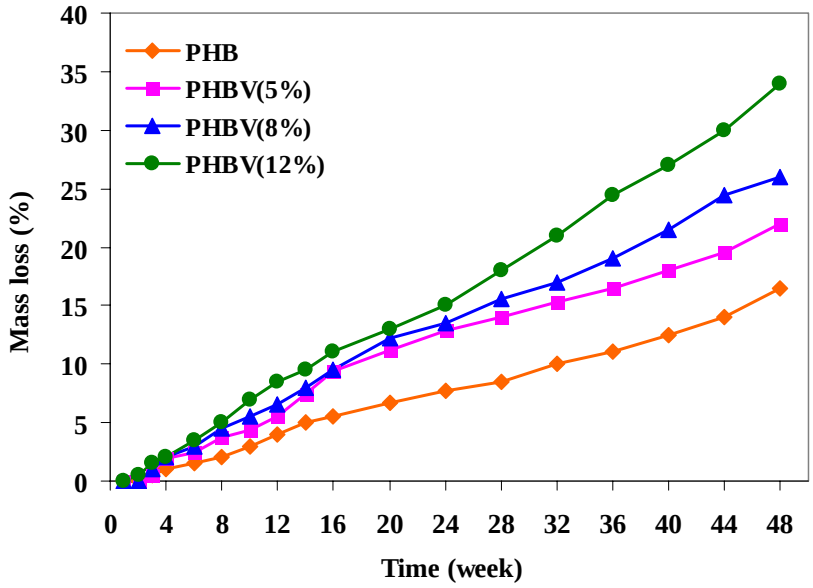

Fig. 4.20. Mass loss analysis of the PHB, PHBV(5%), PHBV(8%) and PHBV(12%) microspheres as a function of time.

From Fig. 4.20, it was observed that the mass remained unchanged for the first few days, as time is required for water molecules to diffuse into the microspheres. The mass loss was low at the beginning, but increases with time from week 2 onwards. Then a drop in mass was observed for up to one year of degradation.

The mass loss of the microspheres was calculated by the following equation:

$$\text{Mass loss}\,(\%) = \frac{m_d}{m_i} \times 100 \qquad (4.1)$$

where,

m_d = mass of the polymer after degradation, mg

m_i = initial mass of the polymer, mg

PHB microspheres were seen to have the slowest mass loss rate of 16.5% while the mass loss rate of PHBV(5%), PHBV(8%) and PHBV(12%) microspheres increased with increasing PHV content, 22%, 26% and 34% respectively. It can be theorized that PHB, having a repeat unit with a shorter methyl side group, has increased crystallinity, thus resulting in the slow degradation rate of PHB. In contrast, the repeat unit of PHV has a longer ethyl group side chain that decreases crystallinity allowing for a faster degradation rate.

Table 4.10. Mass loss of the PHB, PHBV(5%), PHBV(8%) and PHBV(12%) microspheres one year after degradation.

Polymer	Mass loss (%)
PHB	16.5
PHBV(5%)	22.0
PHBV(8%)	26.0
PHBV(12%)	34.0

4.5. Polymer Characterizations

To further study the degradation effects, PHB and PHBV microspheres and thin films were characterized before and after degradation by a few different methods.

4.5.1. Contact Angle measurement

The wettability of the polymer scaffolds is known to be important for cell attachment and so the hydrophilicity of the PHB and PHBV thin films were evaluated by static

water contact angle measurement. Table 4.11 showed the water contact angles of PHB, PHBV(5%), PHBV(8%) and PHBV(12%) before degradation. For PHB films (75.3ºC), the water droplet was more rapidly adsorbed when compared to PHBV. With increasing HV content from 5% to 12%, the wettability of PHBV decreased from 77.7ºC to 81.9ºC. Due to the hydrophobic ethyl side group of PHV, the PHBV copolymers were more hydrophobic than the PHB homopolymer. It is therefore not surprising that, PHBV with a higher HV content would increase its hydrophobicity.

Table 4.11. Contact angle measurements of the PHB, PHBV(5%), PHBV(8%) and PHBV(12%) thin films.

Polymer	Contact angle (º)
PHB	75.3
PHBV(5%)	77.7
PHBV(8%)	79.6
PHBV(12%)	81.9

Langer and Peppas previously reported that the degradation rate of the polymers was affected by their hydrophilic/hydrophobic properties. Polymers with relatively high hydrophilicity degrade by bulk erosion, allowing more water to penetrate into the bulk before degradation begins throughout the microspheres, whereas relatively more hydrophobic polymers with extremely water-labile bonds degrade by surface erosion, breaking the bonds at the surface before allowing water to penetrate [Langer and Peppas, 1983].

For this reason, the more hydrophilic PHB microspheres should be degraded faster than PHBV microspheres. However the mass loss and molecular weight loss of PHB was less than that of PHBV and thus was not in agreement with the theory. A possible

reason could be due to the higher crystallinity of PHB that dominates the degradation rate of PHB microspheres rather than its hydrophobicity. Furthermore, the most hydrophobic PHBV(12%) microspheres degraded with the fastest rate of mass loss and molecular weight loss since it possessed less crystalline and more amorphous regions than PHB.

4.5.2. Gel Permeation Chromatography (GPC) Analysis

The molecular weight and molecular weight distribution are important factors governing the degradation of the microspheres. Hence, the number- and weight-average molecular weights (M_n and M_w) and polydispersity (M_w/M_n or standard deviation) of the polymer microspheres before and after *in vitro* degradation were determined using gel permeation chromatography (GPC). The molecular weight loss of the microspheres was calculated by the following equation:

$$\text{Molecular weight loss}\,(\%) = \frac{M_{w,d}}{M_{w,i}} \times 100 \qquad (4.2)$$

where,

$M_{w,d}$ = molecular weight of the polymer after degradation, Da

$M_{w,i}$ = initial molecular weight of the polymer, Da

Table 4.12. GPC results of PHB, PHBV(5%), PHBV(8%) and PHBV(12%) microspheres before and after degradation.

Polymer	Before degradation M_w (Da)	After one year degradation		
		M_w (Da)	M_w/M_n	M_w loss (%)
PHB	851,100	459,140	1.38	46
PHBV(5%)	754,820	318,240	1.93	58
PHBV(8%)	575,980	270,320	1.77	53
PHBV(12%)	680,970	351,260	1.66	48

GPC results from Table 4.12 shows that the molecular weights of non-degraded polymers reduced one year after degradation. In addition, the polydispersity of the polymers was different with respect to the different polymers of different molecular weights. PHBV(5%) has the largest molecular weight distribution of 1.93 and its molecular weight loss is the highest of 58%. However, PHB microspheres, which degraded with the slowest rate with molecular weight loss of 46%, have the narrowest polydispersity of 1.38. M_w/M_n of PHBV(12%) was 1.66, which is lower than that of PHBV(8%) (1.77). This corresponds to the rate of molecular weight loss for PHBV(12%) of 53%, which was slower than that for PHBV(8%) of 48%.

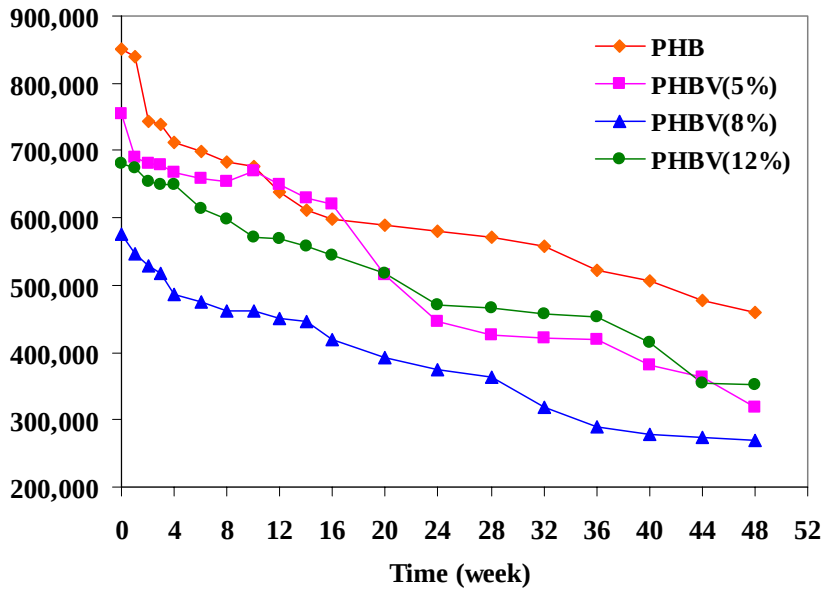

Fig. 4.21. Changes in weight average molecular weight of the PHB, PHBV(5%), PHBV(8%) and PHBV(12%) microspheres as a function of degradation time.

Fig. 4.21 shows the weight average molecular weight loss profiles for the PHB and PHBV microspheres as measured by GPC for up to one year. Molecular weight loss occurred within the first month because water diffused homogeneously into the polymer matrix and enhanced random chain scissions of the ester linkages. Then a

continual drop in molecular weight (M_w and M_n respectively) was observed, with the molecular weight loss increasing with time.

4.5.3. Differential Scanning Calorimetry (DSC) Measurement

Thermal analysis of the PHB and PHBV microspheres was carried out using a differential scanning calorimeter (DSC). Thermal properties of the polymer depend on the glass transition temperature (T_g), melting temperature (T_m), crystallization temperature (T_c), enthalpy of fusion (ΔH) and degree of crystallinity (X_c). The T_m value was taken as the peak value of the respective endotherm in the DSC curves. The T_g value was computed as the midpoint of heat capacity increase.

The degree of crystallinity of the polymer was calculated by using the following equation:

$$X_c(\%) = \frac{\Delta H_f}{\Delta H_o} \times 100 \qquad (4.3)$$

where,

ΔH_f = the enthalpy of fusion of the polymer, J/g

ΔH_o = the enthalpy of fusion of 100 percent crystalline PHB = 146 J/g

PHB is a stiff and brittle polymer, and its brittleness depends on the degree of crystallinity and glass transition temperature. When PHB was copolymerized with the more amorphous PHV, the brittleness was moderately reduced. Table 4.13 shows the crystallinity (%), T_g and T_m of PHB and PHBV microspheres before and after one year

degradation. Due to the difficulty in determining the T_gs for the degraded polymer microspheres, these data were not shown.

Table 4.13. DSC results of PHB, PHBV(5%), PHBV(8%) and PHBV(12%) microspheres before and after degradation.

Polymer	Before degradation			One year after degradation	
	T_m (°)	T_g (°)	Cr (%)	T_m (°)	Cr (%)
PHB	176	6	62	177	92
PHBV(5%)	154	2	32	155	67
PHBV(8%)	149	– 1	30	150	61
PHBV(12%)	148	– 3	25	149	40

It is well known that the crystallinity is one of the main controlling factors for the degradation rate of the polymers. After one year degradation, the crystallinity of all the microspheres increased significantly. During degradation, diffusion of water into the amorphous regions of the polymer occurred and produced random hydrolytic scission at the susceptible ester linkage. As the amorphous regions degraded faster than the crystalline regions, there was a characteristic increase in the percentage crystallinity of the polymers. For this reason, the crystallinity of PHB, PHBV(5%), PHBV(8%) and PHBV(12%) after one year degradation increased from 62%, 32%, 30% and 25% to 92%, 67%, 61% and 40% respectively.

In addition, the composition of the copolymers also affected the thermal properties. The Cr (%), T_g and T_m for the PHBV copolymers was significantly lower than that for the PHB homopolymer. By increasing the PHV content from 0 to 12%, the crystallinity decreased from 62 to 25%, glass transition temperature decreased from 6

to –3ºC, and melting temperature decreased from 176 to 148ºC, respectively. After one year degradation, PHBVs were found to be more amorphous because of the ethyl group side chains, which were longer than methyl group side chains possessed by PHB. This promoted the flexibility for molecular movement in the PHBV polymer bulk and hence, decreased the crystallinity.

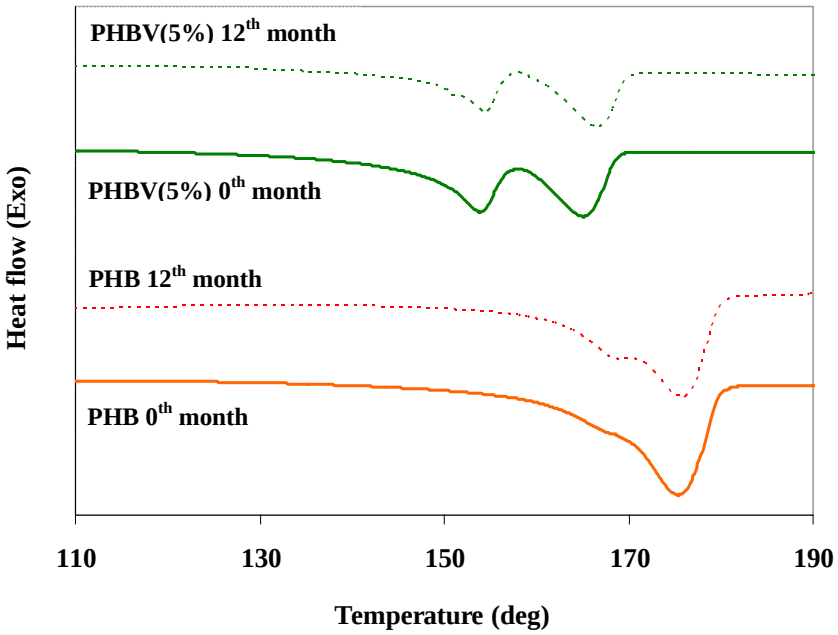

Fig. 4.22. Melting endotherms of the representative PHB and PHBV(5%) microspheres before (solid line) and one year after degradation (dashed line).

From Fig. 4.22, the DSC curve of PHB has only one melting peak and the T_m value of PHB microspheres slightly shifted from a sharp peak of 176ºC to a more broadened peak of 177ºC after degradation. However, PHBV polymers have two melting peaks. The higher temperature peak was due to the melt-recrystallization process. The lower temperature peaks showed the melting temperatures of the crystalline polymers, and therefore the lower melting peaks were taken as the T_m and tabulated in Table 4.12. The T_m slightly increased after one year degradation and the melting peaks shifted to

higher temperatures. It can be seen from Fig. 4.22 that the melting endotherms of the representative PHBV(5%) microspheres shifted from 154 to 155ºC after degradation.

Figure 4.24 shows the crystallization peak of representative PHBV(5%) microspheres. Before degradation (solid line), the crystallization peak was sharp and T_c was found at 53ºC. After degradation (dashed line) crystallization increased only slightly and a broader exotherm was observed at 54ºC.

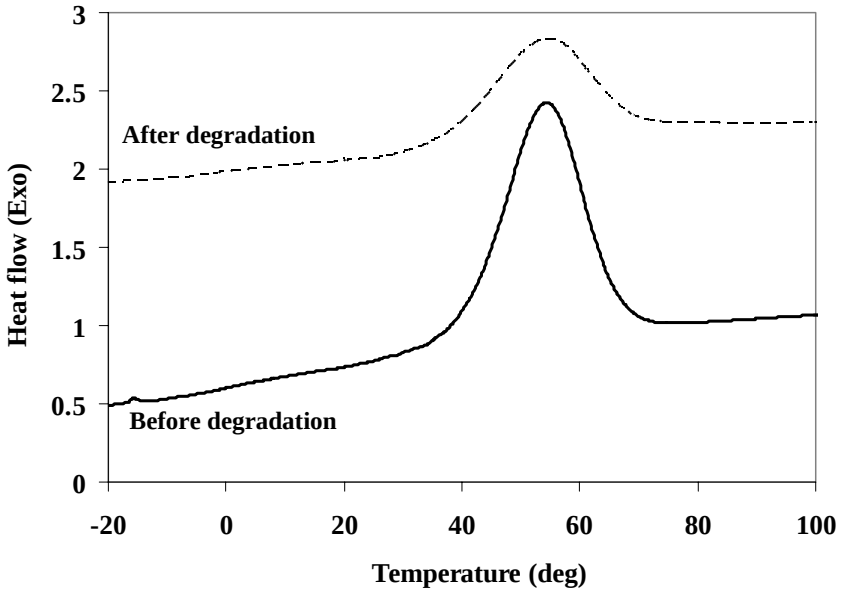

Fig. 4.23. Crystallization exotherms of the representative PHBV(5%) microspheres before (solid line) and one year after degradation (dashed line).

As mentioned above, the crystallinity had a large effect on the degradation rate of the polymers. The degradation and DSC results in this work are in agreement with those of Chen and Wang who have previously reported that a higher degree of crystallinity led to a lower degradation rate of polymer [Chen and Wang, 2002]. Fig. 4.24, which represents the relation between mass loss and crystallinity of the PHB and PHBV microspheres, thus shows a significant decrease of the mass from PHBV(12%) to

PHB. The lowest crystallinity, of PHBV(12%), was found to lead to the highest degradation rate because hydrolysis of the amorphous phase was faster than the crystalline phase. Therefore, the rate of mass loss of PHBV copolymers increased with increasing PHV content because of decreasing crystallinity.

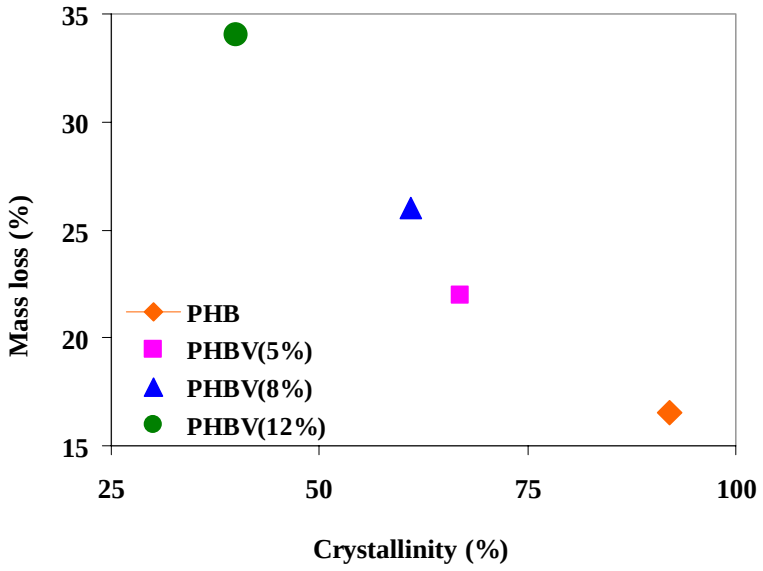

Fig. 4.24. The relation between degradation rate (mass loss %) and crystallinity % of the PHB, PHBV(5%), PHBV(8%) and PHBV(12%) microspheres.

4.5.4. Proton-Nuclear Magnetic Resonance (^{1}H-NMR) Analysis

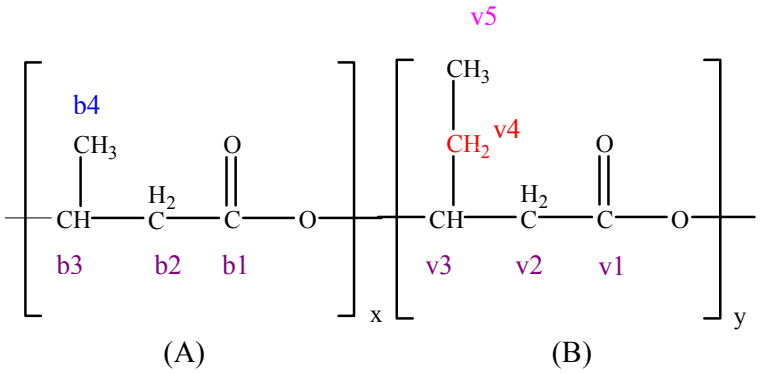

Fig. 4.25. Chemical formula of PHBV copolymer: (A) PHB and (B) PHV. The letters (b1 to b4 and v1 to v5) correspond to the specific chemical shift regions identified by ^{1}H-NMR spectroscopy in Fig. 4.26.

^{1}H-NMR spectra of PHB and PHBV were carried out not only to determine their chemical structures but also to confirm the degradation products of the PHB and PHBV microspheres and to compare with the data obtained by GPC and DSC. The ^{1}H-NMR spectra of the representative PHBV(8%) microspheres before (A) and after (B) degradation are shown in Fig. 4.26. The peak signals in Fig. 4.26 were labeled to correspond to an appropriate proton of the polymer repeat units as presented in Fig. 4.25.

As shown in Fig. 4.26, a characteristic resonance peak between 1.2 to 1.3 ppm corresponds to the proton in the methyl groups ($–CH_3$) of PHB (b4). The chemical shifts of $–CH_2$ (v4) and $–CH_3$ (v5) found in ethyl groups of PHV appeared at 1.6 and 0.9 ppm respectively. These peaks were not observed in the ^{1}H-NMR of PHB (data not shown). Before degradation (Fig. 4.26A), the peaks of v4 and v5 were strong. After the commencement of hydrolysis, the signals seemed to weaken; however, they were still observed in the microspheres (Fig. 4.26B) after a degradation period of one year. This is consistent with the degradation results obtained by GPC and DSC, i.e., the degradation rate of the microspheres was relatively slow and PHB and PHBV microspheres were not completely degraded after a one year period, as mentioned previously.

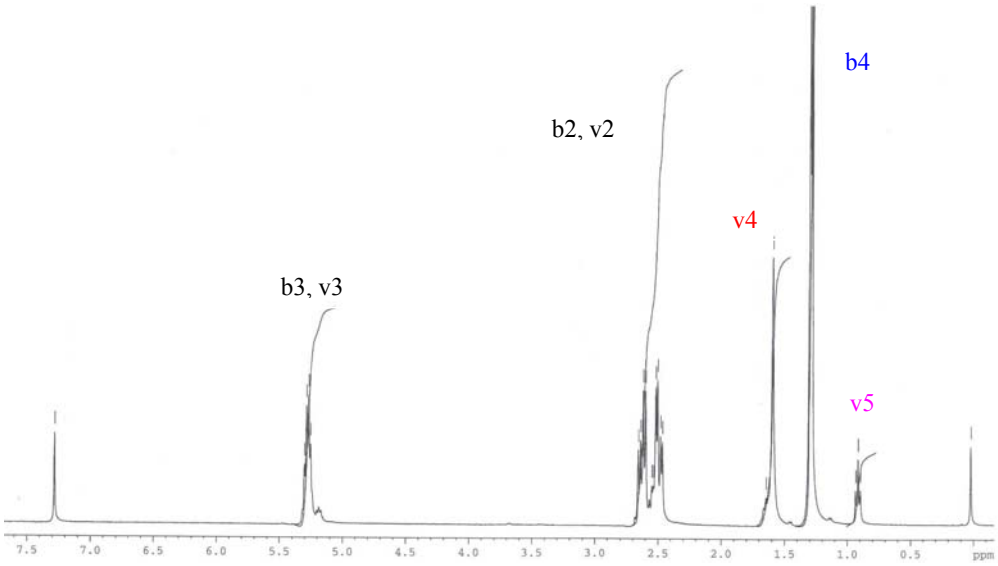

(A)

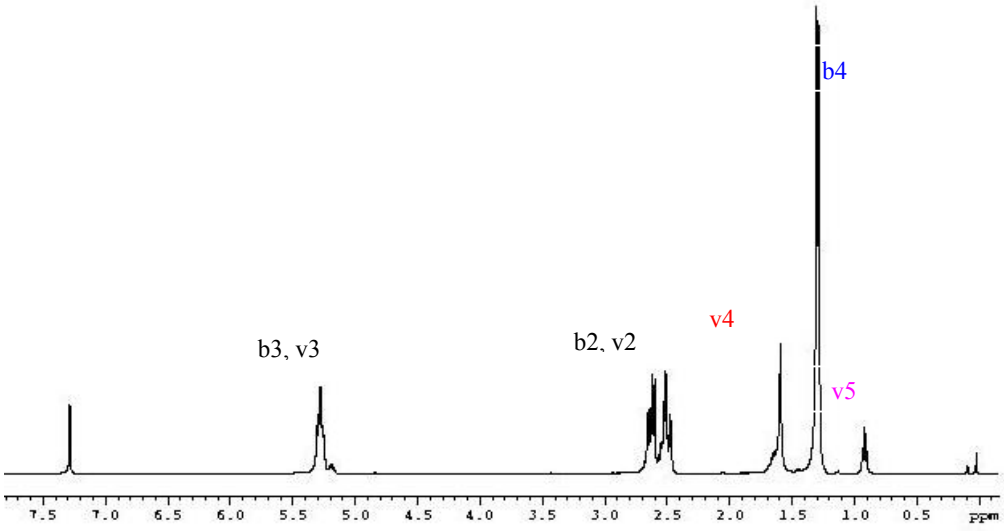

(B)

Fig. 4.26. The 400 MHz ^{1}H-NMR spectra of the representative PHBV(8%) microspheres (A) before and (B) after degradation.

Table 4.14. ^{1}H-NMR integrated area assignments for the representative PHBV(8%) microspheres.

	Area of shift (ppm)	
	Before degradation	After degradation
$-CH_3$ (b4)	3.008	3.029
$-CH_3$ (v5)	0.340	0.274
$-CH_2$ (v4)	1.240	1.009

Table 4.14, which shows the areas for the HB and HV protons, the initial integrated area (v4 and v5) of the representative PHBV(8%) microspheres decreased while that of b4 increased after degradation. This is due to the more amorphous PHV degrading faster than the more crystalline PHB. Therefore, PHB content increases and PHV content decreases with degradation. Moreover, the degradation rate increased with increasing PHV content in the PHBV copolymers. This can be proved by the signal intensity ratio of protons b4/v4, which decreased from 3.247 to 2.878 when PHV content increased from 5% to 12% (Table 4.15).

Table 4.15. The signal intensity ratio of protons b4 and v4 for PHBV(5%), PHBV(8%) and PHBV(12%) microspheres after degradation.

Polymer	b4 / v4
PHBV(5%)	3.247
PHBV(8%)	3.002
PHBV(12%)	2.878

4.5.5. X-ray Photoelectron Spectroscope (XPS) Analysis

X-ray photoelectron spectroscopy (XPS) was used to investigate the chemical compositions of the surface of a polymer. Fig. 4.26 shows the XPS C_{1s} scan of PHB and PHBV(5%) microspheres.

From Fig. 4.26, the peak at the lowest binding energy of 285 eV is indicative of C–C bonds, while the peak at 286 eV represents C–O bonds. The peak at the highest binding energy of 289 eV is due to the presence of C=O bonds. All these peaks can be seen both in Fig. 4.26A & B since both PHB and PHBV possess C–C, C–O and C=O bonds.

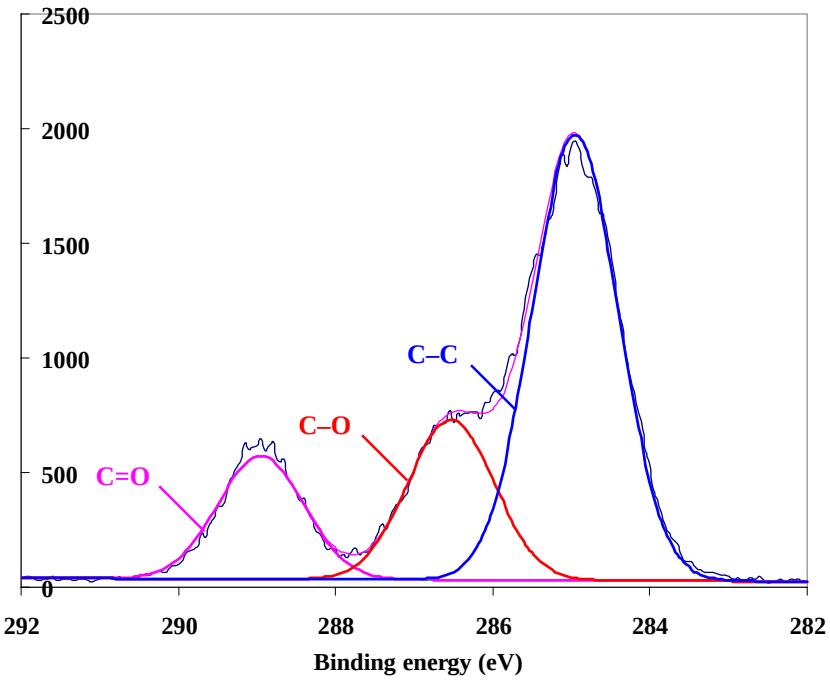

(A)

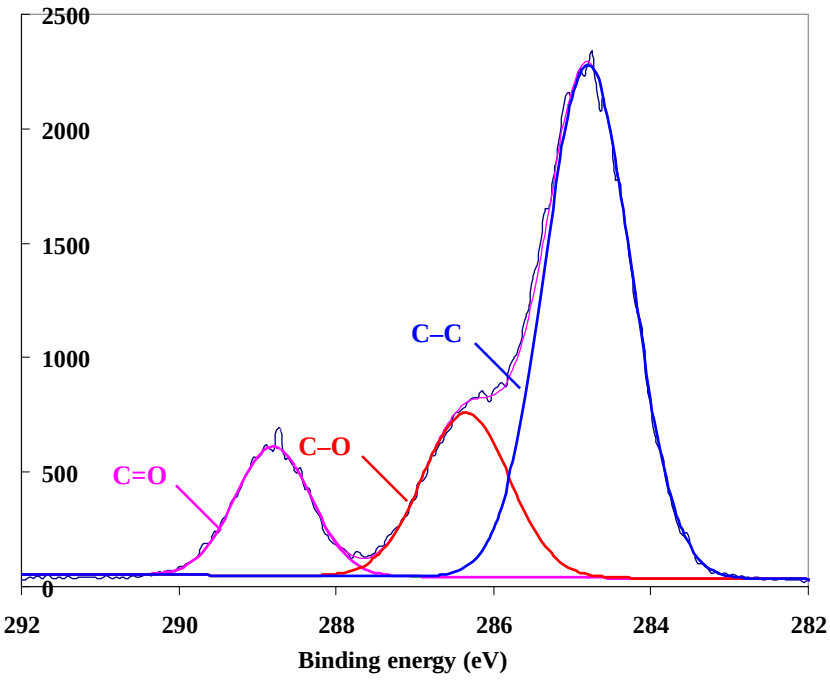

(B)

Fig. 4.27. C_{1s} regions of XPS spectra of the representative (A) PHB and (B) PHBV(5%) microspheres.

From the XPS data, the C and O percentage of PHB and PHBV microspheres were tabulated in Table 4.16. Together with the Cls scans, the atomic compositions indicate the presence of carboxylic groups in the microspheres. The results show that the surfaces for all of the different microspheres had similar chemistry, even though the copolymer compositions are different.

Table 4.16. Atomic percentage of carbon and oxygen elements on the PHB and PHBV microspheres before degradation.

Polymer	C %	O %
PHB	71.87	27.87
PHBV(5%)	74.11	25.45
PHBV(8%)	72.84	26.57
PHBV(12%)	65.86	28.53

4.5.6. Fourier Transform Infrared (FTIR) Examination

Fourier transform infrared (FTIR) spectroscopy was employed to determine chemical structure (functional groups) of the polymers. Fig. 4.28 represents the IR spectra of the PHB and PHVB microspheres before and after degradation. It can be seen that the weak absorption bands at about 3428–3440 cm^{-1} corresponded to the O–H stretching, while the absorption band around 2931–2937 cm^{-1} is the indicative of the presence of C–H stretching. The distinctive carbonyl stretching (C=O) of carboxylic groups appeared at 1718–1741 cm^{-1}, which were strong and intense before degradation. The O–C–O stretching was found to exhibit characteristic absorptions in the range of 1060–1186 cm^{-1}. These experimental findings were agreed with the works of Jun et al. and Suthar et al. [Jun, 2002 and Suthar, 2000].

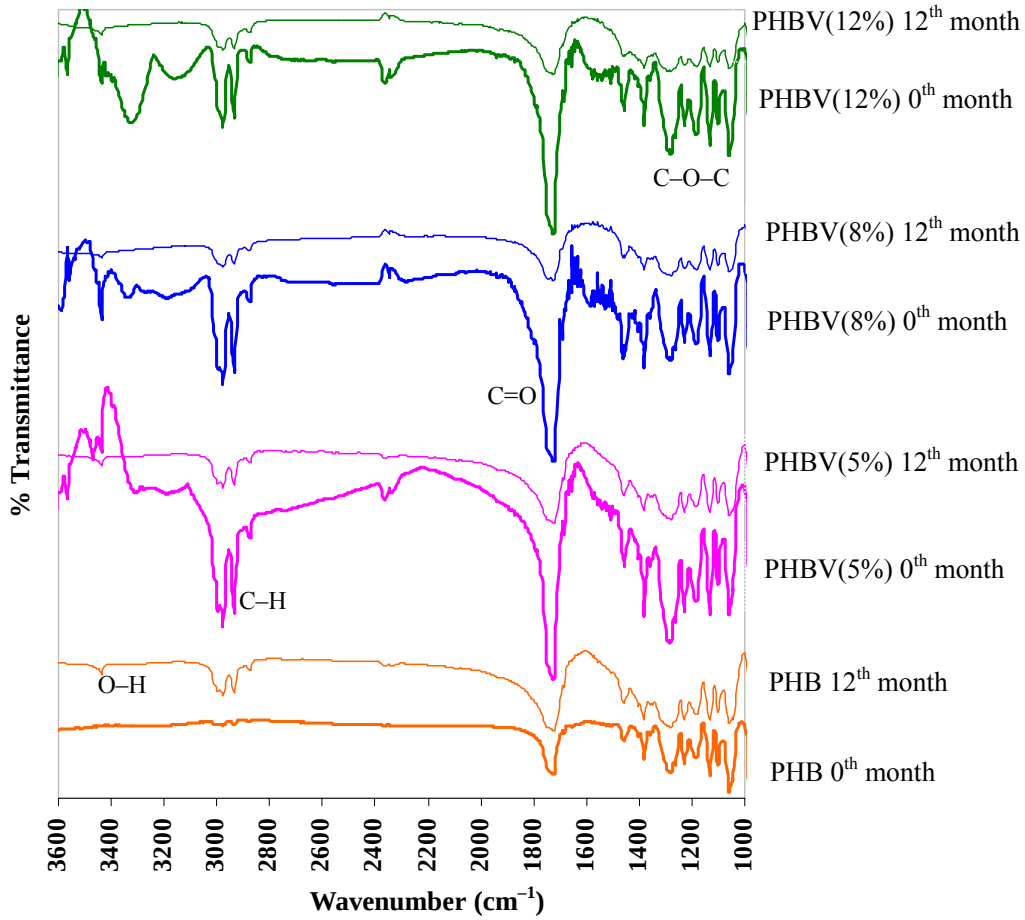

Fig. 4.28. FTIR spectra for the PHB, PHBV(5%), PHBV(8%) and PHBV(12%) microspheres before (thick line) and one year after degradation (dashed line).

From the IR spectrum of PHB microspheres, it may be observed that there were no chemical shifts after degradation. The same phenomena were observed for the PHBVs microspheres, as the characteristic absorption bands were almost identical after degradation. In addition, PHV composition of copolymers had no affect on the chemical shifts. This was not agreeable with Bloembergen et al., who previously reported that the shapes and intensities of some IR bands were very sensitive to the crystallinity of the polymer [Bloembergen, 1986]. However, the peaks in IR spectra of all degraded microspheres became broader and weak which might be due to the decreasing molecular weight of the microspheres. Another possibility is that the intensity of the C=O ester peaks were sent to decrease after degradation, indicating

that hydrolysis of the PHB and PHV ester bonds have occurred, and therefore confirming our previous results.

4.6. Direct Contact Cytotoxicity Test

Besides biodegradability, biocompatibility is another critical factor that determines whether a scaffold can be used in biomedical applications. In this work, the direct contact cytotoxicity test was performed according to the recommended ISO 10993-5 standard, using a mouse connective tissue fibroblast cell line (L-929). L-929 is commonly used for the cytotoxicity tests because they are easy to maintain in culture and exhibit a high proliferation rate [BS EN ISO 10993-5, 1999]. The initial cell density of 2.5 x 10^5 cells was cultured in DMEM, with 80% confluence being reached after 48 h. Fig.4.29 shows optical micrographs of L-929 cells at different cultured days. It can be seen that these cells are monolayer, adherent cells with spindle shapes.

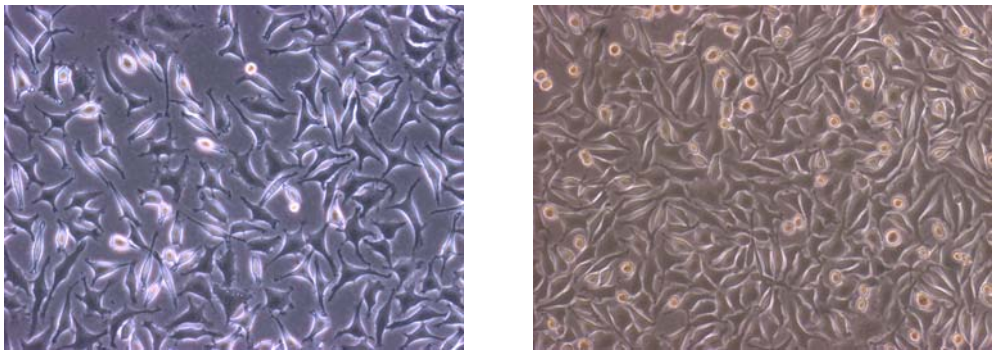

(A) (B)

Fig. 4.29. Optical micrographs of mouse fibroblast cell line, L-929, cultured on TCP on (A) day 1 and (B) day 3.

Fig. 4.30 represents the qualitative cytotoxicity results performed by an optical microscope for PHB and PHBV films.

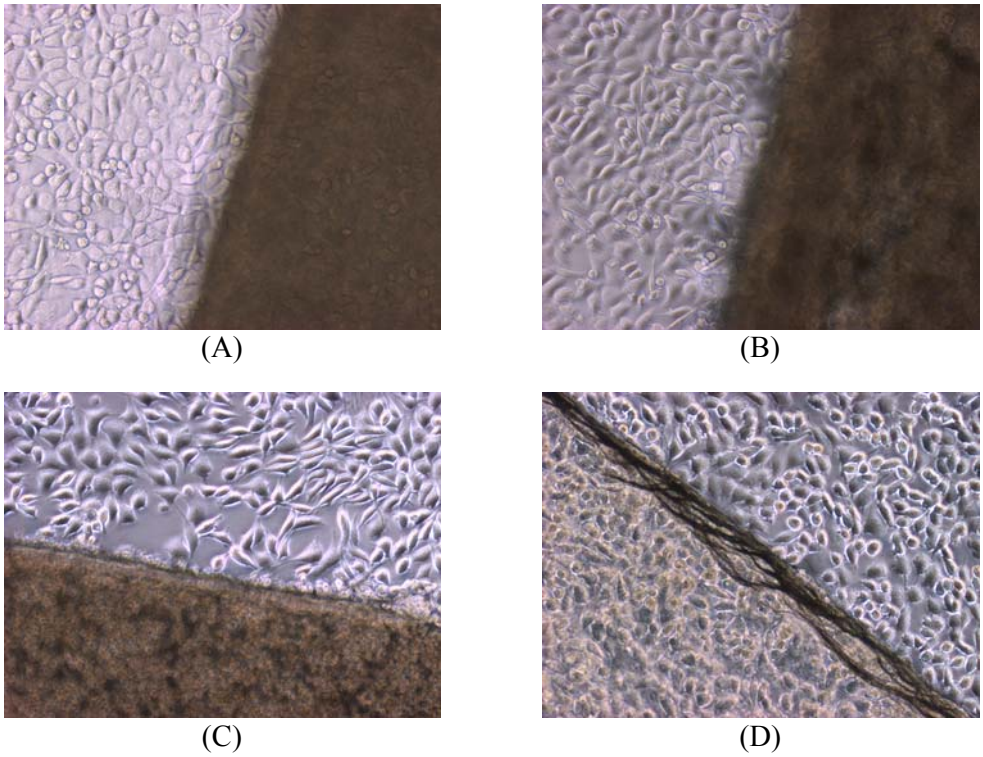

Fig. 4.30. Optical micrographs of L-929 mouse fibroblasts seeded on polymer films, after 48 h incubation: (A) PHB, (B) PHBV(5%), (C) PHBV(8%) and (D) PHBV(12%).

The quantitative cytotoxicity test results were calculated by averaging five replicates for the negative control, positive control and samples. The inhibition zone of the specimen was recorded as diameter (mm) / area (mm^2).

The cytotoxicity percent was calculated by the following equation:

$$\text{Cytotoxicity}\,(\%) = \frac{S - N}{P - N} \times 100 \tag{4.4}$$

where,

S = diameter of zone by sample (mm)

P = diameter of zone by positive control (mm)

N = diameter of zone by negative control (mm)

Fig. 4.31 shows the quantitative results of the cytotoxicity test for the positive control (PC), negative control (NC) and the polymers of PHB, PHBV(5%), PHBV(8%) and PHBV(12%) thin films. While the cytotoxicity was 100% for the positive control, PHB, PHBV(5%), PHBV(8%) and PHBV(12%) films showed cytotoxicities of 18.4%, 12.7%, 10.6% and 12.7% respectively, which clearly illustrates very low cytotoxic effects of PHB and PHBV polymers. Therefore, the PHB and PHBV polymers used here for tissue engineering are deemed non-toxic and further biocompatibility testing with liver cells are indicated.

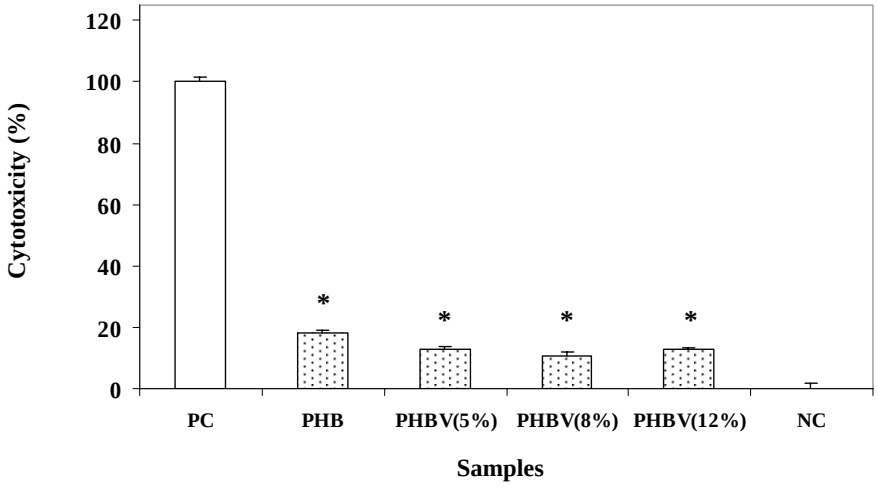

Fig. 4.31. Cytotoxicity results for positive control (white bar), negative control (black bar) and polymer thin films (dotted bars). Values represent means ± SD, n = 5. Statistical analysis was performed by Student t-test. *$p < 0.01$.

4.7. Liver Cells Seeding on Polymer Scaffolds

From the optical microscope images of Hep3B cells cultured on TCP in Fig. 4.32, the hepatocytes were observed to have rounded-structures for the first 30 min after attachment (Fig. 4.32A); after 4 days of cultures (Fig. 4.32B), they spread and flatten to form polygonal shape, 20-40 μm in dimension. The cells firmly adhered to the substrate and formed tight contact with each other, forming a confluent monolayer of

cells. Hepatocytes are anchorage-dependent cells, and therefore need a solid substratum or a scaffold for adhesion, growth, proliferation and function. For this reason, biodegradable and biocompatible PHB and PHBV scaffolds were used in the forms of two-dimensional thin films and three-dimensional microspheres for liver cells growth in this research.

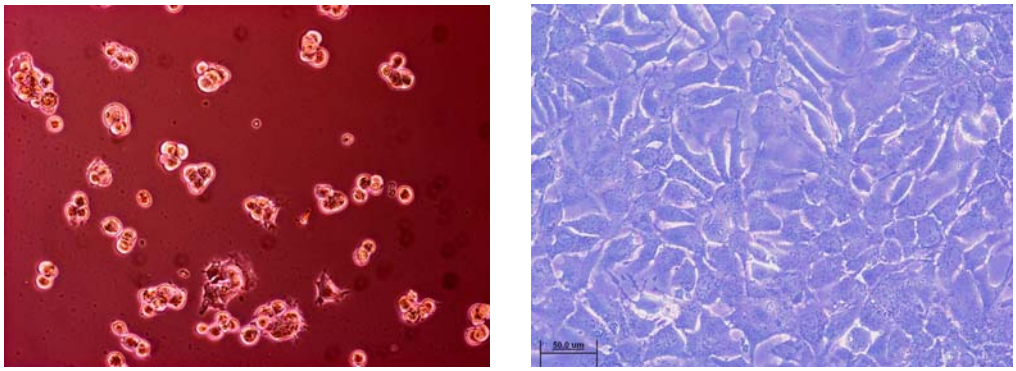

(A) (B)

Fig. 4.32. Optical micrographs of Hep3B attached on TCP: (A) 30 min and (B) 4 days, after seeding.

4.7.1. Liver Cells Growth on 2D Polymer Thin Films

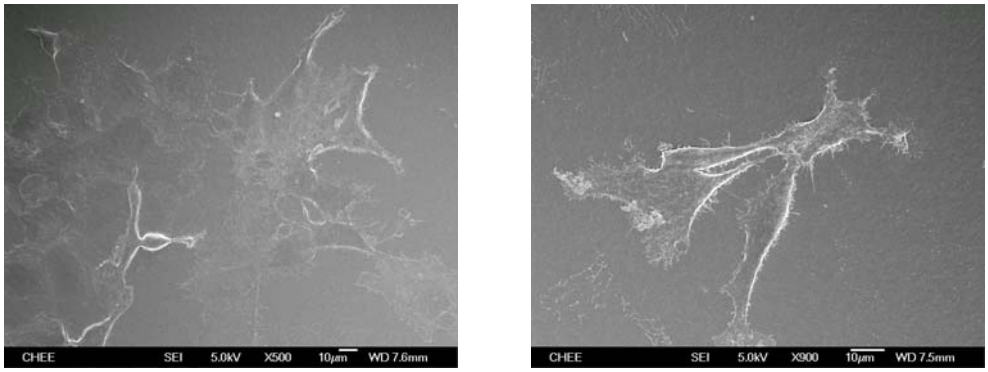

Fig. 4.33. Scanning electron micrographs of Hep3B cells adhere on the typical PHBV(5%) thin films, 3 days after culture. Size of the scale bar is 10 µm.

Fig. 4.33 highlights the SEM scans of Hep3B cells grown on the representative PHBV(5%) thin film after fixation. The adherent cells on the film were spread and

flattened to form a monolayer. The same phenomena were observed for the PHB, PHBV(8%) and PHBV(12%) films.

In order to investigate the viability of Hep3B cells seeded on the polymer thin films, the cells were stained with a two-color fluorescent live/dead stain, incubated at 37ºC for 1 h and the cells were observed using a laser scanning confocal microscope (LSCM). The LSCM micrograph in Fig. 4.34 shows the florescent green-colored live cells attached on the representative PHBV(8%) thin film. No dead cells were observed in this figure.

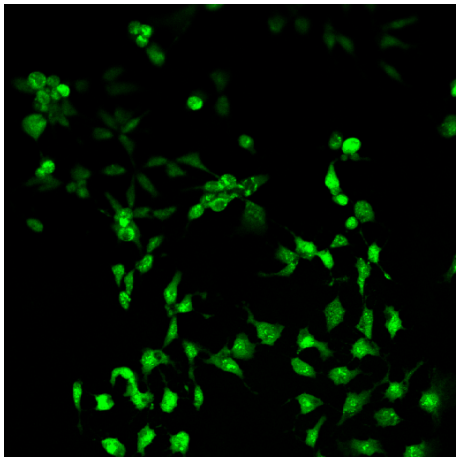

Fig. 4.34. Laser confocal micrograph of Hep3B grow on the representative PHBV(8%) thin film.

4.7.2. Liver Cells Growth on 3D Polymer Microspheres

Cellular morphology and hepatic specific functions of Hep3B cells on two-dimensional thin films were compared with Hep3B cells on three-dimensional microspheres. The morphology of the seeded cells on the representative PHBV(12%) microspheres at various days of culture is shown in the optical micrograph images in Fig. 4.35.

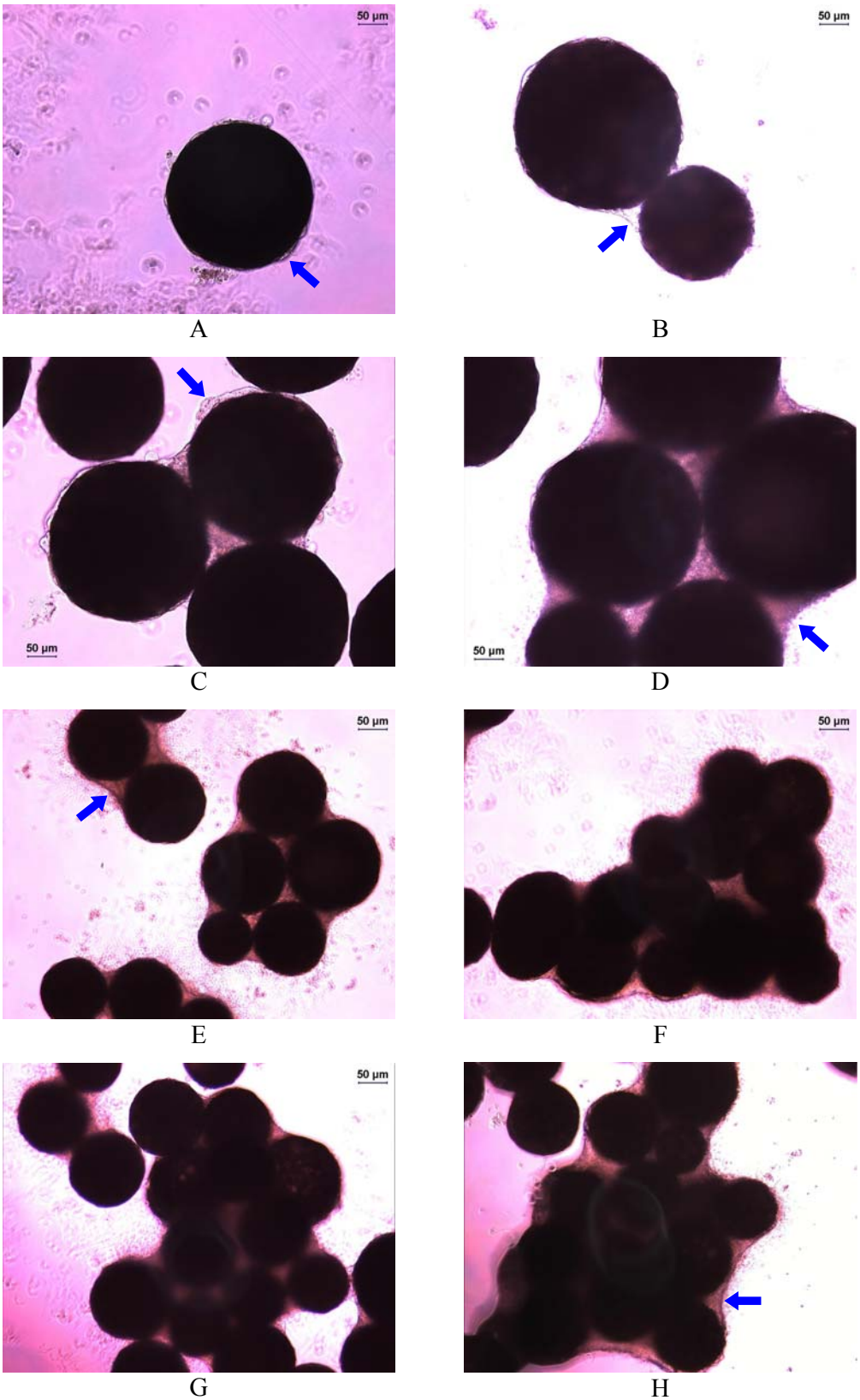

Fig. 4.35. Optical micrographs of Hep3B growth characteristics on the representative PHBV(12%) microspheres. (A) day 2, (B) day 4, (C) day 6, (D) day 8, (E) day 10, (F) day 12, (G) day 14 and (H) day 16.

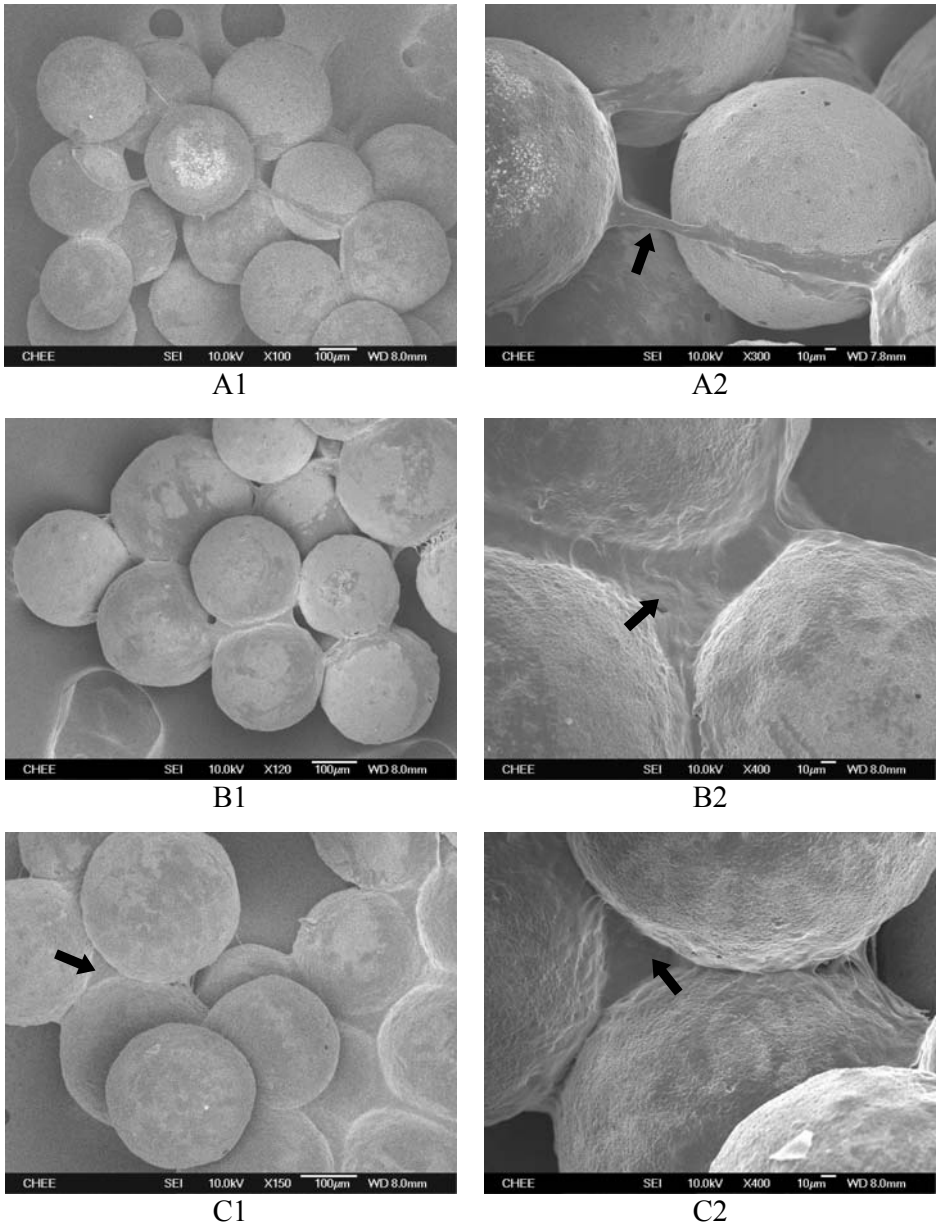

Fig. 4.36. SEM micrographs of Hep3B seeded on the microspheres after 2 weeks: (A) PHB, (B) PHBV(5%) and (C) PHBV(8%). Size of the scale bar of A1, B1 and C1 is 100 µm and that of A2, B2 and C2 is 10 µm.

From Fig. 4.35, few cells (see arrows) were found attached to the microspheres after 2 days of culture (A). Cell-cell contacts between two microspheres occurred after 4 days of culture (B). From day 6 onwards, cells were observed to bridge one microsphere to other microspheres (C-F) as well as stretching to fill the gaps between the microspheres, forming multilayers of cells. After 2 weeks of culture, cells were seem

to become confluent on the microspherical scaffolds and developed cell-polymer aggregates that led to a tissue-like structure (G-H). Therefore, it can be seen that three-dimensional microspheres are suitable as adhesive substrates for cells during *in-vitro* culture that encourages subsequent formation of artificial liver tissue.

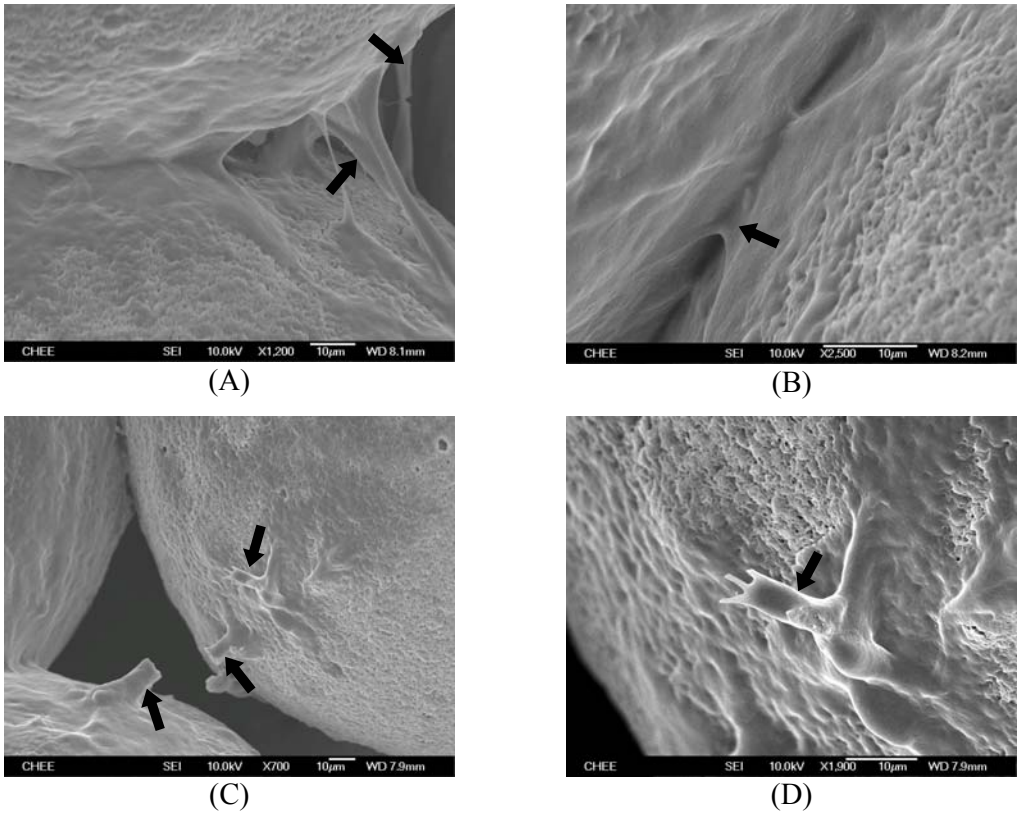

Fig. 4.37. SEM scans of cell-cell and cell-substrate interactions on the (A & B) PHBV(8%), and (C & D) PHBV(5%) microspheres after two weeks. Size of the scale bar is 10 μm.

As shown in Fig. 4.36, cellular morphologies of adhered cells on the microspheres after 2 weeks observed by SEM were similar from those taken by an optical microscope. The adhered cells (see arrows), in the forms of bridge-like structures, connected the gaps between the microspheres to achieve artificial tissue formation. Moreover, magnified SEM images of fixed cells in Fig. 4.37 clearly show strong cell-cell interaction as well as cell-substratum interaction of the liver cells and the polymer

microspheres. It can be seen that multilayers of cells bridged the microspheres and covered the surfaces; and therefore, the porous surface of the microspheres could not be seen in these area. This confirms the cells were seeded well on the microspheres.

The laser confocal images (Fig. 4.38) were also taken to reveal the morphologies of cells adhered on the microspheres by live/dead assay, where the bright green color represents live cells. No dead cells were observed in these figures.

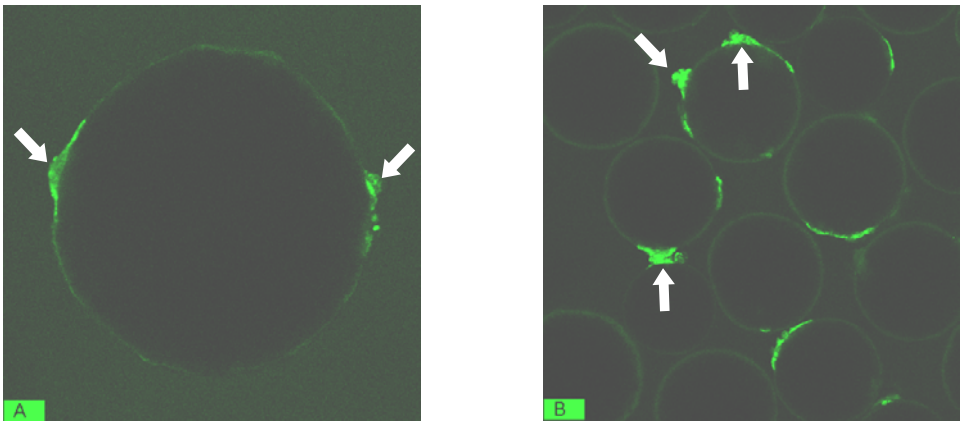

Fig. 4.38. 2D confocal microscopy images of Hep3B cells seeding on the typical PHB microspheres at 5 days of culture.

4.8. Cell Viability Test

The viability and proliferation of cultured cells can be measured by various techniques, including dye exclusion (trypan blue), dye penetration (MTT and live/dead assay), cell functional assays (EROD, ELISA), the rate of DNA synthesis, the rate of protein synthesis or the intracellular adenylate energy charge [Butler, 1997]. In this study, we measured cell viability and proliferation by trypan blue exclusion, live/dead staining and MTT assay.

4.8.1. Cell Proliferation Determination by MTT assay

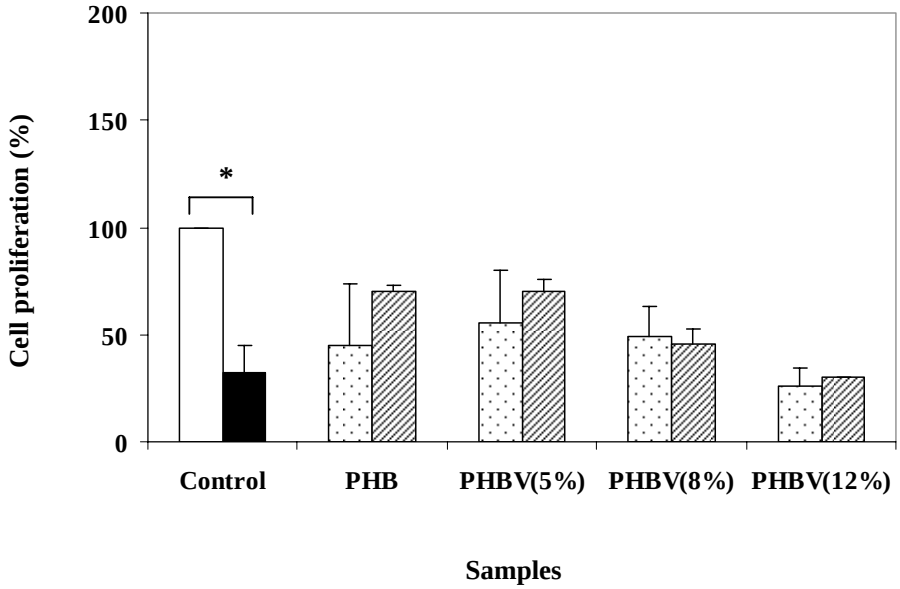

Fig. 4.39. MTT results of Hep3B viability at 2 days culture onto positive control (white bar), negative control (black bar), thin films (dotted bars) and microspheres (hatched bars). Values represent means ± SD, $n = 2$. Statistical analysis was performed by Student *t*-test. * $p < 0.05$.

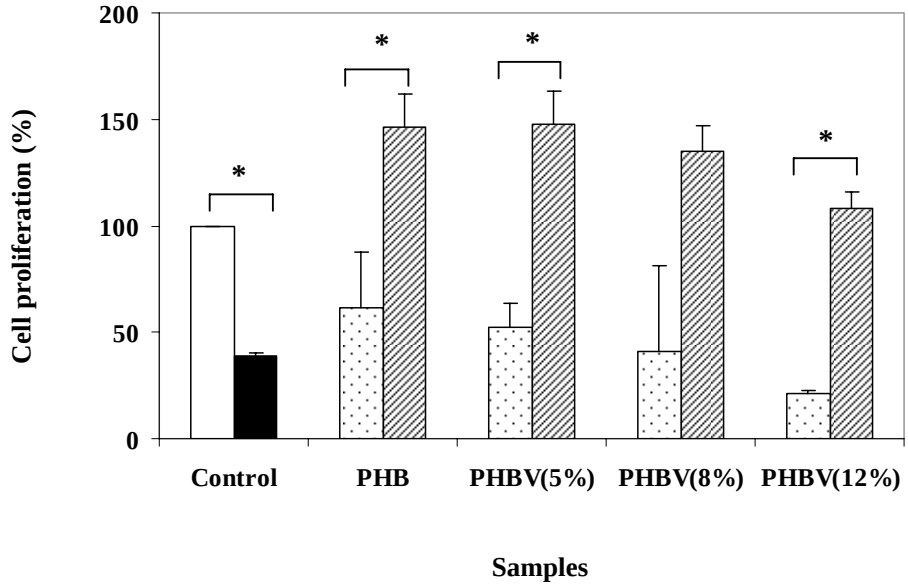

Fig. 4.40. MTT results of Hep3B viability at 6 days culture onto positive control 0(white bar), negative control (black bar), thin films (dotted bars) and microspheres (hatched bars). Values represent means ± SD, $n = 2$. Statistical analysis was performed by Student *t*-test. *$p < 0.05$.

The proliferation of Hep3B cells on both films and microspheres, including positive control and negative control, were validated using a colorimetric methylthiazol tetrazolium (MTT) assay. The results of the MTT assay for Hep3B proliferation on the scaffolds after 2 days and 6 days culture are shown in Fig. 39 and Fig. 4.40 respectively.

The proliferation of the cells was calculated by the following equation:

$$\text{Cell proliferation}\,(\%) = \frac{S}{PC} \times 100 \tag{4.5}$$

where,

S = formazan concentration on the sample scaffold

PC = formazan concentration on the positive control

The quantitative MTT results showed that the cell proliferation on thin films and microspheres were not significantly different at 2 days of culture (Fig. 4.39). On day 2 of culture, the proliferations on the PHB, PHBV(5%), PHBV(8%) and PHBV(12%) thin films were 45%, 55%, 50% and 26% respectively, while the cell proliferations on the respective microspheres were slightly increased at 70%, 70%, 45% and 30%. It was observed that the cell proliferation on the PHB, PHBV(5%) and PHBV(8%) scaffolds were between the positive control and negative control at 2 days of culture period. At 6 days of culture, the proliferations of the cells on the PHB, PHBV(5%), PHBV(8%) and PHBV(12%) thin films were 62%, 52%, 41% and 21% respectively based on 100% proliferation on the positive control (Fig. 4.40). At the same culture period, the cell proliferations on the respective microspheres were evidently raised to

146%, 148%, 135% and 108% respectively. These were significantly grater than the two-dimensional thin films for all of the copolymers.

Many paper have been previously reported that cellular morphology, cell adhesion, proliferation and function depended on the shape of the scaffolds, types of polymer and surface properties of the polymer scaffold, including wettability and copolymer composition [Catapano, 2001, Deng, 2002 and Krasteva, 2002]. From the results obtained by this work, it might be theorized that the cell proliferation was related to the shape of the polymer scaffolds since the cell proliferation on 3D microspheres were more than 2-5 times higher than that on 2D thin films at day 6. In addition, the cells prefer to proliferate on a more hydrophilic and smoother surface of the scaffold. The results showed that the proliferation of the cells observed at 6 days on the more hydrophilic PHB (146%), PHBV(5%) (148%) and PHBV(8%) (135%) microsphere scaffolds are much more than that onto the most hydrophobic PHBV(12%) (108%). Cell proliferation was also hypothesized to depend on the surface smoothness of the scaffold as cells proliferate better to a smoother surface. Among PHB, PHBV(5%), PHBV(8%) and PHBV(12%) microspheres, the latter has a rougher surface compared with the formers, corresponding to the results of having the lowest cell adhesion. This phenomenon is in agreement with by Yang et al. who has reported that mouse fibroblast cell line, L-929, grew better on lipase treated PHB film with a smooth surface than on untreated film with a rough surface [Yang, 2002].

4.9. Measurement of Liver Cell Functionalities

Hepatocytes perform many specific functions including albumin secretion, cytochrome P-450 activity, coagulation proteins, lipoprotein expression and so forth

[Michalopoulos, 1999]. In general, human hepatocytes readily dedifferentiate and lose their functions within a few days when cultured *in vitro*. Many researchers have attempted to retain the hepato-specific functions and viability for longer periods by coculturing hepatocytes with other cell types such as hepatic stellate cells (HSCs), which are known to be the main ECM producing cells within the liver [Riccalton-Banks, 2003], or 3T3 fibroblast cells [Bhandari, 2001], and by modifying the culture surface with ECM [Bissell, 1985]. In this present work, hepatospecific functions of the liver cells including cytochrome P-450 activity and albumin secretion were analyzed at various time points, to determine if the functionalities can be better retained when cultured on 3D microspheres.

4.9.1. Cytochrome P-450 Activity

Cytochrome P-450 activities of Hep3B on 2, 4 and 6 days culture times were evaluated by EROD assay as shown in Fig. 4.41. Although the EROD activities of Hep3B significantly increased up to 6 days of culture on 3D microspheres, it showed no significant difference on 2D thin films. P-450 activities of hepatocytes cultured on day 6 on the microspheres were significantly higher than those on thin films. The highest P-450 activity was observed with PHBV(5%) microspheres on day 6, comparable to PHB and PHBV(8%). In these figures, PHB, PHBV(5%), PHBV(8%) and PHBV(12%) thin films were represented as T0, T5, T8 and T12 while M0, M5, M8 and M12 represent PHB, PHBV(5%), PHBV(8%) and PHBV(12%) microspheres, respectively.

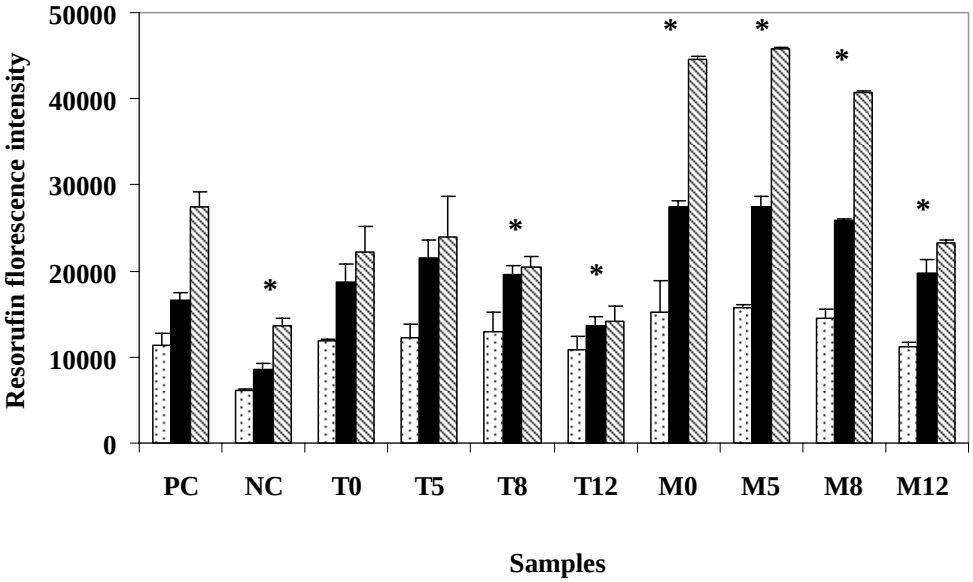

Fig. 4.41. Cytochrome P-450 activity of Hep3B cells attached onto controls, thin films and microspheres on 2 days (dotted bars), 4 days (black bars) and 6 days (hatched bars). Values represent means ± SD, n = 3. Statistical analysis was performed by Student t-test. *$p < 0.05$.

To determine the liver cell activity for P-450, P-450 activity/cell was calculated (data not shown) by dividing the activity value with the MTT data. The P-450 activity/cell of the liver cells seeded on the PHB (0.45), PHBV(5%) (0.48) and PHBV(8%) (0.41) thin films on day 6 were nearly double compared with that on 2 days culture, 0.24, 0.24 and 0.26 respectively. In contrast, P-450 activity/cell of the PHB (0.30), PHBV (0.32) and PHBV(8%) (0.29) microspheres on day 2 were significantly increased to about 3 folds, 0.89, 0.92 and 0.81 respectively at 6 days of culture. Although the same number of cells (5 x 10^4 cells/well/mL) was used for all culture periods, P-450 activity was higher at day 6 due to cell proliferation. In addition, P-450 activity on PHB, PHBV(5%) and PHBV(8%) microspheres increased 3 folds at day 6 while it showed the same activity on the respective this films. From these results, liver specific function of P-450 activity was better on 3D microspheres than on 2D thin films as well as after a longer culture period of 6 days.

4.9.2. Synthesis of Albumin Secretion

Fig. 4.42 shows the level of albumin secreted by liver cells seeded on the controls, thin films and microspheres. No significant differences were found for the different polymer thin films over the entire culture period. However, significant differences between thin films and microspheres were observed at 6 days of culture. The expression level of albumin was significantly increased at 6 days culture on the PHB (7.36), PHBV(5%) (7.9) and PHBV(8%) (6.7) microspheres compared to that on the respective thin films of 4.1, 3.8 and 3.8 on day 2. It can be observed that Hep3B attached on the microspheres secreted albumin 1-2 times more than that on the positive control (3.8) on day 6.

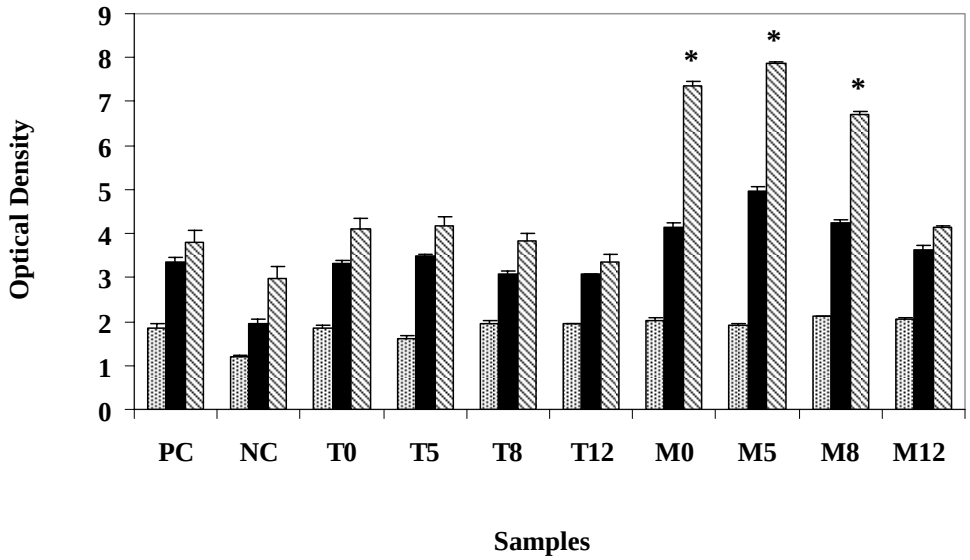

Fig. 4.42. Albumin secretion of Hep3B cells attached onto controls, thin films and microspheres on 2 days (dotted bars), 4 days (black bars) and 6 days (hatched bars). Values represent means ± SD, $n = 3$. Statistical analysis was performed by Student *t*-test. *$p < 0.05$.

The albumin secretion activity/cell was also calculated for the determination of albumin secretion by the liver cells by dividing the albumin activity by the MTT assay.

The albumin secretion activity/cell on the PHB (4.0×10^{-4}), PHBV(5%) (3.8×10^{-4}) and PHBV(8%) thin films (42×10^{-4}) increased from day 2 to (14.7×10^{-4}), (15.8×10^{-4}) and (13.4×10^{-4}) respectively on day 6. On the contrary, the albumin activity/ cell of the PHB (0.30), PHBV (0.32) and PHBV(8%) (0.29) microspheres on day 2 were significantly increased 3-4 folds, to 0.89, 0.92 and 0.81 respectively at 6 days of culture. Moreover, the albumin secretion activity/cell was 1.2-2 times higher on the microspheres than on thin films on day 6 while it was almost the same for both thin films and microspheres on day 2. According to the results obtained by ELISA, it can be seen that the level of albumin secretion by Hep3B were higher on the microsphere scaffolds than both the polymer thin films and the positive control. In addition, the liver specific function of albumin secretion in the culture medium was better on longer term on day 6 culture period. Therefore, 3D microsphere scaffolds show higher support for liver cells to function and have a potential role for fabricating artificial liver tissue formation *in vitro*.

Chapter 5

Conclusions and Recommendation

5.1. Conclusions

Tissue engineering is one of the biomedical strategies that support the regeneration of injured or wounded body tissue by growing cells on scaffolds into tissues. In particular, anchorage dependent cells require artificial scaffolds to form engineered tissue *in vitro*. Recently, microbial PHB and PHBV polyesters have attracted much attention for biomedical application due to their biodegradability, biocompatibility, low toxicity, thermoplasticity, piezoelectricity, optical activity and stereospecificity. In this research, PHB, PHBV(5%), PHBV(8%) and PHBV(12%) were specifically chosen to be fabricated into two-dimensional thin films, and also three-dimensional microspheres to be used as artificial scaffolds. The porous microspherical polymer scaffolds are hypothesized to assist in enabling a significant increase in liver cell growth, proliferation and liver specific functions.

The optimum values of the microsphere synthesis parameters on the size, shape and surface morphology of the microspheres were found to be copolymer compositions (5% and 8%), polymer solution concentration (5%), emulsifier concentration (0.05%), oil/first aqueous volume ratio (10:1), solvent (chloroform), homogenizing speed (16000 rpm) and time (15 s), stirrer height ($\approx$ 1 inch), stirring speed (300 rpm), stirring

time (3 h), evaporation temperature (38ºC), lyophilization time (72 h) and molecular weight of the polymers (see Table 4.12).

Hydrolytic degradation of the microspheres was monitored for up to one year to study the behaviour in a simulated physiological environment. After one year of degradation, the weight loss of the PHB, PHBV(5%), PHBV(8%) and PHBV(12%) microspheres were 16.5%, 22%, 26% and 34%, respectively. The molecular weight decrease was observed to be slow up to 3 months of degradation but the decrease accelerated after 8 months. GPC results showed that the molecular weight of the PHB, PHBV(5%), PHBV(8%) and PHBV(12%) microspheres was reduced to 46%, 58%, 53% and 48% of the respective initial value after a one-year-period.

The SEM images showed the external and internal morphologies of the microspheres before and after degradation. In general, the microspheres were spherical with rough surfaces with many vesicles in the core. The microspheres possessed smaller pores before degradation, with pore sizes increasing as the degradation proceeded. The results also showed that degradation occurred both by surface and bulk erosion. Contact angle measurement of polymer thin films was selected to characterize the hydrophilicity and hydrophobicity of PHB and PHBV polymers as the wettability plays an important role for cell viability. The PHBV(12%) thin films exhibited the largest contact angle (81.9ºC), resulting in it having the lowest cell viability compared with PHB (75.3ºC), PHBV(5%) (77.7ºC) and PHBV(8%) (79.6ºC).

Degradation of the microspheres was found to lead to an increase in the crystallinity in the remaining polymer as a result of amorphous regions being subjected to faster

degradation than the crystalline regions. Therefore, the degradation of more crystalline PHB was seen to be slower than that of the more amorphous PHBV copolymers. Before degradation, DSC results proved that PHB was the most crystalline (62%), having the highest molecular weight (851100 Da), melting temperature (176ºC) and glass transition temperature (6ºC). At the same time, the crystallinity of PHBV(5%), PHBV(8%) and PHBV(12%) are 32%, 30% and 25%, respectively. The T_m and T_g of the copolymers also decreased with increasing PHV content. The T_m of PHBV(5%), PHBV(8%) and PHBV(12%) are 154ºC, 149ºC and 148ºC, while the T_g are 2ºC, –1ºC and –3ºC, respectively.

The proton NMR spectra of PHB and PHBV microspheres were used to characterize their chemical structures and confirm the degradation results obtained by GPC and DSC. The peak at 1.6 ppm was found to correspond to ethyl groups in PHV, and the peaks at 1.3 ppm and 0.9 ppm were found to correspond to methyl groups in PHB and PHV respectively. ^{1}H-NMR data showed that the mole percent of PHB content increased and that of PHV decreased from its initial value after one year degradation. Hence, the hydrolytic degradation was greater for the amorphous PHV than more crystalline PHB, which is consistent with the degradation results obtained by GPC and DSC.

The chemical composition of the microspheres was investigated using XPS. The peaks at binding energy 285 eV, 286 eV and 289 eV are indicative of C–C bond, C–O bond and C=O bond, respectively. The atomic percentages of carbon element on the PHB and PHBV microspheres were 71.87%, 74.11%, 72.84% and 65.86% while that of the respective oxygen element are 27.87%, 25.45%, 26.57% and 28.53% before

degradation. FTIR spectroscopy was employed to determine the chemical structure (functional groups) of the microspheres. The presence of O–H, C–H, C=O and C–O–C bond was evident at the absorption bands between 3428–3440 cm^{-1}, 2931–2937 cm^{-1}, 1718–1741 cm^{-1} and 1060–1186 cm^{-1}, respectively.

To evaluate the biocompatibility of the polymers, a direct contact cytotoxicity test was performed according to the ISO 10993-5 standard using the mouse fibroblast cell line, L-929. A HDPE film was used as the negative control while a ZDBC film was used as the positive control. The cytotoxicities of PHB, PHBV(5%), PHBV(8%) and PHBV(12%) were 18.4%, 12.7%, 10.6% and 12.7% respectively while the cytotoxicity of the positive control is 100%. Therefore, it can be observed that PHB and PHBV polymers are of very low cytotoxicity.

The unique physical properties, biodegradability, biocompatibility and low cytotoxicity is considered advantageous to the use of PHB and PHBV scaffolds for *in vitro* culture of human hepatoma cell line, Hep3B. The cells seeded on the microspheres remained viable for up to 20 days of culture. The optical and LSCM micrographs showed that Hep3B cells adhered in spread and flattened monolayers on 2D thin films. However, the microspheres permitted the cells to grow and adhere in multilayer forming three-dimensional structures. SEM images proved that Hep3B cells were firmly attached and grew well on the scaffolds, developing into cell-polymer aggregates.

The cell proliferation both on the thin films and microspheres were measured by MTT assay. The statistical results indicated that the cells on both thin films and

microspheres were not different at 2 days of culture. However, on day 6, a significant increase of the cells was found on the microspheres in comparison to the thin films. The cell proliferation increased 2 to 5 folds on the microspheres from day 2 to day 6. A hydrophilic smooth surface of a scaffold enhances cell growth while hydrophobic rough surfaces reduce cell-substrate interaction. Therefore, for both thin film and microsphere scaffolds, the cell proliferation on more hydrophilic and smoother surface of PHB and PHBV(5%) scaffolds were higher than that on more hydrophobic and rougher surface of PHBV(8%) and PHBV(12%) scaffolds. The highest cell proliferations were observed on the PHB thin films (62%) and the PHBV(5%) microspheres (148%), while the lowest cell proliferations were observed on the PHBV(12%) thin films (21%) and the PHBV(12%) microspheres (108%) on 6 days of culture.

Among the various functions performed by a liver, the most important hepatic functions such as cytochrome P-450 activity and albumin secretion were evaluated for both the microspheres and thin films up 2 and 6 days of culture. P-450 activity for detoxification of the liver cells was measured by an ethoxyresorufin-O-deethylase (EROD) assay. The P-450 activity of Hep3B cultured on the thin films and microspheres was not significantly different at day 2 of culture. However, the activity on the PHB, PHBV(5%) and PHBV(8%) microspheres at 6 days of culture was 2 times higher than that of thin films. The highest P-450 activity was observed on the PHBV(5%) microspheres on day 6, followed by PHB and PHBV(8%) microspheres. The secretion of albumin (blood serum protein) of the liver cells was also evaluated by an enzyme-linked immunosorbent (ELISA) assay. ELISA results showed that albumin secreted by Hep3B cultured on the microspheres was 2 to 4 times increasing up to day

2 to day 6. Hep3B attached on the PHBV(5%) microspheres secreted the highest level of albumin (7.9 OD), followed by PHB (7.4 OD) and PHBV(8%) microspheres (6.7 OD). In contrast, Hep3B on thin films secreted the albumin double from day 2 to day 6 culture.

In conclusion, the PHB, PHBV(5%) and PHBV(8%) microspheres can be considered as promising polymer scaffolds for liver tissue engineering because of the relatively good liver cell growth and display of specific functional activities on these scaffolds in addition to its biodegradability, biocompatibility and low cytotoxicity.

5.2. Recommendation

Some recommendations for future investigations include:

1. Although PHB and PHBV dissolve well in chloroform, it is one of the toxic solvents known to cause liver cancer. Therefore, other suitable solvent should be used in making PHB and PHBV scaffolds, especially for liver cell growth.
2. To attain faster degradation rate, the degradation should be carried out enzymatically instead of hydrolytically.
3. To achieve long-term maintenance of liver-specific functions, co-culturing of hepatocytes with a range of different cell types should be investigated.

Bibliography

Anderson, J.M. and M.S. Shive. *Biodegradation and biocompatibility of PLA and PLGA microspheres*, Advanced Drug Delivery Reviews, **28**, pp. 5-24. 1997.

Allen, J.W. and S.N. Bhatia. *Engineering liver therapies for the future*. Tissue engineering, **8**, pp. 725-737. 2002.

Amass, W., A. Amass and B.A. Tighe. *Review of biodegradable polymers: Uses, current developments in the synthesis and characterization of biodegradable polyesters, blends of biodegradable polyesters and recent advances in biodegradation studies*, Polymer International, **47**, pp. 89-144. 1998.

Aoyagi, Y., Y. Doi and T. Iwata. *Mechanical properties and highly ordered structure of ultra-high-molecular-weight poly[(R)-3-hydroxybutyrate] films: Effects of annealing and two-step drawing*, Polymer Degradation and Stability, **79**, pp. 209-210. 2003.

Ashby, R.D., F. Shi and R.A. Gross. *Use of Poly(ethylene glycol) to control the end group structure and molecular weight of poly(3-hydroxybutyrate) formed by alcaligenes latus DSM 1122*, Tetrahedron, **53**, pp. 15209-15223. 1997.

Avella, M., E. Martuscelli, G. Qrsello, M. Raimo and B. Pascucci. *Poly(3-hydroxybutyrate)/poly(methyleneoxide) blends: thermal, crystallization and mechanical behavior*. Polymer, **38**, pp. 6135-6143. 1997.

Avella, M. and E. Martuscelli. *Poly-D(—)(3-hydroxybutyrate)/poly-(ethylene oxide) blends: phase diagram, thermal and crystallization behavior*. Polymer, **29**, pp. 1731-1737. 1998.

Azuma, Y., N. Yoshie, M. Sakurai, Y. Inoue and R. Chujo. *Thermal behavior and miscibility of poly(3-hydroxybutyrate)/pol(vinyl alcohol) blends*. Polymer, **33**, pp. 4763-4767. 1992.

Bhandari, R.N.B., L.A. Riccalton, A.L. Lewis, J.R. Fry, A.H. Hammond, S.J.B. Tendler and K.M. Shakesheff. *Liver tissue engineering: A role for co-couture systems in modifying hepatocyte function and viability*, Tissue Engineering, **7**, pp. 345-409. 2001.

Bissell, D.M., J.J. Maher and F.J. Roll. *Cell-matrix interaction in liver: Effects of defined or complex substrata on albumin secretion by rat hepatocytes*, Hepatology, **5**, pp. 1038. 1985.

Bloembergen, S.D., A. Holden, G.K. Hamer and L. Terry. *Studies of composition and crystallinity of bacterial poly(β-hydroxybutyrate-co-β-hydroxyvalerate)*, Macromolecules, **19**, pp. 2865. 1986.

Blumm, E. and A.J. Owen. *Miscibility, crystallization and melting behavior of P(3-hydroxybutyrate)/poly(L-lactide) blends*, Polymer, **36**, pp. 4077-4081. 1995.

Brown, R.A. *Tissue engineering: clinical applications and mechanical control*. In *Future strategies for tissue and organ replacement,* ed by J.M. Polak, L.L. Hench and P. Kemp. pp. 27. London: Imperial College Press. 2002.

Biological evaluation of medical devices-part 5: Test for *in vitro* cytotoxicity, BS EN ISO 10993-5:1999.

Burke, M.D. and R.T. Mayer. *Inherent specificities of purified cytochromes P-450 and P-448 toward biphenyl hydroxylation and ethoxyresorufin deethylation*, Drug Metabolism and Disposition, **3**, pp. 245-253. 1975.

Burkersroda, F., L. Schedl and A. Göpferich. *Why degradable polymers undergo surface erosion or bulk erosion*, Biomaterials, **23**, pp. 4221-4231. 2002.

Butler, M. *Animal cell culture and technology: The basics*. pp. 11, New York: Oxford University Press. 1997.

Cao, A., N. Asakawa, N. Yoshie and Y. Inoue. *Phase structure and biodegradation of the bacterial poly(3-hydroxybutyric acid)/chemosynthetic poly(3-hydroxypropionic acid) blend*, Polym. J., **30**, pp. 743-752. 1998.

Catapano, G., L.D. Bartolo, V. Vico and L. Ambrosio. *Morphology and metabolism of hepatocytes cultured in Petri dishes on films and in non-woven fabrics of hyaluronic acid esters*, Biomaterials, **22**, pp. 659-665. 2001.

Chatterjee, J., Y. Haik and C.J. Chen. *Modification and characterization of polystyrene-based magnetic microspheres and comparison with albumin-based magnetic microspheres*, Journal of Magnetism and Magnetic Materials, **225**, pp. 21-29. 2001.

Chen, L.J. and Wang, M. *Production and evaluation of biodegradable composites based on PHB–PHV copolymer*, Biomaterials, **23**, pp. 2631-2639. 2002.

Chung, T.W., J. Yang, T. Akaike, K.Y. Cho, J.W. Nah, S.I. Kim and C.S. Cho. *Preparation of alginate/galactosylated chitosan scaffold for hepatocyte attachment*, Biomaterials, **23,** pp. 2827-2834. 2002.

Dave, B., M. Parikh, M.S. Reeve, R.A. Gross and S.P. McCarthy. *Morphological and blend miscibility effects on the biodegradability of poly(3-hydroxybutyrate-co-3-hydroxyvalerate) and blends*, Polym. Mater. Sci. and Eng., Am. Chem. Soc., **63**, pp. 726. 1990.

Deng, X.M., J.Y. Hao, M.L. Yuan, C.D. Xiong and S.J. Zhao. *Miscibility, thermal behavior, morphology and mechanical properties of binary blends of poly[(R)-3-hydroxybutyrate] with poly(γ-benzyl-L-glutamate)*. Polym. Int., **50**, pp. 37-44. 2001.

Deng, Y., K. Zhao, X.F. Zhang, P. Hu and G.Q. Chen. *Study on the three-dimensional proliferation of rabbit articular cartilage-derived chondrocytes on polyhydroxy-alkanoate scaffolds*, Biomaterials, **23**, pp. 4049-4056. 2002.

Doyle, C., E.T. Tanner and W. Bonfield. *In vitro and in vivo evaluation of polyhydroxybutyrate and of polyhydroxybutyrate reinforced with hydroxyapatite*, Biomaterials, **12**, pp. 841-847. 1991.

Doyle, A. and J.B. Griffiths. (ed). *Cell and tissue culture for medical research*. England: John Wiley & Sons. 2001.

Dufresne, A. and M. Vincendon. *Poly(3-hydroxybutyrate) and poly(3-hydroxyoctanoate) blends: morphology and mechanical behavior*, Macromolecules, **33**, pp. 2998-3008. 2000.

Dunn, J.C., R.G. Tompkins and M.L. Yarmush. *Long-term in vitro function of adult hepatocytes in a collagen sandwich configuration*, Biotechnol. Prog., **7**, pp.237. 1991.

Duvernoy, O., T. Malm, J. Ramström and S. Bowald. *A biodegradable patch used as a pericardial substitute after cardiac surgery: 6 and 24 month evaluation with CT*, Thorac. Cardiovasc. Surg., **43**, pp. 271-274. 1995.

Elisseeff, J.H., R. Langer and Y. Yamada. *Biomaterials for tissue engineering*. In *Tissue engineering and biodegradable equivalents: Scientific and clinical applications*. ed by K.U. Lewandrowski, D.L. Wise, D.J. Trantolo, J.D. Gresser, M.J. Yaszemski and D.E. Altobelli, pp. 145-164, New York: Marcel Dekker Inc. 2002.

Ertl, B., P. Platzer, M. Wirth and F. Gabor. *Poly(D,L-lactide-co-glycolic acid) microspheres for sustained delivery and stabilization of camptothecin*, Journal of Controlled Release, **61**, pp. 305-317. 1999.

Flendrig, L.M., J.W. la Soe, G.G. Jorning, A. Steenbeek, O.T. Karlsen and W.M. Bovee. *In vitro evaluation of a novel bioreactor based on an integral oxygenator and a spirally wound nonwovan polyester matrix for hepatocyte culture as small aggregates*, J. Hepatol., **26**, pp. 1379-1392. 1997.

Gerlach, J.C., J. Encke, O. Hole, C. Miiller, C.J. Ryan and P. Neuhaus. *Bioreactor for a larger scale hepatocyte in vitro perfusion*, Transplantation, **58**, pp. 984. 1994.

Géze A., M.C.V. Julienne, P. Saulnier. P. Varlet, C.D. Duport, P. Devauchellec and J.P. Benoit. *Modulated release of IdUrd from poly(D,L-lactide-co-glycolide)*

microspheres by addition of poly (D,L-lactide) oligomers, Journal of Controlled Release, **58**, pp. 311-322, 1999.

Ghobrial, R.M., H. Yersiz, D.G. Farmer, F. Amersi, J. Goss, P. Chen, S. Dawson, S. Lerner, N. Nissen, D. Imagawa, S. Colquhoun, W. Araout, S.V. McDiarmid and R.W. Busuttil. *Predictors of survival after in vivo split liver transplantation: Analysis of 110 consecutive patients*, Ann. Surg, **232**, pp. 312. 2000.

Giessen, V.W.J., AM. Lincoff, R.S. Schwartz, H.M. van Beusekom, P.W. Serruys, D.R. Holmes, S.G. Ellis and E.J. Topol. *Marked inflammatory sequalae to implantation of biodegradable and nonbiodegradable polymers in porcine coronary arteries*, Circulation, **94**, pp. 1690-1697. 1996.

Gillard, J., B. Baras, M.A. Benoit and B.B.C. Youan. *Protein-loaded poly(ε-caprolactone) microparticles: I. Optimization of the preparation by (water-in-oil)-in-water emulsion solvent evaporation*, Journal of microencapsulation, **16**, pp. 587-599. 1999.

Gogolewski, S., M. Jovanovic, S.M. Perren, J.G. Dillon and M..K. Hughes. *Tissue response and in vivo degradation of selected polyhydroxyacids: polylactides (PLA), poly(3-hydroxybutyrate) (PHB), and poly(3-hydroxybutyrate-co-3-hydroxyvalerate) (PHB/VA)*, J. Biomed. Mat. Res., **27**, pp. 1135-1148. 1993.

Göpferich, A. *Mechanism of polymer degradation and elimination*. In *Handbook of biodegradable polymers*. ed by A.J. Domb, J. Kost and D.M. Wiseman, pp. 451-71, Amsterdam: Harwood Academic Publishers. 1997.

Gotfredsen, K., L. Nimb and E. Hjirting-Hansen. *Immediate implant placement using a biodegradable barrier, polyhydroxybutyrate-hydroxyvalerate reinforced with polyglactin 910. An experimental study in dogs*, Clin. Oral Implants Res., **5**, pp. 83-91. 1994.

Greco, P. and E. Martuscelli. *Crystallization and thermal behavior of poly(D(—)-3-hydroxybutyrate)-based blends*. Polymer, **30**, pp. 1475-1483. 1989.

Hashikura, Y., M. Makuuchi, S. Kawasaki, H. Matsunami, T. Ikegami, Y. Nakazawa, K. Kiyosawa and T. Ichida. *Successful living-related partial liver transplantation to an adult patient*, Lancet, **343**, pp. 1233. 1994.

Hocking, P.J. and R.H. Marchessault. Biopolyesters. In *Chemistry and technology of biodegradable polymers.* Ed. by G.J.L. Griffin, pp. 48-50. London: Chapman & Hall. 1994.

Holmes, P.A. *Applications of PHB - a microbially produced biodegradable thermoplastic,* Phys. Technol., **16**, pp. 32-36. 1985.

http://www.livertransplant.org.

Hu, S.G., C.H. Jou and M.C. Yang. *Protein adsorption, fibroblast activity and antibacterial properties of poly(3-hydroxybutyric acid-co-hydroxyvaleric acid) grafted with chitosan and chitooligosaccharide after immobilized with hyaluronic acid*, Biomaterials, **24**, pp. 2685-2693. 2003.

Iriondo, P., J.J. Iruin and M. Fernandez-Berride. *Thermal and infra-red spectroscopic investigations of a miscible blend composed of poly(vinyl phenol) and poly(hydroxybutyrate)*, Polymer, **36**, pp. 3235-3237. 2000.

Jain, R.A. *The manufacturing techniques of various drug loaded biodegradable poly(lactide-co-glycolide) (PLGA) devices*, Biomaterials, **21**, pp. 2475-2490. 2000.

Joly, A., J.F. Desjardins, B. Fremond, M. Desille, J.P. Campion, Y. Malledant, Y. Lebreton, G. Semana, F. EdwardsLevy, M.C. Levy and B. Clement. *Survival, proliferation, and functions of porcine hepatocytes encapsulated in coated alginate beads: A step toward a reliable bioartificial liver*, Transplantation, **63**, pp. 79. 1997.

Jun, X., B.H. Guo, R. Yang, Q. Wu, G.Q. Chen and Z.M. Zhang. *In situ FTIR study on melting and crystallization of polyhydroxyalkanoates*, Polymer, **43**, pp. 6893-6899. 2002.

Kassab, A.C., K. Xu, E.B. Denkbas, Y. Dou, S. Zhao and E. Piskin. *Rifampicin carrying polyhydroxybutyrate microspheres as a potential chemoembolization agent*, J. Biomater. Sci. Polym. Ed., **8**, pp. 947-961. 1997.

Kassab, R., H.P. Lopez, H. Fessi, J. Menaucourt, R. Bonaly and J. Coulon. *Molecular recognition by Kluyveromyces of amphotericin B-loaded, galactose-tagged, poly (lactic acid) microspheres*, Bioorganic and Medicinal Chemistry, **10**, pp. 767-1775. 2002.

Kepes, A. and Péaud Lenoël, C. Bull. Soc. Chim. Biol., **34**, pp. 563-575. 1952.

Kim, M.N., A.R. Lee, K.H. Lee, I.J. Chin and J.S. Yoon. *Biodegradability of poly(3-hydroxybutyrate) blended with poly(ethylene-co-vinyl acetate) or poly(ethylene oxide)*, European Polymer Journal, **35**, pp. 1153-1158. 1999.

King, P.P. *Biotechnology: An industrial view*. J. Chem. Tech. Biotechnol., **32**, pp. 2-8. 1982.

Kiss, É and E.I. Vargha-Butler. *Novel method to characterize the hydrolytic decomposition of biopolymer surfaces*, Colloids and Surfaces B: Biointerfaces, **15**, pp.181-193. 1999.

Kneser, U., P.M. Kaufmann, H.C. Fiegel, J.M. Pollok, X. Rogiers and D. Kluth. *Interaction of hepatocytes and pancreatic islets cotransplanted in polymeric matrices*, Virchows. Arch., **435**, pp. 125-132. 1999.

Köse, G.T., H. Kenar, N. Hasırcı and V. Hasırcı. *Macroporous poly(3-hydroxybutyrate-co-3-hydroxyvalerate) matrices for bone tissue engineering*, Biomaterials, **24**, pp. 1949-1958. 2003.

Kostopoulos, L. and T. Kaning. *Augmentation of the rat mandible using guided tissue regeneration*, Clin. Oral Implants Res, **5**, pp. 75-82. 1994.

Krasteva, N., U. Harms, W. Albrecht, B. Seifert, M. Hopp, G. Altankov and T. Groth. *Membranes for biohybrid liver support systems–investigations on hepatocyte attachment, morphology and growth*, Biomaterials, **23**, pp. 2467-2478. 2002.

Langer, R. and N. Peppas. *Chemical and physical structure of polymers as carriers for controlled release of bioactive agents: A review*, Journal of Macromolecular Science - Reviews in Macromolecular Chemistry and Physics, **23**, pp. 61-126. 1983.

Lee, S.Y. *Bacterial polyhydroxyalkanoates*, Biotechnol. Bioeng., **49**, pp. 1-14. 1996.

Li, A.P., D. Beck, S. Colburn, R. Monsell and C. Pellegrin. *Culturing of primary hepatocytes as entrapped aggregates in a packed bed bioreactor: A potential bioartificial liver*. In Vitro Cell. Dev. Biol., **3**, pp. 249-254. 1993.

Lim, F. (ed). *Biomedical applications of microencapsulation*. Boca Raton: CRC Press. 1984.

Lotti, N., M. Pizzoli, G. Ceccoruli and M. Scandola. *Binary blends of microbial poly(3-hydroxybutyrate) with polymethacrylates*, Polymer, **34**, pp. 4935-4940. 1993.

Malm, T., S. Bowald, S. Karacagil, A. Bylock and C. Busch. *A new biodegradable patch for closure of atrial septal defect. An experimental study*, Scand. J. Thorac. Cardiovasc. Surg., **1**, pp. 9-14. 1992.

Malm, T., S. Bowald, A. Bylock, C. Busch and T. Saldeen. *Enlargement of the right ventricular outflow tract and the pulmonary artery with a new biodegradable patch in transannular position*, Eur. Surg. Res., **26**, pp. 298-308. 1994.

Matsumura, K.N., G.R. Guevara, H. Huston, W.L. Hamilton, M. Rikimaru, G. Yamasaki and M.S. Matsumura. *Hybrid bioartificial liver in hepatic failure: Preliminary clinical report*, Surgery, **101**, pp. 99. 1987.

Matthew, H.W.T. *Polymers for tissue engineering scaffolds*. In *polymeric biomaterial*. 2nd ed, ed by S. Dumitriu, pp. 167-186. New York: Marcel Dekker, Inc.. 2002.

Michalopoulos, G.K. *Hepatocyte primary cultures*. In *Tissue engineering methods and protocols*. ed by Morgan, J.R. and M.L. Yarmush, pp. 227-243. NJ: Humana Press. 1999.

Mooney, D., L. Hansen, J. Vacanti, R. Langer, S. Farmer and D. Ingber. *Switching from differentiation to growth in hepatocytes: Control by extracellular matrix*, Journal of Cell Physiology, **151**, pp. 497-505. 1992.

Nebe, B., C. Forster, H. Pommerenke, G. Fulda, D. Behrend, U. Bernewski, K.P. Schmitz and J. Rychly. *Structural alterations of adhesion mediating components in cells cultured on poly-β-hydroxy butyric acid*, Biomaterials, **22**, pp. 2425-2434. 2001.

O'lkhov, A.A., A.L. Iordanskii and G.E. Zaikov. *Morphologically special features of poly(3-hydroxybutyrate)/low-density polyethylene blends*, Polym-Plast. Technol., **39**, pp. 783-792. 2000.

Paglia, E.D., P.L. Beltrame, M. Cannetti, A. Seves, B. Marcanall and E. Martuscelli. *Crystallization and thermal behavior of poly(D(—)-3-hydroxybutyrate)/poly-(epichlorohydrin) blends*, Polymer, **34**, pp. 996-1001. 1993.

Park, T.G. *Degradation of poly(D,L-lactic acid) microspheres: effect of the molecular weight*, J. Control. Release, **30**, pp. 161-173. 1994.

Peppas, N.A. and R. Langer. *New challenges in biomaterials*, *Science*, **264**, pp. 1065–1067. 1994.

Piskin, E. *Biomaterials in different forms for tissue engineering: An overview*. In *Porous materials for tissue engineering*. ed by D.M. Liu and V. Dixit, pp. 1-14. Switzerland: Trans Tech Publications. 1997.

Raja, S., J.R. Nery and S. Mies. *Liver transplantation from live donors*, Lancet, **2**, pp. 497. 1989.

Ramsay, J. A. and B.A. Ramsay. Appl. Phycol. Forum, **7**, 1990.

Ranucci, C.S., A. Kumar, S.P. Batra and P.V. Moghe. *Control of hepatocyte function on collagen foams: sizing matrix pores toward selective induction of 2-D and 3-D cellular morphogenesis*, Biomaterials, **21**, pp. 783-793. 2000.

Recum, A.F. (ed). *Handbook of biomaterials evaluation. Scientific, technical, and clinical testing of implant materials*. 2nd ed. pp. 211-385. US; Edwards Brothers. 1999.

Reusch, R.N. *Transmembrane ion transport by polypohosphatepoly-R-3-hydroxybutyrate complexes,* Biochem. Engl. Trans., **65**, pp. 280-295. 2000.

Riccalton-Banks, L., C. Liew, R. Bhandari, J. Fry and K. Shakesheff. *Long-term culture of functional liver tissue: Three-dimensional coculture of primary hepatocytes and stellate cells*, Tissue Engineering, **9**, pp. 401-409. 2003.

Rivard, C.H., C.J. Chaput, E.A. DesRosiers, L.H. Yahia and A. Selmani. *Fibroblast seeding and culture in biodegradable porous substrates*, J. Appl. Biomater., **6**, pp. 65-68. 1995.

Rubinsky, B. *Low temperature preservation of biological organs and tissues*. In *Future strategies for tissue and organ replacement*. ed by J.M. Polak, L.L. Hench and P. Kemp, pp. 27. London: Imperial College Press. 2002.

Saad, B., G. Ciardelli, S. Matter, M. Welti, G.K. Uhlschmid, P. Neuenschwander and U.W. Suter. *Characterization of the cell response of cultured macrophages and fibroblasts to particles of short chain poly[(R)-3-hydroxybutyric acid]*, J. biomed. Mater. Res., **30**, pp. 429-439. 1996.

Saito, T., K. Tomita, K. Juni and K. Ooba. *In vivo and in vitro biodegradation of poly(3-hydroxybutyrate) in rat*, Biomaterials, **12**, pp. 309-12. 1991.

Savenkova, L., Z. Gercberga, V. Nikolaeva, A. Dzene, I. Bibers and M. Kalnin. *Mechanical properties and biodegradation characteristics of PHB-based films*, Process. Biochem., **35**, pp. 573-580. 2000.

Scandola, M., G. Ceccoruli and M. Pizzoli. *Miscibility of bacterial poly(3-hydroxybutyrate) with cellulose esters***,** Macromolecules, **25**, pp. 6441. 1992.

Scherzer, T., *Barrier layers against oxygen transmission on the basis of electron beam cured methacrylated gelatin,* Nucl. Instrum. Meth. Phys. Res. B, **131**, pp. 382. 1997.

Selden, C. and H. Hodgson. *Engineering the liver*. In *Future strategies for tissue and organ replacement,* ed by J.M. Polak, L.L. Hench and P. Kemp, pp. 27. London: Imperial College Press. 2002.

Sendil, D., I. Gursel, D.L. Wise and V. Hasirci. *Antibiotic release from biodegradable PHBV microparticles*, J. Control. Rel., **19**, pp. 207-217. 1999.

Sharp, D.W.A. *The penguin dictionary of chemistry.* pp. 302. England: Penguin Books. 1985.

Shuai, X., Y. He, Y.H. Na and Y. Inoue. *Miscibility of block copolymers of poly(ε-caprolactone) and poly(ethylene glycol) with poly(3-hydroxybutyrate) as well as the compatibilizing effect of these copolymers in blends of poly(ε-caprolactone) and poly(3-hydroxybutyrate)*. J. Appl. Polym. Sci., **80**. pp. 2600-2608. 2001.

Simon. F.W., P.M. David, M.H. Daniel and P.P. Horowitz. *PHA applications: addressing the price performance issue: I. Tissue engineering*, International Journal of Biological Macromolecules, **25**, pp. 111–121. 1999.

Sodian, R., J.S. Sperling, D.P. Martin, A. Egozy, U. Stock, J.E. Mayer and J.P. Vacanti. *Fabrication of a trileaflet heart valve scaffold from a poly-hydroxyalkanoate biopolyester for use in tissue engineering*, Tissue Eng., **6**, pp. 183-188. 2000.

Starzl, T.E., T.L. Marchioro, K.N. Von Kaulla, G. Hermann, RS. Brittain and W.R. Waddell. *Homotransplantation of the liver in humans*, Surg. Gynecol. Obstet, **117**, pp. 659-676. 1963.

Starzl, T.E. *Liver allo-transplantation and xenotransplanation*, Transplant. Proc., 25, pp. 15. 1993.

Sun, A.M., Z. Cai, Z. Shi, F. Ma and G.M. O'Shea. *Microencapsulated hepatocytes: An in vitro and in vivo study*, Biomater. Artif. Cells Artif. Organs, **15**, pp. 483. 1987.

Sussman, N.L, G.T. Gislason, C.A. Conlin and J.H. Kelly. *The hepatic extracorporeal liver assist device: Initial clinical experience*. Artif. Organs., **18**, pp. 390-396. 1994.

Suthar, V., A. Pratap and H. Raval. *Studies on poly(hydroxy alkanoates)/(ethylcellulose) blends*, Bull. Mater. Sci., **23**, pp. 215-219. 2000.

Williamson, D.H., J.F. Wilkinson and J. Gen. Microbiol., **19**, pp. 198. 1958.

Vert M., P. Christel, F. Chabot and J. Leray. *Macromolecular materials*. pp. 119. Ch 4. FL: CRC Press. 1984.

Yang, Y.Y., H.H. Chia and T.S. Chung. *Effect of preparation temperature on the characteristics and release profiles of PLGA microspheres containing protein fabricated by double-emulsion solvent extraction/evaporation method*, Journal of Controlled Release, **69**, pp. 81-96. 2000.

Yang, Y.Y., J.P Wan, T.S. Chung, P.K. Pallathadka, S. Ng and J. Heller. *POE-PEG-POE triblock copolymeric microspheres containing protein: I. Preparation and characterization*. Journal of Controlled Release, **75**, pp. 115-128. 2001.

Yang, X., K. Zhao and G.Q. Chen. *Effect of surface treatment on the biocompatibility of microbial polyhydroxyalkanoates*, Biomaterials, **23**, pp. 1391-1397. 2002.

Youan, B.B.C., T.L. Jackson, L. Dickens, C. Hernandez, G.O. Ababio. *Protein release profiles and morphology of biodegradable microcapsules containing an oily core*, Journal of Controlled Release, **76**, pp. 313-326. 2001.

Zhang, L., C. Xiong and X. Deng. *Miscibility, crystallization and morphology of poly(β-hydroxybutyrate/poly(D,L-lactide) blends*, Polymer, **37**. pp. 235-241. 1996.

Zinn, M., B. Witholt and T. Egli. *Occurrence, synthesis and medical application of bacterial Polyhydroxyalkanoate*, Advanced Drag Delivery Reviews, **53**, pp. 5-21. 2001.